A 2-D THERMO-MECHANICAL FINITE ELEMENT MODEL FOR RESIDUAL STRESS DETERMINATION DURING WELDING AND ANNEALING

By

B. K. Dutta

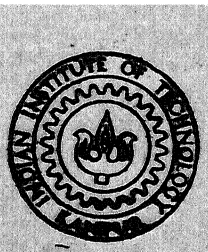

DEPARTMENT OF MECHANICAL ENGINEERING

INDIAN INSTITUTE OF TECHNOLOGY, KANPUR

JULY, 1983

A 2-D THERMO-MECHANICAL FINITE ELEMENT MODEL FOR RESIDUAL STRESS DETERMINATION DURING WELDING AND ANNEALING

A Thesis Submitted
In Partial Fulfilment of the Requirements
for the Degree of
MASTER OF TECHNOLOGY

By

B. K. Dutta

to the
DEPARTMENT OF MECHANICAL ENGINEERING
INDIAN INSTITUTE OF TECHNOLOGY, KANPUR
JULY, 1983

ME-1983-M-DUT-THE

CERTIFICATE

This is to certify that the thesis entitled 'A 2-D Thermo-Mechanical Finite Element Model for Residual Stress Determination During Welding and Annealing' by B.K. Dutta is a record of work carried out under our supervision and has not been submitted elsewhere for a degree.

(B. P. Singh)
Assistant Professor
Dept. of Mechanical Engineering
Indian Institute of Technology
Kanpur.

(V. Sundararajan)
Professor
Dept. of Mechanical Engineering
Indian Institute of Technology
Kanpur.

To

My Father Shri B.N. Dutta and Mother Smt. Mira Dutta
Who Dedicated Their Whole Lives
For
Better Education of Their Children

ACKNOWLEDGEMENTS

My studies under the M.Tech. program at I.I.T. Kanpur were performed under the auspices of the Department of Atomic Energy, Government of India. I am grateful to Shri S.K. Mehta, Head, Reactor Engineering Division and Shri A. Kakodkar, Head, Component Analysis Section, for getting sanctioned of necessary leave and financial support for my studies.

I thank Shri V.K. Mehra, my group leader and Shri H.S. Kushwaha, my immediate superior in BARC for their constant help and encouragement during the course of my studies.

I am greatly indebted to Prof. V. Sundararajan and Dr. B.P. Singh under whose supervision this thesis was completed. I thank them for their inspiring guidance, cheerful discussions and driving influence.

The help of the staff of the Computer Centre, I.I.T. Kanpur has been invaluable in developing the computer programs. I would like to thank Mr. R.N. Srivastava for his patience and care in typing a difficult manuscript.

Finally, I thank my parents, my brother, Sanjay Dutta and my sisters Mrs. Dipti Mitra and Miss Tripti Dutta for their abundant encouragement and support for my higher education.

- B.K. Dutta

CONTENTS

LIST OF FIGURES

NOMENCLATURE

T	:	Temperature
t	:	Time
C, X	:	Constants
H', E_T	:	Isotropic hardening factors
k	:	Yield point corresponds to shear
S_x, S_y, S_z	:	Three components of deviatoric stresses
E	:	Young's modulus
G	:	Shear modulus
$\dot{E}$	:	Variation of E with respect to temperature
r	:	Radius
K_x, K_y	:	Conductivity in x and y directions
C_p	:	Specific heat
q	:	Boundary heat flux
h	:	Coefficient of thermal convection
T_∞	:	Atmospheric temperature
$\tilde{Q}$	:	Volumetric heat generation
n_x, n_y	:	Normal vectors in x and y directions
n_r, n_z	:	Normal vectors in r and z directions
h_r	:	Coefficient of heat loss due to radiation
T_{at}	:	Temperature at which no heat loss due to radiation
L_H	:	Latent heat
C_{PS}	:	Specific heat of solid
C_{Pl}	:	Specific heat of liquid
C_{Pe}	:	Equivalent specific heat
T_S	:	Solidus temperature

T_l	:	Liquidus temperature
N	:	Shape function
u, v	:	Nodal displacements in x and y directions
ε	:	Strain
$\bar{\varepsilon}$	:	Effective strain
$\sigma_1, \sigma_2, \sigma_3$	:	Three principal stresses
σ_{YP}	:	Yield point
$\bar{\sigma}$	:	Effective stress
τ	:	Shear stress
$\dot{\varepsilon}^c$	:	Creep strain rate
ν	:	Poisson's ratio
$\dot{\nu}$	:	Change of Possion's ratio with respect to temperature
α	:	Coefficient of thermal expansion
ρ	:	Density
r	:	Absorbtivity
σ_r	:	Boltzmann constant
ξ, η	:	Local coordinates
$\{\delta\}$	:	Global vector of nodal displacements
$\{\sigma\}$	:	Stress vector
$\{\varepsilon\}$	:	Strain vector
$\{R\}$	:	Global load vector
$\{F\}$	:	Elemental load vector
$\{P\}$	:	Plastic load vector
$[B]$	:	Strain-nodal displacement matrix
$[D]$	:	Stress-strain matrix
$[\bar{D}]$	:	Stress-strain matrix considering creep
$[D_{ep}]$	:	Elastic-plastic material matrix

$[K_o]$	:	Initial stiffness matrix
$[K_T]$	:	Tangential stiffness matrix
$[N]$	:	Matrix of shape functions
$[\bar{B}]$	:	Strain-displacement matrix at a point

Superscript

e	:	Elastic
p	:	Plastic
-1	:	Inverse
Th	:	Thermal
TP	:	Temperature dependent properties
t	:	Total
T	:	Transpose
cr	:	Creep
(e)	:	Corresponds to element
(ne)	:	Elemental nodal values
i	:	Iteration number

Subscript

x, y, x	:	Corresponding directions
xy	:	x-y plane
θ	:	Hoop direction
eq	:	Equivalent

Prefix

d	:	Infinitesimal difference
Δ	:	Finite difference
$\frac{\partial}{\partial x}, \frac{\partial}{\partial y}, \frac{\partial}{\partial z}$	:	Partial derivatives

SYNOPSIS

A 2-D THERMO-MECHANICAL FINITE ELEMENT MODEL FOR RESIDUAL STRESS DETERMINATION DURING WELDING AND ANNEALING

A Thesis Submitted
In Partial Fulfilment of the Requirements
for the Degree of
MASTER OF TECHNOLOGY

by
B.K. DUTTA
Department of Mechanical Engineering
Indian Institute of Technology, Kanpur
July, 1983

A formulation for thermo-plastic analysis of plane strain case by finite element technique, has been derived. A computer program has been developed for elasto-plastic and thermo-plastic analysis of 2-D structures.

The formulation for thermo-plastic analysis of plane strain case and the computer program have been then modified for taking into consideration the effect of creep.

The program has been tested for number of sample problems, including problems involving creep. Program is used to compute stress transients during welding and annealing of two long plates. The results have been compared with the available results and found in good agreement.

The program is then used to compute stress transients during welding and annealing of a long cylinder and results are reported in the thesis.

PART I

THEORY

CHAPTER 1

INTRODUCTION

1.1 General Review

1.2 A Problem Definition

1.3 Computational Task

1.4 The Finite Element Method

1.1 General Review

Behaviour of solids under different conditions is always a field of interest for engineers and scientists. Before the introduction of digital computers, the application of solid mechanics largely rested on the simplification of analytical formulations, which are sometimes approximate in themselves. The gap between application and theory made the whole spectacle unreal. The development of digital computers and their application have brought radical changes in this area. The literature of last ten years clearly reflects this change. This is due to the important role played by numerical methods. Today an ever increasing number of engineers and scientists are using classical equations of solid mechanics on digital computers for solving real-life problems and the power of these equations is being extended beyond the dreams of their inventors. As a result, one hears frequently from engineers, questions as to the arbitrary idealisation of the classical analytical equations. A better appreciation of the idealisation involved and ways of improving them are often presented.

1.2 A Problem Definition

Modern industries fabricate large components (such as calandria, end shield etc. in case of nuclear industry), which require different mechanical processes, such as welding, casting, grinding etc. These operations in turn introduce large residual stresses of different nature. Determination of these residual stresses is of utmost interest to designers

as well as fabricators, as they influence the buckling strength of the structure and also structure is susceptible to brittle fracture, which gets enhanced in presence of nuclear radiations. The fatigue life of the structures is also affected considerably and structures are susceptible to cold cracking because of high nill ductility temperature (NDT) if large residual stresses are introduced during manufacturing.

Complexity of the determination of residual stresses, are characterized as follows:

1. Large temperature change in a small area
2. Inelastic deformation
3. Temperature dependency of material properties
4. Phase change of the some portion of the component
5. Complex boundary conditions.

Before the development of digital computers, most of the work for determining residual stresses were confined to either experimental or analysis of a very simplified one-dimensional model which is solvable by conventional mathematics. But the introduction of digital computers brought a revolution in this area and engineers are now in a position to compute these stresses more accurately and reliably by the help of powerful numerical techniques, such as the finite difference and finite element methods.

1.3 Computational Task

During mechanical processes, the thermomechanical transients control the evolution of the residual stresses and deformations. Therefore, the thermal stress analysis of the

mechanical processes requires both the time hystory analysis of temperatures and associated stresses. These are due to:

i) heat flow to the component and

ii) quasi-static response behavior of the structural component.

For an efficient numerical solution, these two computational steps are combined and fully integrated. The two field problems are resolved sequentially within the staggered solution scheme for transient heat transfer and thermoelastic-viscoplastic material behavior on the basis of interpolation in space and time. Therefore, the numerical aspects of stability and accuracy govern the appropriate selection of time steps for the incremental solution of the response history.

The computational task for determining residual stresses reliably is complicated by several facts:

1. The structural component is subjected to highly localised heat flow in the form of conduction, convection and radiation.

2. The fusion of the molten bead with the base material involves a moving contact problem with phase changes and moving boundaries.

3. The mechanical response during heating and cooling behavior spans the entire temperature range from room to melting temperature and vice versa.

4. The change of the internal material structure introduces latent heat effects on the thermal side as well as additional volume changes and transformation plasticity in the region of rapid cooling.

5. The degradation of stiffness and strength during heating causes full unloading and stress relief in the heat affected zone of high temperature.

6. The residual stresses depend on the entire history, thus the full heating-cooling cycle has to be traced taking due account of the temperature and deformation hystory.

1.4 The Finite Element Method

In one operation, it is difficult for a human mind to analyse and understand the behavior of its complex surroundings and creations. Hence it is a common tendency to divide a system to subsystems or 'elements', for which behavior is readily understood. The collective behavior of all the subsystems is an indication of the original system. This natural way of analysing a system is adopted by engineers, scientists and even economists for many years.

In general for getting exact behavior of a system, one has to go for infinite subdivisions and the problem can only be defined using the mathematical fiction of an infinitesimal, which ultimately leads to differential equations or equivalent statements. Such systems are called "continuous system". If a finite number of subdivisions can predict the exact behavior of the original system, the system is termed as "discrete system".

With the introduction of high speed digital computer, a discrete problem can be solved readily even if the number of elements is very large. This gives rise to a tendency of approximating a continuous system by a discrete system of

large number of elements. Since capacity of all computers is finite, hence this 'large' cannot be infinite. Hence continuous problems can only be solved exactly by mathematical manipulation. Here, the available mathematical techniques usually limit the possibilities to oversimplified situations.

The various methods had been proposed time to time to approximate a continuous system by a discrete system, also termed as 'discretization'. All these methods involve an approximation which, hopefully, is of such a kind that it approaches, as closely as desired, the true continuum solution as the number of discrete variables increases.

The discretization of continuum problems has been approached differently by mathematician and engineers. The first have developed general techniques applicable directly to differential equations governing the problem, such as finite difference technique. On the other hand, engineers often approach the problem more intuitively by creating an analogy between real discrete elements and finite portions of a continuum domain.

It is for the engineering 'direct analogy' view that the term 'finite element' has been born. Clough appears to be first to use this term, which implies in it a direct use of standard methodology applicable to discrete systems. Both conceptually and from the computational viewpoint, this is of the utmost importance. The first allows an improved understanding to be obtained; the second the use of a unified approach to the variety of problems and the development of standard computational procedures.

CHAPTER 2

LITERATURE SURVEY AND SCOPE OF THE PRESENT WORK

2.1 Development of Finite Element Technique

2.2 Development of Numerical Techniques for Plasticity Analysis

2.2.1 Some Basic Relations

2.2.2 Solution of Plasticity Problems

Tangential Stiffness Method

Initial Strain Method

Initial Stress Method

2.3 Development in Thermo-plastic Analysis

2.4 Development of Residual Stress Analysis During Welding

2.4.1 One-Dimensional Analysis

2.4.2 Two-Dimensional Analysis

Thermal Analysis

Stress and Distortion Analysis

2.5 Scope of the Present Work

2.1 Development of Finite Element Method

The development of the finite element method (FEM) can be described in the following five stages.

Stage 1 - Initial intuitional development in which Turner[1] (1956), Argyris[2] (1955), Clough[3] (1960) presented the method as an approximation of continuum in the context of structural analysis and Clough for the first time used the name "finite element".

Stage 2 - Wide recognition of FEM in the field of structural mechanics in which the basis for compatible model by Melosh[4] (1963), equilibrium model by Fraeijs de Verbeke[5] (1964) and hybrid model by Pian[6] (1964) depending upon different variational principles in elasticity were derived. Numerous finite element models and their applications were being reported everyday and a proper classification and treatment of the subject is given in reference by Argyris[7] (1965), Zienkiewicz and Cheung[8] (1967) and Prezemieniecki[9] (1968).

Stage 3 - The mathematical interpretation of the FEM and convergence are consolidating the fundamentals and are making FEM a powerful, universal technique. Zienkiewicz and his coworkers [1] have pioneered many non-structural applications of the FEM. Thus other useful processes of finite element derivation[10,11] exist which widen its scope beyond the problems in which a well defined variational functional exists.

Stage 4 - The widening of scope of FEM was first pioneered in the classic paper by Irons[12] (1966) in which future

strategy of handling finite element programs is outlined. As a result, a family of isoparametric and allied numerically integrated elements have been investigated. Most of these are reported by Zienkiewicz [1]. Now many practical aspects of reduced and selective integration rules and best sampling points for stresses etc. have come to the forefront. The research workers have been liberated from the time-wasting effort of deducing and programming various matrices afresh for each new problem and have directed their attention to efficient programs capable of breaking 'cost barriers'. The effect of this phase of development on the future applications and extensions such as in nonlinear analysis is enormous and far-reaching.

Stage 5 - The developments in FEM today can be seen mainly in three directions. In one direction, we find engineers, mathematicians and scientists are engaged in improving the present solution methods, assembly procedures, stiffness computing procedures and also different convergence criteria by the help of numerical mathematics. Impact of this work can be seen from the development of frontal solution procedure, skyline assembly technique [37], macro stiffness computation procedure, R.L. Taylor [1] and also from the publication of enormous number of books in FEM written in purely mathematics point of view.

In the second direction, we find engineers and scientists engaged in applying existing finite element solution technique to solve engineering and scientific problems. Such as use of FEM for analysing temperature distribution in

large components, mechanical processes [11], large civil structures, fatigue [9], creep [18], neutron flux distribution in reactor core etc. Even though ASME Codes have not specifically advocated the use of FEM, it is the most popular tool today to compute the detailed stress distribution as required by the ASME Code, Section III.

In the third direction, engineers and scientists are engaged in applying FEM in more and more new fields such as fluid mechanics, magnets and electro dynamic problems [1] etc.

2.2 Development of Numerical Techniques for Plasticity Analysis

Theoretical as well as practical interest in plasticity has stimulated much work in the numerical solution of elasto-plastic problems by the FEM and other procedures. The literature on small strain displacement elastic-plastic solutions using FEM is now large[13-15] [6,33,36], difference lie between the apparent forms of the non-linear solution algorithms used, and the form of constitutive relations postulated.

Before 1971, in most of the literature on the subject, simple, constant stress, elements have been used. This was largely motivated by the situation in which an exact integration of an element containing both elastic and plastic regimes would be difficult or impossible. Such difficulties disappear in the case of numerically integrated elements. Numerical integration was then introduced extensively into the formulation of complex elements [1] in linear elastic analysis and the higher order elements were proved to be remarkably efficient. Adoption of isoparametric formulation

for materially nonlinear problems was done for the first time by G.C. Nayak (1971) [6] and showed that even greater advantages arise once a smooth distribution of the displacement throughout the element is postulated by a shape function definition. So state of stress at each integrating point can be examined individually and the resulting element properties obtained by a suitable weighted summation over the integrating points.

2.2.1 Some Basic Relations

To discuss developments in solution procedures for plasticity analysis, some basic relations of plasticity, are given here for further reference. Derivations of these relations are given in Chapter 3.

incremental strain-displacement relation $\{d\varepsilon\} = [B]\{d\delta\}$ (2.1)

incremental equation of equilibrium $\{dR\} - \int_V [B]^T \{d\sigma\} dV = \{0\}$ (2.2)

tangent stiffness matrix $[K_T] = \int_V [B]^T [D]_{ep} [B] dV$ (2.3)

incremental plastic strain $\{d\varepsilon\}^p = d\bar{\varepsilon}^p \{\frac{\partial \bar{\sigma}}{\partial \sigma}\} = \frac{d\bar{\sigma}}{H'} \{\frac{\partial \bar{\sigma}}{\partial \sigma}\}$

$$= \frac{\{\frac{\partial \bar{\sigma}}{\partial \sigma}\} \lfloor \frac{\partial \bar{\sigma}}{\partial \sigma} \rfloor \{d\sigma\}}{H'} \quad (2.4)$$

incremental elastic-plastic stress strain relation

$$\{d\sigma\} = [D]_{ep} \{d\varepsilon\} = [[D] - [D]^p] \{d\varepsilon\}$$

$$= \{d\sigma\}^e - \{d\sigma\}^p \quad (2.5)$$

where

$$[D]^P = \frac{[D] \left\{\frac{\partial \bar{\sigma}}{\partial \sigma}\right\} \left[\frac{\partial \bar{\sigma}}{\partial \sigma}\right] [D]}{H' + \left[\frac{\partial \bar{\sigma}}{\partial \sigma}\right] [D] \left\{\frac{\partial \bar{\sigma}}{\partial \sigma}\right\}} \qquad (2.6)$$

Hence any plasticity problem now involves the solution of equilibrium Equation (2.2) together with incremental stress strain relations given by Equations (2.5) and (2.6).

2.2.2 Solution of Plasticity Problems

Tangential Stiffness Method [33] - By substituting $\{d\sigma\}$ and $\{d\varepsilon\}$ from Equation (2.5) and Equation (2.1) into equilibrium Equations (2.2), we have

$$\{dR\} - \int_V [B]^T [D]_{ep} [B] \, dV \; \{d\delta\} = \{0\} \qquad (2.7)$$

which from Equation (2.3) reduces to

$$\{dR\} - [K_T] \{d\delta\} = \{0\} \qquad (2.8)$$

hence $$\{d\delta\} = [K_T]^{-1} \{dR\} \qquad (2.9)$$

This method of solving was presented by Pope[16] (1965) for plane stress problems for strain hardening Von Mises solid. He advocated the use of small increments of load which just caused yield in the next simple triangular element. Yamada, Yoshimura and Sakurai (1968) [32] used the method presented by Pope by allowing one triangular element to yield at a time. They have clearly shown that the problem is very much dependent on the mesh type and sizes and there can be some elastic elements surrounded by plastic ones near to the elastic-plastic interface.

Marcal and King (1967) [33] advocated a large size increment of load (based on initial yield load factor L) and solved the Equations (2.9) by using a mean value of tangential stiffness (partial stiffness) for elastic perfectly plastic and strain hardening Von Mises solid with simple triangular elements in plane stress, plane strain and axysymmetry. The necessity of partial stiffness coefficients arose because of the 'transition region' which is usually adjacent to the elastic plastic interface and for correct solution of Equations (2.9). The transition region must be correctly known.

Partial stiffness matrix for an element under transition is calculated by

$$[D_{ep}] = [D] - (1 - m)[D]^p \tag{2.10}$$

where $$m = \frac{\sigma_y - \sigma_{n-1}}{\sigma_n - \sigma_{n-1}} \quad \text{and} \quad \sigma_n > \sigma_y > \sigma_{n-1} \tag{2.11}$$

More explanations on this method can be seen in Chapter 3.

Initial Strain Method - Another modification of Equations (2.2) is based on the idea of modifying the right hand side of elastic equations of equilibrium to compensate for the fact that the plastic strains do not cause any change in stress and can be treated in the same way as the thermal strains. Since

$$\{\Delta\sigma\} = [D]\{\Delta\varepsilon\}^e = [D](\{\Delta\varepsilon\}^t - \{\Delta\varepsilon\}^p) \tag{2.12}$$

hence using Equation (2.4) in Equation (2.12), we have

$$\{\Delta\sigma\} = [D]\left(\{\Delta\varepsilon\}^t - \frac{\{\frac{\partial\bar{\sigma}}{\partial\sigma}\}\left[\frac{\partial\bar{\sigma}}{\partial\sigma}\right]\{\Delta\sigma\}}{H'}\right) \tag{2.13}$$

Using Equation (2.13) in Equation (2.2) we have

$$\{\Delta R\} = [K_o]\{\Delta\delta\} - \int_V [B]^T [D] \left(\frac{1}{H'} \left\{\frac{\partial \bar{\sigma}}{\partial \sigma}\right\} \left[\frac{\partial \bar{\sigma}}{\partial \sigma}\right] \{\Delta\sigma\}\right) dV \tag{2.14}$$

where

$$[K_o] = \int_V [B]^T [D] [B] \, dV$$

Hence

$$[K_o]\{\Delta\delta\} = \{\Delta R\} + \{\Delta P\} \tag{2.15}$$

where

$$\{\Delta P\} = \int_V \frac{1}{H'} \left([B]^T [D] \left\{\frac{\partial \bar{\sigma}}{\partial \sigma}\right\} \left[\frac{\partial \bar{\sigma}}{\partial \sigma}\right] \{\Delta\sigma\}\right) dV \tag{2.16}$$

Obviously solution of Equations (2.15) is impossible if $H' = 0$ (that is, no hardening).

Gallagher et al[17] (1962) and Argyris[18] (1965) have effectively used Equation (2.16). The essential difference from the tangential stiffness method is the evaluation of $\{\Delta P\}$ by iterations.

Evidently the method satisfies the equilibrium equations and stress-strain relationships. The method is not applicable for ideal elastic-plastic material but can be made to work with hardening non-associated flow laws. For solution, $[K_o]^{-1}$ can be stored once and for all. It is, therefore, not likely to be as costly as the tangential stiffness method. However as the yielding of material increases the number of iterations required are more.

Initial Stress Method - Since the 'initial strain method' is not applicable to ideally elastic-plastic material an alternative method called 'initial stress method' was

introduced by Zienkiewicz, Valliappan and King[19] (1968-1969). Here Equations (2.2) are written as

$$\{\Delta P\} = [K]_o \{\Delta\delta\} - \int_V [B]^T \{\Delta\sigma\}^p \, dV \tag{2.17}$$

where

$$\{\Delta\sigma\}^p = [D]^p \{\Delta\varepsilon\} \tag{2.18}$$

hence the initial load

$$\{\Delta P\} = [K]^p \{\Delta\delta\} = \int_V [B]^T \{\Delta\sigma\}^p \, dV \tag{2.19}$$

This method has the advantage of being easily interpreted physically and is simple and presents no problems for cyclic loading as the unloading proceeds on purely elastic basis. There are no problems as regards the consideration of non-associated flow laws and has an obvious advantage of operating with $[K_o]^{-1}$ stored once and for all. However its preference over other methods such as tangential stiffness method depends mainly on the rate of convergence. The initial stress method converges very rapidly in the beginning and becomes very slow near general yield.

There are various other methods which are being used such as method of residual forces [6], alpha constant stiffness method[20], method of plastic multiplier [6] etc. But the three methods explained above seems to be popular. A computer program developed by the present author, uses the tangential stiffness method as devised by Marcal and King. One of the reasons of using this method is variations in material properties with loading (because of their temperature dependency) and hence matrix $[K_o]^{-1}$ cannot be stored

and used for further iterations. Since it is now necessary to calculate stiffness matrix for every loading step, it is better to calculate $[K]_T$ instead of $[K]_o$, as in former case convergence is faster.

2.3 Development in Thermo-Plastic Analysis

A thermo-plastic analysis can be treated very much similar to elasto-plastic analysis. But in case of thermo-plastic analysis beside elastic and plastic strains, two more strains corresponding to the temperature change and the temperature dependent material properties, are to be considered. Tangential stiffness method seems to be a popular choice because of necessity of computation of stiffness matrix in every loading step due to the dependency of the material properties on temperature. One of the oldest paper in this analysis is that of UEDA et al (1971) [19]. The formulation presented in [19] and also in [17] by the same authors, seems to be applicable for 1-D, 2-D plane stress and axisymmetric and 3-D structures. But no formulation was reported for plane strain case in which a systematic elimination of z direction incremental stress is required. Subsequently many authors used the above formulations in their work such as [9], [12], [3] etc. For plane strain case a method is suggested by Friedman (1975) [20], by postulating an expression for $d\bar{\varepsilon}^p$. In the present work systematic derivation of different expressions for thermo-plastic analysis of plane strain case is done and shown in Chapter 3.

2.4 Development of Residual Stress Analysis During Welding

The welding process is one of the most widely used structural fabrication techniques, and has therefore received much study as a mechanical process. The objective of such work is the identification of problems associated with welding. Among these the residual stresses and distortions resulting from the extreme thermal conditions during welding are one most important. The residual state of stress has a strong influence on the strength and life of the resulting structure, and welds are usually the critical determinants of the overall structural integrity. Both experimentally and analytically, the problem poses severe difficulties, and inspite of the extent of the experimental effort, there have been few analytical studies of the residual stresses in a weld. Analytically most of the studies available can be divided into two categories. These are the studies done before the development of FEM and the studies done after the development of FEM. Before the development of FEM most of the available work is one-dimensional and uses a line solution for the thermal analysis. Whereas after 1970s, work done in this context is of 2-D analysis by FEM. Studies on the transient thermal stresses during welding started in the 1930s. Boulton and Lance-Martin[21] discussed the transient thermal stresses that occur along the edge of a plate during welding.

The first significant attempt to use a computer in the analysis of thermal stresses during welding was done by Tall[22,23] in a Ph.D. thesis in 1961. He developed a simple program on thermal stresses during bead welding along the

center line of a strip. The temperature distribution was treated as two-dimensional; however, in analyzing stresses it was assumed that (1) longitudinal stress, σ_X, is a function of the lateral distance Y only and (2) that σ_Y and τ_{XY} are zero.

In 1968 Masubuchi et al[24] of Battelle Memorial Institute developed based upon Tall's analysis, a FORTRAN program on the one-dimensional analysis of thermal stresses during welding. Since 1970 the computer analysis of transient thermal stresses during welding has become more common at several laboratories around the world [4].

Commission X (Residual stress, stress relieving and brittle fracture) of the International Institute of Welding established in 1972 a working group of "Numerical analyses of stresses, strains and other effects produced by welding". The working group has prepared reports covering the studies made in various laboratories of the World[25].

In this section a general one-dimensional analysis done before 1970s and two-dimensional analysis after 1970s and inherent assumptions in both the analysis separately are presented.

2.4.1 One-Dimensional Analysis [10]

Temperature distribution around the moving arc is calculated as a two-dimensional heat-conduction problem. The temperature distribution can be expressed by the following equation [4]:

$$\textcircled{H} = \frac{q}{2\pi\lambda} e^{-\frac{V}{2}\xi} K_o \frac{V}{2K} r$$

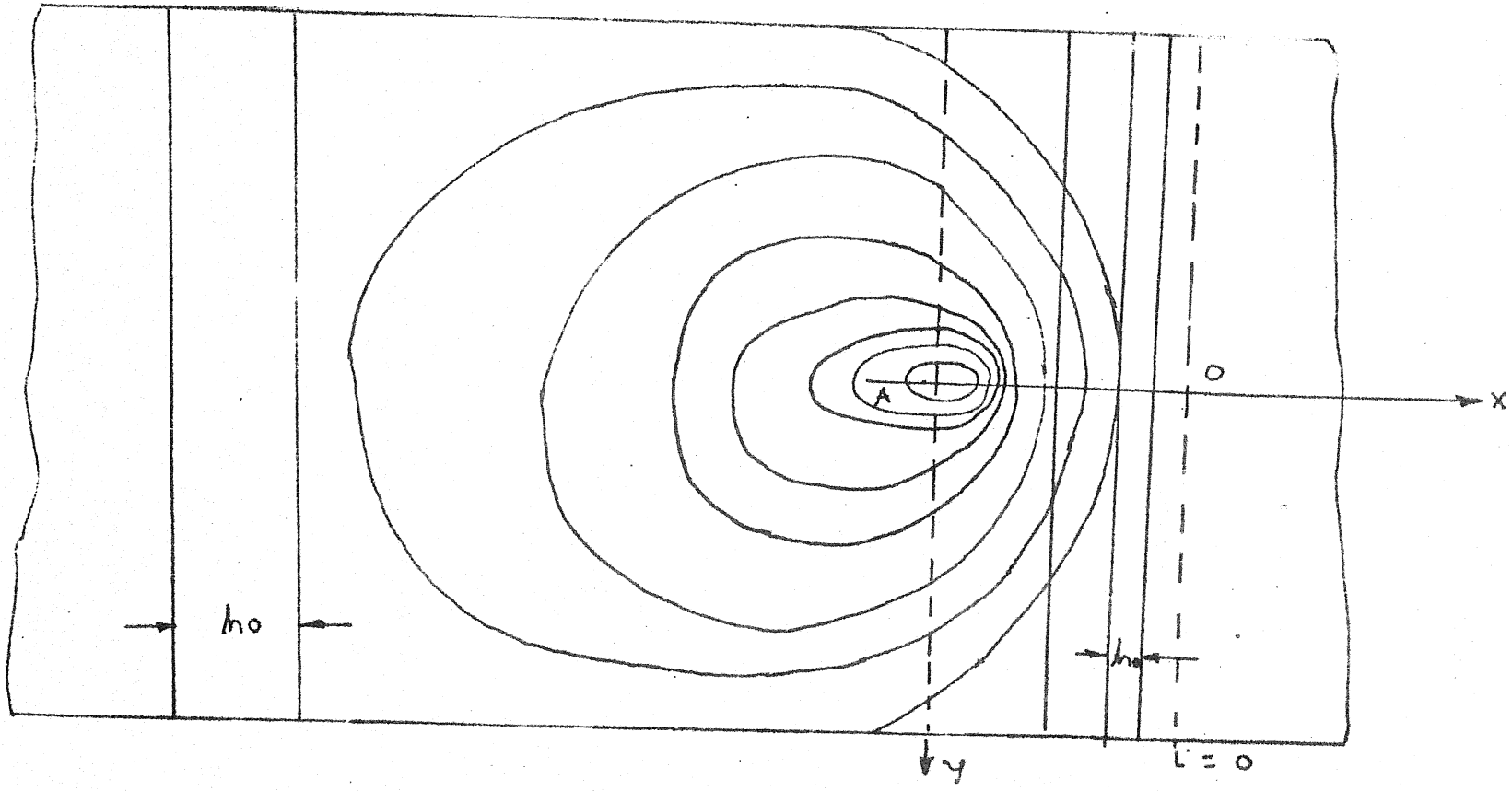

FIG.- 2·1 DIVISION OF STRESS FIELD INTO TRANSVERSE STRIPS FOR CALCULATING THERMAL & RESIDUAL STRESSES.

where

Θ = temperature change

q = intensity of the linear heat source

λ = heat conductivity

κ = thermal diffusivity

V = arc travel speed

$\xi = x - Vt$ = longitudinal ordinate in the moving coordinate system

t = time

$r = \sqrt{\xi^2 + y^2}$

$K_o(Z)$ = zero order modified Bessel function of the second kind.

The intensity of the linear heat source, q, is expressed by:

$$q = \frac{\eta V I}{T}$$

where η = thermal efficiency of welding arc, or arc efficiency

V = arc voltage

I = arc current

T = plate thickness

For calculating stresses, the field is divided into a set of transverse strips of width h_o, as shown in Figure 2.1. The time intervals represented by the strip width must be narrow enough so that the temperature and thermal stress for each increment may be regarded as being constant. Since the greatest changes in temperature occur near the arc, narrow strips are used in areas near the arc.

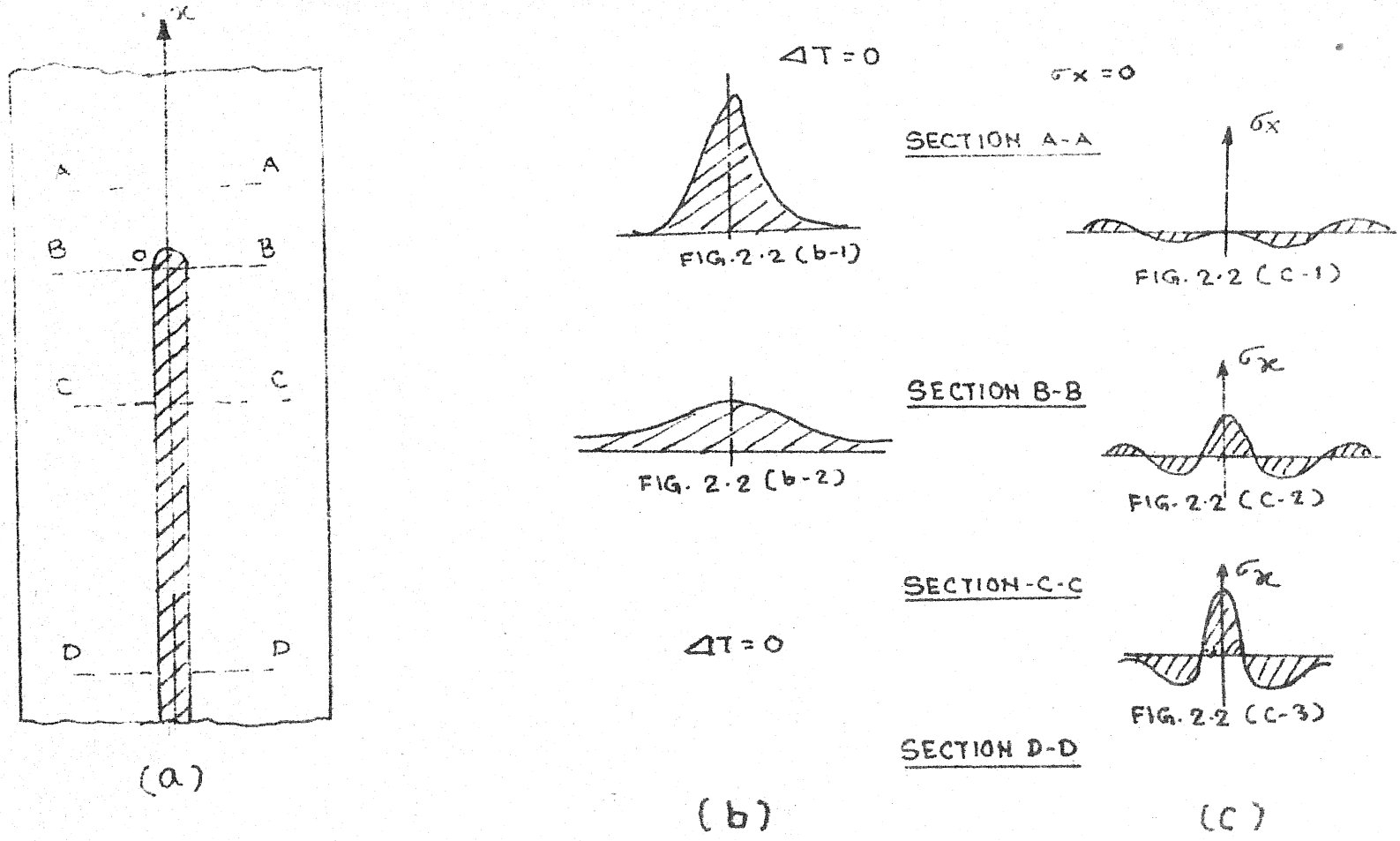

FIG.-2·2 SCHEMATIC REPRESENTATION OF TEMPERATURE & STRESS DISTRIBUTIONS DURING WELDING [4]

Key assumptions in the one-dimensional programs are that

(a) both sides of each strip remain straight during welding, which produces longitudinal stresses, σ_x, creating a sort of plane-strain condition in each strip; and

(b) the longitudinal stresses along the entire length of each strip are balanced.

Figure 2.2 shows schematically changes of temperature and stresses during welding as predicted by 1-D analysis. A bead-on-plate weld is being made along the X-axis. The welding arc, which is moving at a speed v, is presently located at the origin 'O', as shown in Figure 2.2(a). Figure 2.2(b) shows temperature distribution along several cross sections. Along section A-A, which is ahead of the welding arc, the temperature change due to welding, ΔT, is almost zero. Along section B-B which crosses the welding arc, the temperature distribution is very steep. Along section C-C which is some distance behind the welding arc, the distribution of temperature change is as shown in Figure 2.2(b-2). Along section D-D, which is very far from the welding arc, the temperature change due to welding again diminishes. Figure 2.2(c) shows the distribution of stresses along these sections in the x direction.

Along section A-A, thermal stresses due to welding are almost zero. The stress distribution along section B-B is shown in Figure 2.2(c-1). Stresses in regions underneath the welding arc are close to zero, because molten metal does not support loads. Stresses in regions some distance away

from the arc are compressive, because the expansion of these areas is restrained by surrounding metal that is at lower temperatures. Since the temperatures of these areas are quite high and the yield strength of the material is low, stresses in these areas are as high as the yield strength of material at corresponding temperatures. The magnitude of the compressive stress passes through a maximum with increasing distance from the weld or with decreasing temperature. However, stresses in areas away from the weld are tensile, and balance with compressive stresses in areas near the weld. In other words $\int \sigma_x \, dy = 0$ across section B-B. Thus, the stress distribution along section B-B is as shown in Figure 2.2(c-1). Stresses are distributed along section C-C as shown in Figure 2.2(c-2). Since the weld-metal and base-metal regions near the weld have cooled, they begin to shrink, causing tensile stresses in regions close to the weld. As the distance from the weld increases, the stresses first change to compressive and then become tensile. Figure 2.2(c-3) shows the stress distribution along section D-D. High tensile stresses are produced in regions near the weld, while compressive stresses are produced in regions away from the weld. The distribution of residual stresses that remain after the welding is completed, is shown in figure.

2.4.2 Two-Dimensional Analysis

A two-dimensional model was first developed and applied by Hibbitt and Marcel successfully[26]. Comparison with available experimental work was made, with gross

quantitative agreement. The same model was used by Nickell and Hibbitt [39], who compared temperature results (including the prediction of fusion zone) with a well instrumented experiment on a complex geometry with good accuracy. A similar model has been developed by Friedman [20], who studied butt welds, but no experimental comparison has been made. Buyukozturk and Hibbit[27] applied this technique to a large, multipass butt weld, again without experimental verification. In all these cases the authors reported that their main difficulty and source of possible error was the lack of basic material and parametric data.

Thermal Analysis

Heat Input - The mechanisms involved in heat input are extremely complex and physics of the weld arc are not fully understood [11]. The heat of the arc may be related to

$$Q = \eta V I$$

where Q is the net heat flux, η is the arc efficiency, V is the electrical input voltage and I is the electrical input current.

The distribution of flux on the facing surface is assumed to be normal and radially symmetric. That is

$$q = q_o \bar{e}^{c r^2}$$

where q_o and c are chosen based on the radius of the welding electrode. The most effective method of obtaining these two parameters is from a well instrumented test.

In most welds it is readily shown that the arc speed is large compared to heat transfer rates, so that the heat transfer parallel to the line of motion of the electrode may be neglected. That is, the temperature history of any section normal to the line of motion of the weld head is the same as that of any other such section, except for a shift in time. This is an important consideration, since it allows a reduction from a three-dimensional to a two-dimensional thermal analysis. Hence

$$q(s, t) = q_o \, e^{-cs^2} \, e^{-cV^2(t - t_o)^2}$$

where 's' measures distance, on the surface, from the centerline of the weld electrode. V is the electrode velocity and t_o is the time of peak heating for this section.

Heat Transfer - The mechanism which carries the heat applied to the surfaces described above, into the bulk material of the filler and base material adjacent to the joint is that of conductive heat transfer. The Fourier law $q_i = -K_{ij} T_{,j}$ governs this mechanism, where $K_{ij}(T)$ is the conductivity.

In addition, specific and latent heat effects must be included, since the problem is a transient one, with melting and re-solidification occurring in the material. Since both the specific heat and conductivity are known to vary with temperature, it is necessary to have their values available for the complete temperature range of the analysis. Usually the investigators resort to extrapolation of known

data, since high temperature values are difficult to measure experimentally [19,20].

The FEM as conventionally applied to heat transfer problems is not well suited to latent heat calculations. The reason for this is that the method is based on the assumption of a local solution, $T = \emptyset^N(x)\ T^N$, which is assumed C^1 continuous on the interior of the elements. When phase change takes place at a unique temperature (as in a pure phase) the latent heat requires a discontinuity in the temperature gradients. Such discontinuities are only admitted at the element interfaces, so that it is not realistic to resolve the fusion front any finer than the element dimension. Apparent increase in heat capacity seems to be a popular method for phase change consideration [14].

Boundary Conditions - The third mechanism of importance in the heat transfer is the surface boundary conditions. Two heat transfer mechanisms are usually considered: radiation effects dominate at higher temperatures, but later in the cool-down history the primary mechanism is convection. The difficulty in the latter case is the inside variation in convection coefficient depending on surface condition and air flow.

Galerkin finite element method [1] and central difference (Crank-Nicholsen) time stepping algorithm [13] seem to be again popular choice [11].

Stress and Distortion Analysis - The stress analysis also utilizes a finite element geometric model and piecewise

linear time-stepping. The input for this phase of the analysis is the temperature history defined throughout the joint region by the previous thermal analysis.

Finite Element Model - In most cases the geometric model must be modified for the stress analysis [20]. This is because the thermal analysis is a very local solution. But in order to predict residual stress and distortion accurately, it is important to model the flexibility of the rest of the structure, since the constraint provided by the structure outside the region in the immediate neighborhood of the joint plays a significant part in the growth of residual stress.

Material Properties - The residual stresses result from inelastic response of the material to the extremely severe thermal history of the joint constitutive characterization of the material is difficult since all temperature from room temperature to well above the melting point are present. In all the work to date, the assumption is made that the material may be treated as a time-independent elastic-plastic material during welding, with temperature dependent yield and elastic moduli. This characterization was justified in[26] by the argument that welding times are short so that any time-dependent behavior is restricted to sharp primary creep effects of extremely short characteristic times, which cannot be distinguished easily from yield in a material characterization experiment.

An interesting aspect of the weld process is the presence of sharp temporal temperature gradients. The material cools so rapidly that it is clear that unstable material

phases must be present, so that the material properties in regions, where this happens, must be quite different from those of the bulk material. This point has never received attention in the welding analysis that have been performed, except in[27], where the authors use a different material characterization in the heat-affected zone, based on post-weld surface hardness measurements.

Elastic-Plastic Solution Procedure - The use of the FEM for non-isothermal elastic-plastic analysis is by now a routine procedure, and the weld problem is merely a rather severe example of such an analysis. All the authors cited use tangent modulus methods [7,11,12,19,20] where by the system stiffness matrix is reformed at each step in order to account for active plastic loading, or elastic unloading from such a state. The formulation uses a piecewise linear approximation for the classical equations of plasticity, and some scheme is always used to process the thermal analysis results to ensure sufficiently small steps in the stress analysis to satisfy this linearization requirement.

2.5 Scope of the Present Work

Welding of long plates, cylinders etc. can be treated as a plane strain case for stress transients analysis. In the present work, a complete derivations of different expressions for thermo-plastic analysis of plane strain case by FEM, has been carried out. Incremental stress in Z direction is eliminated during this derivation, because of its dependency on other inplane stresses. A computer program

THESIS has been developed for thermo-plastic analysis of plane-stress, plane-strain and axisymmetric structures depending upon the formulations derived. The same program has been also modified for taking into consideration the melting of part of the structure. The program has been tested for different sample problems and then used to compute stress transients during butt welding of two long plates and longitudinal welding of a cylinder.

Upper derivation of different expressions for thermo-plastic analysis of plane strain case has been repeated for taking into consideration creep. Four creep laws such as power creep, experimental creep, time hardening creep and strain hardening creep laws, have been used in the formulation for better representation of creep phenomena of any materials during any temperature range. Program THESIS has been then modified for thermo-plastic analysis with creep of 2-D structures. The program has been again tested for different sample problems and then used for computing stress transients during annealing of two butt welded plates and longitudinal welded cylinder.

Eight noded isoparametric element has been used for the finite element modelling of the structure. 2x2 Gauss point integration, Gaussian elimination solution procedure and macro stiffness computing procedure for fast computation of element stiffness matrices, as suggested in [1], have been used in the program THESIS. Tangential stiffness solution procedure for plasticity analysis has been used as discussed in Section (2.2.2).

CHAPTER 3

ELASTO-PLASTIC AND THERMO-PLASTIC ANALYSIS OF 2-D STRUCTURES

3.1 Introduction

3.2 General Theory of Plasticity

3.2.1 Yield Criteria

3.2.1a Tresca-Yield Criteria

3.2.1b Von-Mises Criteria

3.2.1c Stress Space Representations of Yield Criteria

3.2.2 Stress-Strain Relations (Flow Rule)

3.2.2a Levy-Mises Equations

3.2.2b Prandtl-Reuss Equations

3.2.3 Strain Hardening Theories

3.2.3a Isotropic Strain Hardening Theory

3.2.3b Kinematic Strain Hardening Theory

3.3 A Finite Element Approach to Thermo-Mechanical Problems

3.4 Elasto-Plastic Analysis of Plane Stress and Axisymmetric Problems

3.5 Elasto-Plastic Analysis of Plane Strain Problems

3.6 Thermo-Plastic Analysis of Plane Stress and Axisymmetric Problems

3.1 Introduction

In the present chapter, four sets of formulations are presented for elasto-plastic and thermo-plastic analysis of 2-D structures. The main aim of these formulations is to find expressions for elasto-plastic material matrix $[D_{ep}]$ and corresponding load vector. These expressions are used in finite element formulation presented in Appendix 1, for ultimate analysis of entire structure. In Section 3.2 basic relations for plasticity are presented for further reference. In Section 3.3, a general approach to finite element for elasto-plastic and thermo-plastic analysis is discussed. A formulation is presented in Section 3.4 for elasto-plastic analysis of plane stress and axisymmetric structures. In Section 3.5, above formulation is modified for plane strain case. Formulation for thermo-plastic analysis of plane stress and axisymmetric structures is presented in Section 3.6, which is an extension of Section 3.4. Finally a new approach for thermo-plastic analysis of plane strain case is presented in Section 3.7, developed during the course of this work.

An incremental solution algorithm is given in Section 3.8. Section 3.9 deals with solved examples to show capability of these formulations to attack different types of problems.

3.2 General Theory of Plasticity

'Plastic' behavior of solids is characterized by a non-unique stress-strain relationship, as opposed to that of linear elasticity. One definition of plasticity may be

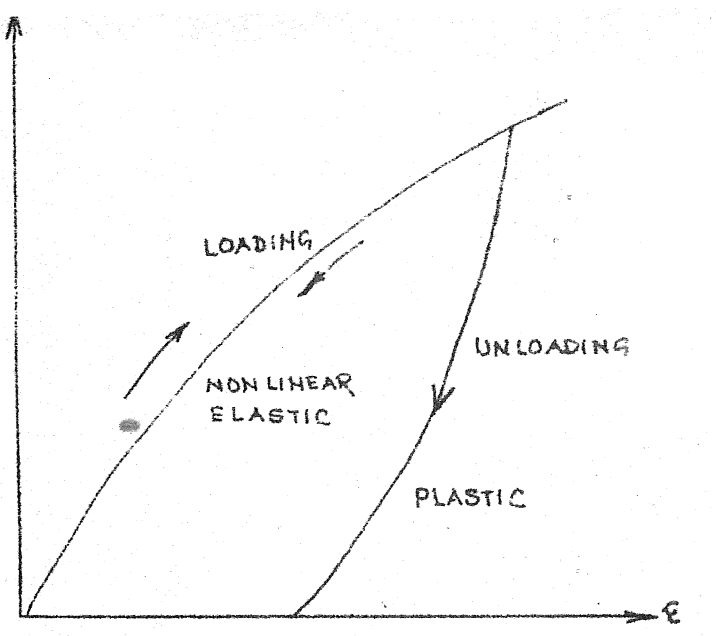

FIG. 3·1(a) NONLINEAR ELASTICITY & PLASTICITY

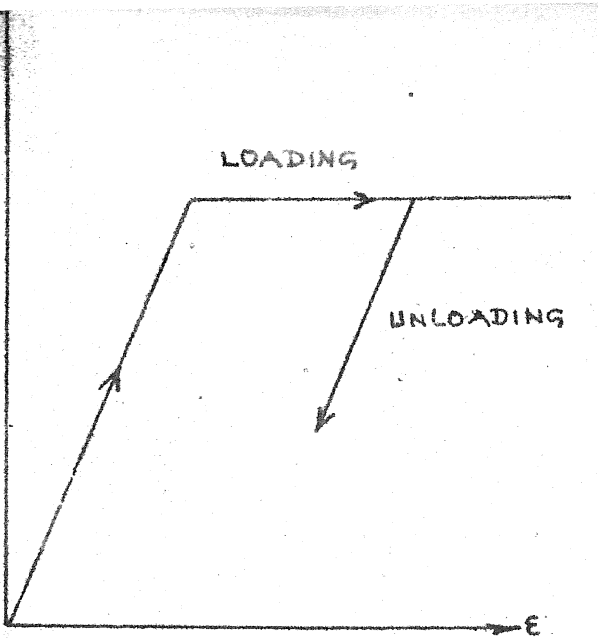

FIG. 3·1(b) IDEAL PLASTICITY

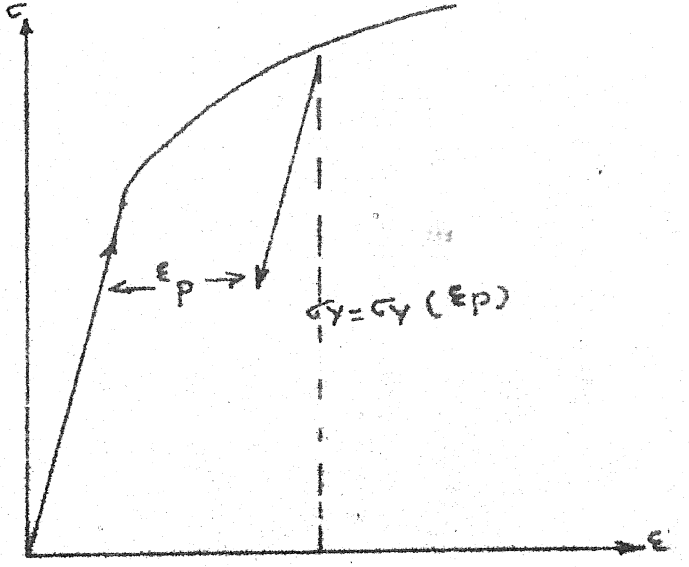

FIG. 3·1(c) STRAIN HARDENING PLASTICITY

FIG.-3·1 UNIAXIAL BEHAVIOR

the presence of irrecoverable strains on load removal. If uniaxial behavior of a material is considered, as shown in Figure 3.1(a), a non-linear relationship on loading alone does not determine whether non-linear elastic or plastic behavior is exhibited. Unloading will immediately discover the difference with the elastic material following the same path and the plastic material showing a history dependent, different path. Many materials show an ideal plastic behavior in which a limiting yield stress, σ_{YP}, exists at which the strains are indeterminate, as shown in Figure 3.1(b). For all stresses below σ_{YP} a linear (or non-linear) elasticity relationship is assumed. A further refinement of this model is one of hardening/softening plastic material in which the yield stress depends on some parameter, such as ε_p as shown in Figure 3.1(c).

Because of non-uniqueness of stress-strain relationship, one has to consider the following three points, before proceeding to plasticity analysis.

3.2.1 Yield Criteria

A yield criteria is a hypothesis concerning the limit of elasticity under any possible combination of stresses. The suitability of any proposed yield criteria must be checked by experiment.

If a point in a ductile material is subjected to the principal stresses σ_1, σ_2, σ_3 and is represented by a Mohr circle, if the principal stresses are changed to $(\sigma_1 + \sigma_m)$, $(\sigma_2 + \sigma_m)$ and $(\sigma_3 + \sigma_m)$, then the size of Mohr

circle, for this new state of stress, remains same but is shifted by a distance σ_m along the σ-axis. The additional stresses σ_m make up a hydrostatic (tensile or compressive) stress system. It is found that the absolute size of the Mohr circle alone determines the limit of elasticity and is independent of its position. This is to say that the yield criteria is a function of $(\sigma_1 - \sigma_2)$, $(\sigma_2 - \sigma_3)$ and $(\sigma_3 - \sigma_1)$ and is independent of hydrostatic stress component $(\sigma_1 + \sigma_2 + \sigma_3)/3$.

Thus yielding occurs when some scalar function of the principal stress differences reaches a critical magnitude, or to say mathematically:

$$f(\sigma_1 - \sigma_2, \sigma_2 - \sigma_3, \sigma_3 - \sigma_1) = \text{Constant} \qquad (3.1)$$

3.2.1a Tresca-Yield Criteria

Perhaps the simplest function imaginable which satisfies Equation (3.1) is of the form

$$\sigma_i - \sigma_j = \text{Constant} \qquad (3.2)$$

Equation (3.2) interprets when largest of the three magnitudes $\sigma_1 - \sigma_2$, $\sigma_2 - \sigma_3$, $\sigma_3 - \sigma_1$ attains a critical constant value (for a given material) yielding begins.

Equation (3.2) was first suggested by Tresca in 1864. Hence this states: 'yielding occurs when the greatest absolute value of any one of the three maximum shear stresses in the material reaches a certain value'.

Since yield criteria should be valid for any combination of stresses, the constant in Equation (3.2) may

be determined from uniaxial stress state. Denoting yield shear stress by k for a state of pure shear and tensile yield stress by σ_{YP}, since for pure shear stress $\sigma_1 = -\sigma_3 = k$ and the intermediate principal stress $\sigma_2 = 0$, the value of the constant is 2k. Also for pure tension we have $\sigma_1 = \sigma_{YP}$ and $\sigma_2 = \sigma_3 = 0$, hence for $\sigma_1 > \sigma_2 > \sigma_3$, one gets for yielding by Tresca criteria

$$|\sigma_1 - \sigma_3| = \sigma_{YP} = 2k \qquad (3.3)$$

3.2.1b Von-Mises Criteria

Another admissible function, which satisfies Equation (3.1) is of the form

$$(\sigma_1 - \sigma_2)^2 + (\sigma_2 - \sigma_3)^2 + (\sigma_3 - \sigma_1)^2 = \text{Constant} \qquad (3.4)$$

The incorporation of $(\sigma_1 - \sigma_2)$ etc., as quadratic terms, dispenses with the need to use the modulus sign. In this type of function, each of the principal stresses contributes to yielding. This function was proposed by Huber (1904), Von-Mises (1913) and by J.C. Maxwell in a letter to Kelvin in 1856 [31]. The criteria was then interpreted by Hencky as 'yielding begins when the shear strain energy reached a critical value'.

The value of the constant in Equation (3.4) can be again determined from the simple tension yielding, i.e. $\sigma_1 = \sigma_{YP}$, $\sigma_2 = 0$, $\sigma_3 = 0$ and pure shear yielding i.e. $\sigma_1 = -\sigma_3 = k$, $\sigma_2 = 0$. Hence yield criteria becomes

$$(\sigma_1 - \sigma_2)^2 + (\sigma_2 - \sigma_3)^2 + (\sigma_3 - \sigma_1)^2 = 2\sigma_{YP}^2 = 6k^2 \qquad (3.5)$$

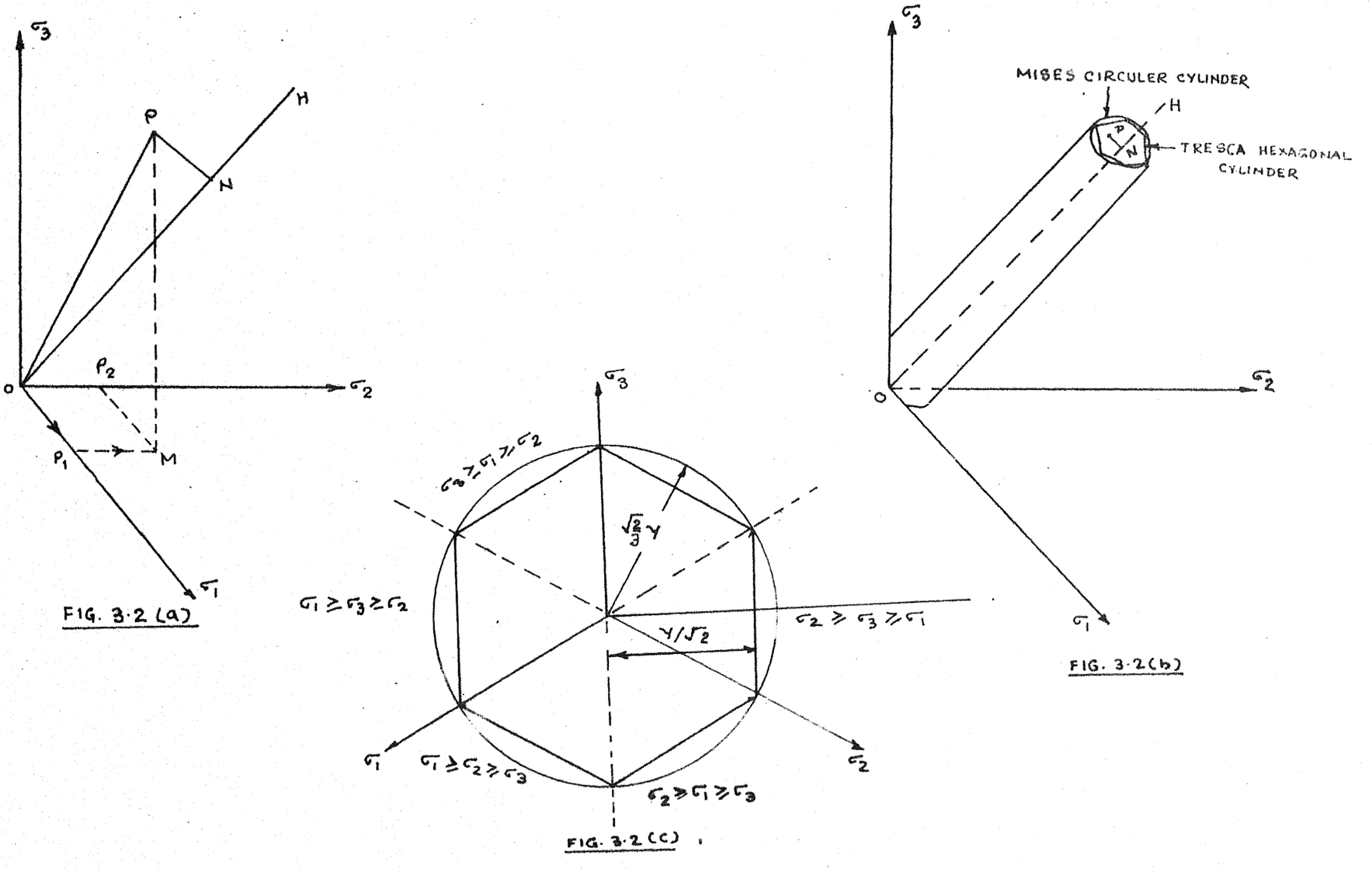

FIG.-3·2 STRESS SPACE REPRESENTATION OF YIELD CRITERIA

Hence the relation between σ_{YP} and k, as per Tresca criterion is $k = 0.5\ \sigma_{YP}$, whereas as per Von-Mises criteria $k = \frac{2}{3}\left(\frac{\sigma_{YP}}{2}\right) = 0.57735\ \sigma_{YP}$.

For a general state of stress (σ_x, σ_y, σ_z, τ_{xy}, τ_{yz}, τ_{zy}), the Von-Mises criteria becomes

$$\frac{1}{\sqrt{2}}\left[(\sigma_x - \sigma_y)^2 + (\sigma_y - \sigma_z)^2 + (\sigma_z - \sigma_x)^2 + 6(\tau_{xy}^2 + \tau_{yz}^2 + \tau_{zx}^2)\right]^{1/2} = \sigma_{YP} \qquad (3.6)$$

The formulations subsequently presented in this chapter and in the following chapters, make use of this criteria for yielding as it is the best available yield criteria and this includes all the principal stresses in one expression.

3.2.1c Stress Space Representations of Yield Criteria

In Figure 3.2(a) three mutually perpendicular axes, O σ_1, O σ_2 and O σ_3 are shown. If the principal stresses at a point in a body are (σ_1, σ_2, σ_3), this state of stress system is represented by a point P in this 'stress space', the coordinates of P being σ_1, σ_2, σ_3. The state may be written as the sum of the three vectors OP_1 (= σ_1), P_1M (= σ_2) and MP (= σ_3).

Let OH be a line, which is equally inclined to all the three axes (i.e. direction cosines of OH are $1/\sqrt{3}$, $1/\sqrt{3}$, $1/\sqrt{3}$). Projection of OP on OH is ON. Hence $ON = \sigma_1/\sqrt{3} + \sigma_2/\sqrt{3} + \sigma_3/\sqrt{3}$ and $PN^2 = \frac{1}{3}\left[(\sigma_1 - \sigma_2)^2 + (\sigma_2 - \sigma_3)^2 + (\sigma_3 - \sigma_1)^2\right]$.

Since according to Von-Mises criteria, yielding occurs when $(\sigma_1 - \sigma_2)^2 + (\sigma_2 - \sigma_3)^2 + (\sigma_3 - \sigma_1)^2 = 2\,\sigma_{YP}^2$ (from Equation (3.6)) hence yield locus may be represented by a circle of radius $PN = \sigma_{YP}\sqrt{2/3}$. It follows that the Von-Mises yield criteria may be represented in principal stress space by a circular cylinder of radius $\sigma_{YP}\sqrt{2/3}$, whose axis is the line through the origin equally inclined to the axes of coordinates, as shown in Figure 3.2(b). Yielding is unaffected by the magnitude of ON which represents a hydrostatic state of stress. ON is the vector sum of the spherical components and NP is the vector sum of the deviatoric components of the stress.

The Tresca criteria may be written $|\sigma_3 - \sigma_1| = \sigma_{YP}$ (from Equation (3.3)) and when drawn in principal stress space it is represented by a regular hexagonal cylinder which is conventionally inscribed within the Von-Mises cylinder, as shown in Figure 3.2(b). This can be also demonstrated by considering the projection of the stress states on to a plane through the origin and perpendicular to OH. This plane is called the π plane and in the original principal stress space has the equation $\sigma_1 + \sigma_2 + \sigma_3 = 0$. The positive principal axes $O\,\sigma_1$, $O\,\sigma_2$, $O\,\sigma_3$ appear in the π-plane, as shown in Figure 3.2(c), inclined to 120° to each other. When the negative axes of principal stress are included, the whole area or plane is divided into six equal sectors. The representation of Von-Mises criteria and Tresca yield criteria on π plane, are shown in Figure 3.2(c).

3.2.2 Stress--Strain Relations (Flow Rules)

3.2.2a Levy-Mises Equations

Saint Venant (1870), first proposed that the principal axes of strain increment coincided with the axes of principal stress [31]. The general relationship between strain increment and the deviatoric stresses was first introduced by Levy (1871) and independently by Von Mises (1913). These equations are now known as the Levy-Mises equations and are written as

$$\frac{d\,\varepsilon_x}{s_x} = \frac{d\,\varepsilon_y}{s_y} = \frac{d\,\varepsilon_z}{s_z} = \frac{d\,\varepsilon_{yz}}{\tau_{yz}} = \frac{d\,\varepsilon_{zx}}{\tau_{zx}} = \frac{d\,\varepsilon_{xy}}{\tau_{xy}} = d\lambda \qquad (3.7)$$

Since in Equation (3.7) elastic strains are not taken into account, the Levy-Mises relations obviously cannot be used to obtain information about 'elastic spring-back' or residual stresses, but are useful for unrestricted plastic flow.

3.2.2b Prandtl-Reuss Equations

The stress-strain relations for an elastic-perfectly plastic solid were first proposed by Prandtl (1924) for the case of plane-strain deformation. The general form of the equations was given by Reuss (1930) [31]. Prandtl's equations are an extension of the Levy-Mises equations.

Reuss assumed that the plastic strain increment at any instant, is proportional to the instantaneous stress deviation and the shear stresses, thus

$$\frac{d\,\varepsilon_x^p}{s_x} = \frac{d\,\varepsilon_y^p}{s_y} = \frac{d\,\varepsilon_z^p}{s_z} = \frac{d\,\varepsilon_{yz}^p}{\tau_{yz}} = \frac{d\,\varepsilon_{zx}^p}{\tau_{zx}} = \frac{d\,\varepsilon_{xy}^p}{\tau_{xy}} = d\lambda$$

or
$$d\,\varepsilon_{ij}^p = s_{ij}\,d\lambda \qquad (3.8)$$

$d\lambda$ is an instantaneous non negative constant of proportionality which may vary throughout loading cycle.

The equations state that a small increment of plastic strain depends on the current deviatoric stress, not on the stress increment which is required to bring it about. Also, the principal axes of stress and plastic strain increment coincide. The equation is only a statement about the ratio of the plastic strain increments in the various X, Y, Z-directions; it gives no direct information about their absolute magnitude.

3.2.3 Strain Hardening Theories

In case of strain hardening plastic materials, though elastic behavior and hence its initial yield condition are same as that of a perfectly plastic material, but once plastic flow begins, its continuation depends on the degree to which the material strain-hardens. The criteria for this continuation may then be formally stated as

$$f_c\,(J_2, J_3) = \text{Constant} \qquad \dot{f}_c > 0$$

where the constant now depends upon the condition of current yielding and, therefore, the plastic-stress history. Here J_2 and J_3 are the second and third invariants of the deviatoric stress.

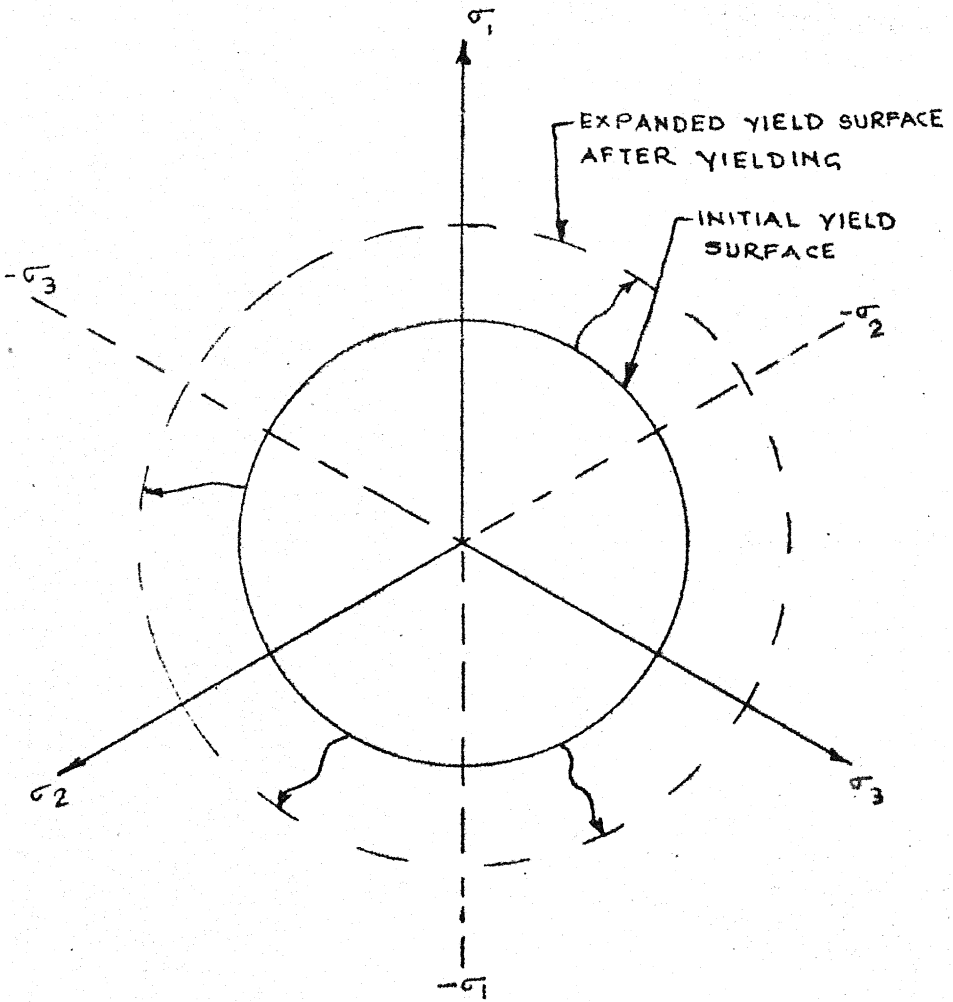

FIG. 3·3(a) ISOTROPIC-STRAIN HARDENING

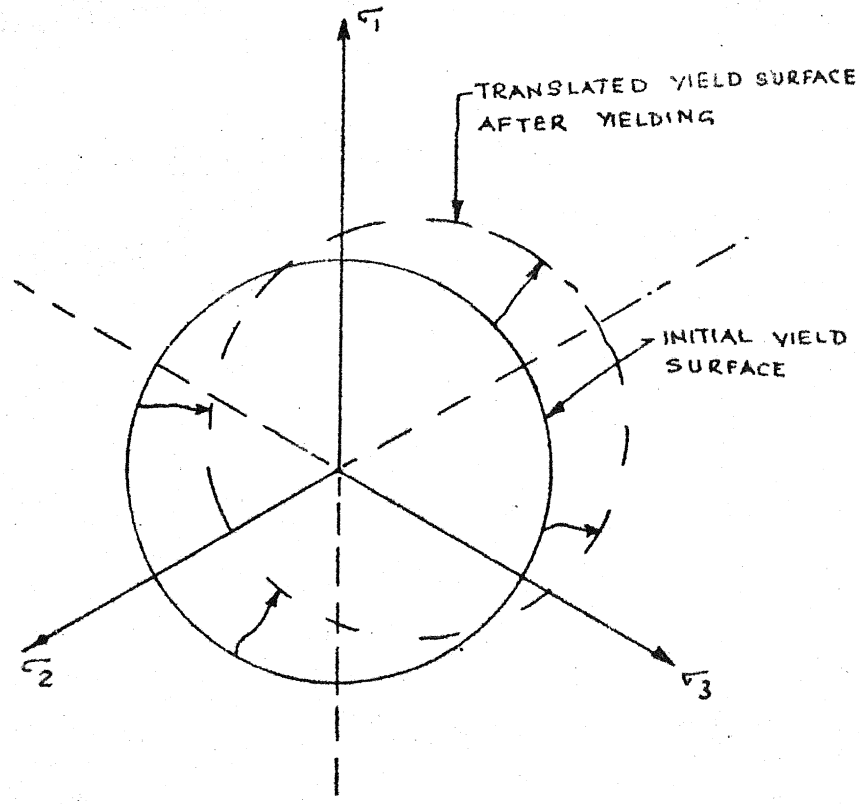

FIG. 3·3(b) KINEMATIC-STRAIN HARDENING

FIG.-3·3 TWO WIDELY ADOPTED STRAIN HARDENING THEORIES

For the development of any theory of strain hardening, a basic requirement is an empirical relation between the degree of strain hardening (represented by the current yield condition) and the plastic-strain rate. Available experimental evidence merely points up the difficulties encountered in the formulation of such a relation. The lack of significant test data has given rise to some theoretical formulations. These theories are as follows.

3.2.3a Isotropic Strain Hardening Theory

This theory is due to Hill and is based on the hypothesis that the degree of strain hardening is a function only of the total plastic work and is independent of the strain path taken to reach a given stress. Hence this theory assumes that the yield surface expands uniformly about the origin while maintaining its shape and orientation, as shown graphically in Figure 3.3(a). In other words, even if yielding occurs in tension, the effect of strain hardening on the yield stress in compression is equal to that in tension. Thus, tensile strain hardening also numerically increases the compressive yield stress and the elastic range.

3.2.3b Kinematic Strain Hardening Theory

Another theory of strain hardening by Prager is based on the use of a kinematic model. The basic assumption of this theory is that, when the material strain-hardens in tension, the elastic unloading range is double the initial tensile yield stress. Thus, tensile strain hardening

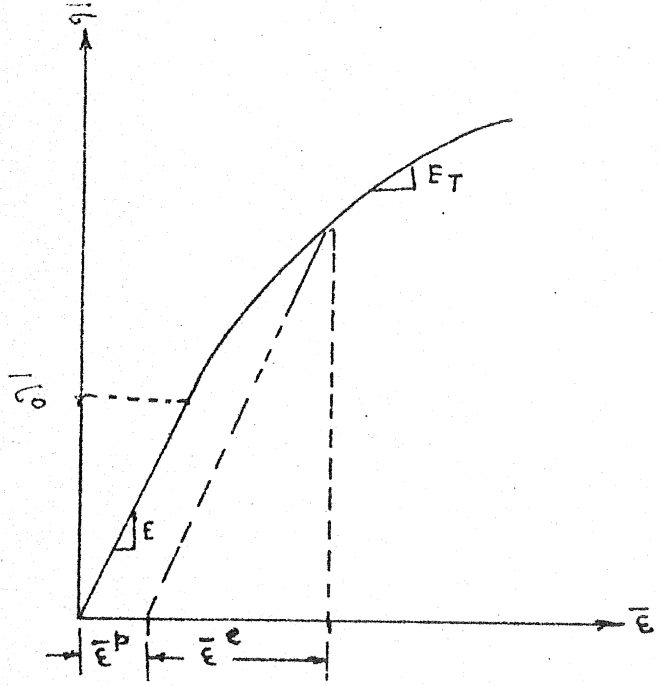

FIG. 3·4(a)

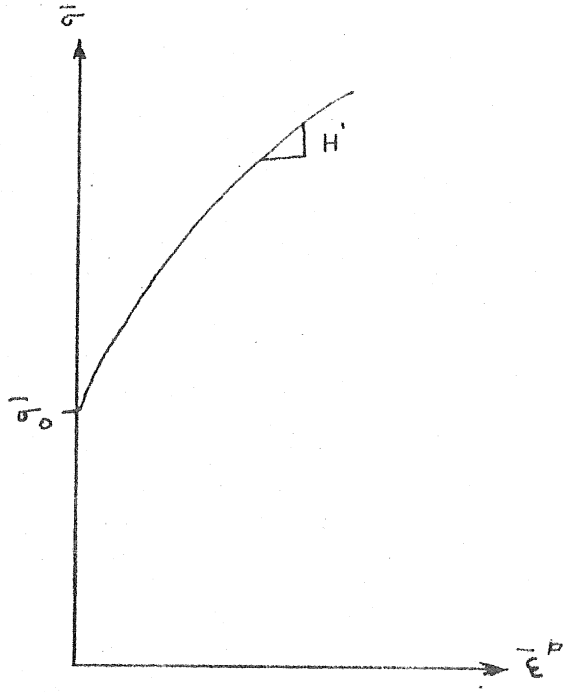

FIG. 3·4(b)

FIG.-3·4 EFFECTIVE STRESS - EFFECTIVE STRAIN RELATIONS

numerically decreases the compressive yield stress. A consequence of this theory is that the yield surface is free to translate as a rigid body while, maintaining its initial shape and size, as shown in Figure 3.3(b).

Yet another theory based on the physical concept of grain slip has been developed by Batdorf and Budiansky. This theory leads to flow laws which are mathematically difficult to handle and a few problem solutions that exist are not in particularly good agreement with experimental results [34]. Other theories combining isotropic hardening and kinematic hardening have also been proposed.

A computer program THESIS, developed during the course of this work, described latter in this chapter, makes use of isotropic strain hardening theory, i.e. same shape of stress-strain curve whether the uniaxial stress is tensile or compressive.

Figure 3.4(a) shows a typical one dimensional stress-strain curve for isotropic strain hardening material, the slope at any point in this curve is given by

$$E_T = \frac{d\bar{\sigma}}{d\bar{\varepsilon}}$$

In Figure 3.4(b), same curve is plotted between one dimensional effective plastic strain. Slope at any point on this curve is given by

$$H' = \frac{d\bar{\sigma}}{d\,\bar{\varepsilon}^p} \qquad (3.9)$$

Also from geometry, $d\bar{\varepsilon}^p = d\bar{\varepsilon} - \frac{d\bar{\sigma}}{E}$

Using the above three relations, we have

$$H' = \frac{EE_T}{E - E_T} \tag{3.10}$$

3.3 A Finite Element Approach to Thermo-Mechanical Problems

In this chapter from Section 3.4 onwards different formulations are presented for different cases of 2-D structures for elasto-plastic and thermo-plastic analysis. Von-Mises yield criteria, Prandtl-Reuss flow rule and isotropic strain hardening rule, are used during the development of these formulations.

In finite element technique, the equilibrium of an element is given by [1]

$$\int_V [B]^T \{d\sigma\}\, dV = \{dF\} \tag{3.11}$$

The most general expression for $\{d\sigma\}$ is given by,

$$\{d\sigma\} = [D]\{d\varepsilon\}, \text{ for elastic case} \tag{3.12}$$

and $$\{d\sigma\} = [D_{ep}]\{d\varepsilon\} + \{dP\} \text{ for plastic case} \tag{3.13}$$

since $$\{d\varepsilon\} = [B]\{d\delta\}$$

we have

$$\int_V [B]^T [D][B]\, dV\, \{d\delta\} = \{dF\} \quad \text{for elastic case} \tag{3.14}$$

and

$$\int_V [B]^T [D_{ep}][B]\, dV\, \{d\delta\} = \{dF\} - \int_V [B]^T \{dP\}\, dV$$

$$\text{for plastic case} \tag{3.15}$$

where $\int_V [B]^T [D] [B] \, dV$ or $\int_V [B]^T [D_{ep}] [B] \, dV$ is called element stiffness matrix and is denoted by $[K]$.

In the next four sections of this chapter, during the development of formulations for elasto-plastic and thermo-plastic analysis, the main aim is to find expressions for $[D_{ep}]$ and $\{dP\}$ for different 2-D cases.

3.4 Elasto-Plastic Analysis of Plane Stress and Axisymmetric Problems

This analysis was first developed by Pope[16] and improved by Marcal-King [33] as described in Section 3.8.2. Total strain is given by

$$\{d\varepsilon\}^t = \{d\varepsilon\}^e + \{d\varepsilon\}^p \tag{3.16}$$

where

$$\lfloor d\varepsilon \rfloor = \lfloor d\varepsilon_x \quad d\varepsilon_y \quad d\gamma_{xy} \rfloor \quad \text{for plane stress cases}$$

and

$$\lfloor d\varepsilon \rfloor = \lfloor d\varepsilon_x \quad d\varepsilon_y \quad d\gamma_{xy} \quad d\varepsilon_\theta \rfloor \quad \text{for axisymmetric cases}$$

Since

$$\{d\sigma\} = [D] \{d\varepsilon\}^e$$

hence using Equation (3.16)

$$\{d\sigma\} = [D] (\{d\varepsilon\}^t - \{d\varepsilon\}^p) \tag{3.17}$$

Denoting the left hand side of Equation (3.6) of Von-Mises yield criteria by , effective stress and

$$\bar{\sigma} = \frac{1}{\sqrt{2}} [(\sigma_x - \sigma_y)^2 + (\sigma_y - \sigma_\theta)^2 + (\sigma_\theta - \sigma_x)^2 + 6\tau_{xy}^2]^{1/2} \tag{3.18}$$

for axisymmetric case. For plane stress case $\sigma_\theta = 0$.

Yielding begins when $\bar{\sigma}$ equals to σ_{yp}.

Hence increment in effective stress

$$d\bar{\sigma} = \frac{\partial \bar{\sigma}}{\partial \sigma_x} d\sigma_x + \frac{\partial \bar{\sigma}}{\partial \sigma_y} d\sigma_y + \frac{\partial \bar{\sigma}}{\partial \tau_{xy}} d\tau_{xy} + \frac{\partial \bar{\sigma}}{\partial \sigma_\theta} d\sigma_\theta \qquad (3.19)$$

Using Equation (3.18) in Equation (3.19) and also using the expressions for deviatoric stresses, i.e.

$$S_x = \sigma_x - \sigma_{mean}$$

$$= \sigma_x - \frac{\sigma_x + \sigma_y + \sigma_\theta}{3}$$

$$= \frac{1}{3}\left[2\sigma_x - \sigma_y - \sigma_\theta\right]$$

and similarly

$$S_y = \frac{1}{3}\left[2\sigma_y - \sigma_\theta - \sigma_x\right] \qquad (3.20)$$

and $$S_\theta = \frac{1}{3}\left[2\sigma_\theta - \sigma_x - \sigma_y\right]$$

We have

$$d\bar{\sigma} = \left[\frac{\partial \bar{\sigma}}{\partial \sigma}\right]\{d\sigma\} \qquad (3.21)$$

where $$\left[\frac{\partial \bar{\sigma}}{\partial \sigma}\right] = \left[\frac{3}{2}\frac{S_x}{\bar{\sigma}} \quad \frac{3S_y}{2\bar{\sigma}} \quad \frac{3\tau_{xy}}{\bar{\sigma}} \quad \frac{3S_\theta}{2\bar{\sigma}}\right] \qquad (3.22)$$

and $\{d\sigma\}$ is the vector of stress increments.

Using Prandtl-Reuss flow rule i.e. Equation (3.8), we have

$$\begin{Bmatrix} d\varepsilon_x^p \\ d\varepsilon_y^p \\ d\varepsilon_{xy}^p \\ d\varepsilon_\theta^p \end{Bmatrix} = d\lambda \begin{Bmatrix} S_x \\ S_y \\ \tau_{xy} \\ S_\theta \end{Bmatrix} \tag{3.23}$$

Calling $d\bar{\varepsilon}^p = \frac{2}{3}\bar{\sigma}\, d\lambda$, we have Equation (3.23) as

$$\begin{Bmatrix} d\varepsilon_x^p \\ d\varepsilon_y^p \\ d\gamma_{xy}^p \\ d\varepsilon_\theta^p \end{Bmatrix} = d\bar{\varepsilon}^p \begin{Bmatrix} \frac{3}{2}\frac{S_x}{\bar{\sigma}} \\ \frac{3}{2}\frac{S_y}{\bar{\sigma}} \\ 3\frac{\tau_{xy}}{\bar{\sigma}} \\ \frac{3}{2}\frac{S_\theta}{\bar{\sigma}} \end{Bmatrix}$$

hence from Equation (3.22)

$$\{d\varepsilon\}^p = d\bar{\varepsilon}^p \left\{\frac{\partial\bar{\sigma}}{\partial\sigma}\right\} \tag{3.24}$$

Here $d\bar{\varepsilon}^p$ is called equivalent one-dimensional plastic strain.

Using Equations (3.17), (3.21) and (3.24), we have

$$d\bar{\sigma} = \left\lfloor \frac{\partial\bar{\sigma}}{\partial\sigma} \right\rfloor [D] \left(\{d\varepsilon\}^t - d\bar{\varepsilon}^p \left\{\frac{\partial\bar{\sigma}}{\partial\sigma}\right\} \right) \tag{3.25}$$

Further using one dimensional strain-hardening Equation (3.9) in Equation (3.25), we have

$$H'\, d\bar{\varepsilon}^p = \left\lfloor \frac{\partial\bar{\sigma}}{\partial\sigma} \right\rfloor [D] \left(\{d\varepsilon\}^t - d\bar{\varepsilon}^p \left\{\frac{\partial\bar{\sigma}}{\partial\sigma}\right\} \right) \tag{3.26a}$$

hence

$$d\bar{\varepsilon}^p = \lfloor W_1 \rfloor \{d\varepsilon\}^t \tag{3.26}$$

where

$$\lfloor W_1 \rfloor = \frac{\lfloor \frac{\partial \bar{\sigma}}{\partial \sigma} \rfloor [D]}{H' + \lfloor \frac{\partial \bar{\sigma}}{\partial \sigma} \rfloor [D] \{ \frac{\partial \bar{\sigma}}{\partial \sigma} \}} \tag{3.27}$$

By Equation (3.26) one can calculate $d\bar{\varepsilon}^p$, since one knows stress level for previous iteration and strain increment vector $\{d\varepsilon\}^t$ is calculated by finite element technique for a load increment. To get expression for $[D_{ep}]$, one proceeds as follows.

Using Equations (3.26) and (3.24) in Equation (3.17), we have

$$\{d\sigma\} = [D] (\{d\varepsilon\}^t - \{ \frac{\partial \bar{\sigma}}{\partial \sigma} \} \lfloor W_1 \rfloor \{d\varepsilon\}^t)$$

$$= [D_{ep}] \{d\varepsilon\}^t \tag{3.28}$$

where

$$[D_{ep}] = [D] - [D] \{ \frac{\partial \bar{\sigma}}{\partial \sigma} \} \lfloor W_1 \rfloor \tag{3.29}$$

Thus the elasto-plastic analysis of plane stress and axisymmetric geometries, in Equation (3.13) expression for $[D_{ep}]$ is given by Equation (3.29) and $\{dp\} = \{0\}$.

3.5 Elasto-Plastic Analysis of Plane Strain Problems

The formulation presented in Section 3.4, cannot be used for elasto-plastic analysis of plane strain problems, since the elimination of $d\sigma_z$ i.e. the stress increment in the third direction is to be done. Method of elimination of $d\sigma_z$ was first shown in [33], and "initial stress" solution procedure was suggested. In the present work same elimination

method of $d\sigma_z$, but 'partial stiffness solution procedure have been adopted.

Total strain is given by Equation (3.16) as

$$\begin{Bmatrix} d\varepsilon_x \\ d\varepsilon_y \\ d\gamma_{xy} \\ d\varepsilon_z \end{Bmatrix}^t = \begin{Bmatrix} d\varepsilon_x \\ d\varepsilon_y \\ d\gamma_{xy} \\ d\varepsilon_z \end{Bmatrix}^e + \begin{Bmatrix} d\varepsilon_x \\ d\varepsilon_y \\ d\gamma_{xy} \\ d\varepsilon_z \end{Bmatrix}^p \qquad (3.30)$$

In case of plane strain problems $d\varepsilon_z^t = 0$, i.e.

$$d\varepsilon_z^e + d\varepsilon_z^p = 0$$

In terms of stresses, this can be written as:

$$\frac{1}{E}[d\sigma_z - \nu(d\sigma_x + d\sigma_y)] + d\varepsilon_z^p = 0$$

or
$$d\sigma_z = \nu(d\sigma_x + d\sigma_y) - E\, d\varepsilon_z^p \qquad (3.31)$$

Writing first three strains of Equation (3.30), in terms of stresses as

$$d\varepsilon_x^t = \frac{1}{E}[d\sigma_x - \nu(d\sigma_y + d\sigma_z)] + d\varepsilon_x^p$$

$$d\varepsilon_y^t = \frac{1}{E}[d\sigma_y - \nu(d\sigma_z + d\sigma_x)] + d\varepsilon_y^p \qquad (3.32)$$

$$d\gamma_{xy}^t = \frac{1}{G}\, d\tau_{xy} + d\gamma_{xy}^p$$

Using Equation (3.31), Equation (3.32) becomes

$$d\varepsilon_x^t = \frac{1}{E}[(1-\nu^2)d\sigma_x - \nu(1+\nu)\, d\sigma_y] + \nu\, d\varepsilon_z^p + d\varepsilon_x^p$$

$$d\varepsilon_y^t = \frac{1}{E}[(1-\nu^2)d\sigma_y - \nu(1+\nu)\, d\sigma_x] + \nu\, d\varepsilon_z^p + d\varepsilon_y^p$$

$$d\gamma_{xy}^{t} = \frac{1}{G} d\tau_{xy} + d\gamma_{xy}^{p}$$

Solving these equations for stress increments, in terms of strain increments, we get

$$\begin{Bmatrix} d\sigma_x \\ d\sigma_y \\ d\tau_{xy} \end{Bmatrix} = \frac{E}{(1+\nu)(1-2\nu)} \begin{bmatrix} 1-\nu & \nu & 0 \\ \nu & 1-\nu & 0 \\ 0 & 0 & \frac{1-2\nu}{2} \end{bmatrix} \begin{Bmatrix} d\varepsilon_x^t - \nu d\varepsilon_z^p - d\varepsilon_x^p \\ d\varepsilon_y^t - \nu d\varepsilon_z^p - d\varepsilon_y^p \\ d\gamma_{xy}^t - d\gamma_{xy}^p \end{Bmatrix} \tag{3.33}$$

Substituting expressions for $d\varepsilon_x^p$, $d\varepsilon_y^p$ and $d\varepsilon_z^p$ (Equation 3.24), in the above equations, we get

$$\begin{Bmatrix} d\sigma_x \\ d\sigma_y \\ d\tau_{xy} \end{Bmatrix} = [D] \begin{Bmatrix} d\varepsilon_x^t - \frac{3}{2\bar{\sigma}}(S_x + \nu S_z) d\bar{\varepsilon}^p \\ d\varepsilon_y^t - \frac{3}{2\bar{\sigma}}(S_y + \nu S_z) d\bar{\varepsilon}^p \\ d\gamma_{xy}^t - \frac{3}{\bar{\sigma}} \tau_{xy} d\bar{\varepsilon}^p \end{Bmatrix} \tag{3.34}$$

where $[D]$ is the conventional plane strain stress-strain matrix.

To have a similarity with the formulation presented in Section 3.4, let Q be an imaginary function, such that

$$\left\lfloor \frac{\partial Q}{\partial \sigma} \right\rfloor = \left\lfloor \frac{3}{2\bar{\sigma}}(S_x + \nu S_z), \quad \frac{3}{2\bar{\sigma}}(S_y + \nu S_z), \quad \frac{3}{\bar{\sigma}} \tau_{xy} \right\rfloor \tag{3.35}$$

Thus Equation (3.34) becomes

$$\{d\sigma\} = [D] \left(\{d\varepsilon\}^t - d\bar{\varepsilon}^p \left\{ \frac{\partial Q}{\partial \sigma} \right\} \right) \tag{3.36}$$

For plane strain case, Equation (3.18) becomes

$$\bar{\sigma} = \frac{1}{\sqrt{2}} \left[(\sigma_x - \sigma_y)^2 + (\sigma_y - \sigma_z)^2 + (\sigma_z - \sigma_x)^2 + 6\tau_{xy}^2 \right]^{1/2}$$

and

$$d\bar{\sigma} = \frac{3}{2} \frac{S_x}{\bar{\sigma}} d\sigma_x + \frac{3}{2} \frac{S_y}{\bar{\sigma}} d\sigma_y + \frac{3\tau_{xy}}{\bar{\sigma}} d\tau_{xy} + \frac{3}{2} \frac{S_z}{\bar{\sigma}} d\sigma_z$$

Eliminating $d\sigma_z$ from above by using Equation (3.31), we get

$$d\bar{\sigma} = \frac{3}{2\bar{\sigma}} (S_x + \nu S_z) d\sigma_x + \frac{3}{2\bar{\sigma}} (S_y + \nu S_z) d\sigma_y + \frac{3\tau_{xy}}{\bar{\sigma}} d\tau_{xy}$$

$$- \frac{9}{4} \frac{S_z^2}{\bar{\sigma}^2} E \, d\bar{\varepsilon}^p$$

$$= \left[\frac{\partial Q}{\partial \sigma} \right] \{ d\sigma \} - \frac{9}{4} \frac{S_z^2}{\bar{\sigma}^2} E \, d\bar{\varepsilon}^p \qquad (3.37)$$

Using Equations (3.9), (3.36) and (3.37), we have

$$d\bar{\varepsilon}^p = \left[W_2 \right] \{ d\varepsilon \}^t \qquad (3.38)$$

where

$$\left[W_2 \right] = \frac{\left[\frac{\partial Q}{\partial \sigma} \right] [D]}{H' + \left[\frac{\partial Q}{\partial \sigma} \right] [D] \{ \frac{\partial Q}{\partial \sigma} \} + \frac{9}{4} \frac{S_z^2}{\bar{\sigma}^2} E} \qquad (3.39)$$

Substituting Equation (3.38) in Equation (3.36), we get

$$\{ d\sigma \} = [D_{ep}] \{ d\varepsilon \}^t$$

where $$[D_{ep}] = [D] - [D] \{ \frac{\partial Q}{\partial \sigma} \} \left[W_2 \right] \qquad (3.40)$$

Hence for a plane strain elasto-plastic analysis expression for $[D_{ep}]$ in Equation (3.13) is given by Equation (3.40) and $\{ dP \} = \{ 0 \}$.

3.6 Thermo-Plastic Analysis of Plane Stress and Axisymmetric Problems

Formulation presented in this section is developed on similar lines, as for elasto-plastic analysis of plane stress and axisymmetric problems (i.e. Section 3.4), and has been used by several authors [12,17,19].

Total strain increment for a thermo-plastic structure is given by

$$\{d\varepsilon\}^t = \{d\varepsilon\}^e + \{d\varepsilon\}^p + \{d\varepsilon\}^{Th} + \{d\varepsilon\}^{TP} \qquad (3.41)$$

where $\{d\varepsilon\}^{Th}$ is the strain increment due to change in temperature and $\{d\varepsilon\}^{TP}$ is the strain increment due to temperature dependent material properties, such as E and ν.

The expression for $\{d\varepsilon\}^p$ is again given by Equation (3.24) and expression for $\{d\varepsilon\}^{Th}$ is given by

$$\{d\varepsilon\}^{Th} = dT \begin{Bmatrix} \alpha \\ \alpha \\ 0 \\ \alpha \end{Bmatrix} = dT \{\alpha\} \qquad (3.42)$$

where dT is the temperature increment.

Expression for $\{d\varepsilon\}^{TP}$ is obtained as follows:

$$\{\varepsilon\} = [D]^{-1} \{\sigma\} = [C]\{\sigma\}$$

where

$$[C] = \begin{bmatrix} \frac{1}{E} & -\frac{\nu}{E} & 0 \\ -\frac{\nu}{E} & \frac{1}{E} & 0 \\ 0 & 0 & \frac{1}{G} \end{bmatrix} \quad \text{for plane stress case} \qquad (3.43)$$

and

$$[C] = \begin{bmatrix} \frac{1}{E} & -\frac{\nu}{E} & 0 & -\frac{\nu}{E} \\ -\frac{\nu}{E} & \frac{1}{E} & 0 & -\frac{\nu}{E} \\ 0 & 0 & \frac{1}{G} & 0 \\ -\frac{\nu}{E} & -\frac{\nu}{E} & 0 & \frac{1}{E} \end{bmatrix} \quad \text{for axisymmetric case} \tag{3.44}$$

Since

$$\{d\varepsilon\}^{TP} = \{\frac{\partial \varepsilon}{\partial T}\} dT = dT \frac{\partial [C]}{\partial T} \{\sigma\} \tag{3.45}$$

and

$$\{d\varepsilon\}^{TP} = -\frac{dT}{E} \begin{bmatrix} \dot{\frac{E}{E}} & \dot{\nu} - \frac{\nu}{E}\dot{E} & 0 \\ \dot{\nu} - \frac{\nu}{E}\dot{E} & \dot{\frac{E}{E}} & 0 \\ 0 & 0 & -2\dot{\nu} + \dot{\frac{E}{G}} \end{bmatrix} \{\sigma\}$$

for plane stress case

and

$$\{d\varepsilon\}^{TP} = -\frac{dT}{E} \begin{bmatrix} \dot{\frac{E}{E}} & \dot{\nu} - \frac{\nu}{E}\dot{E} & 0 & \dot{\nu} - \frac{\nu}{E}\dot{E} \\ \dot{\nu} - \frac{\nu}{E}\dot{E} & \dot{\frac{E}{E}} & 0 & \dot{\nu} - \frac{\nu}{E}\dot{E} \\ 0 & 0 & -2\dot{\nu} + \dot{\frac{E}{G}} & 0 \\ \dot{\nu} - \frac{\nu}{E}\dot{E} & \dot{\nu} - \frac{\nu \dot{E}}{E} & 0 & \dot{\frac{E}{E}} \end{bmatrix} \{\sigma\}$$

for axisymmetric case

(3.46)

Substituting expressions for $\{d\varepsilon\}^p$, $\{d\varepsilon\}^{Th}$ and $\{d\varepsilon\}^{TP}$ from Equations (3.24), (3.42) and (3.45) respectively, in Equation (3.41), we get

$$\{d\varepsilon\}^e = \{d\varepsilon\}^t - d\bar{\varepsilon}^p \{\frac{\partial \bar{\sigma}}{\partial \sigma}\} - dT \{\alpha\} - dT \frac{\partial [C]}{\partial T} \{\sigma\} \quad (3.47)$$

Hence incremental stress vector $\{d\sigma\}$ is given by

$$\{d\sigma\} = [D] \{d\varepsilon\}^e = [D] (\{d\varepsilon\}^t - d\bar{\varepsilon}^p \{\frac{\partial \bar{\sigma}}{\partial \sigma}\} - dT \{\alpha\} - dT \frac{\partial [C]}{\partial T} \{\sigma\}) \quad (3.48)$$

Using Equations (3.21) and (3.48), we have

$$d\bar{\sigma} = \lfloor \frac{\partial \bar{\sigma}}{\partial \sigma} \rfloor [D] (\{d\varepsilon\}^t - d\bar{\varepsilon}^p \{\frac{\partial \bar{\sigma}}{\partial \sigma}\} - dT \{\alpha\} - dT \frac{\partial [C]}{\partial T} \{\sigma\}) \quad (3.49)$$

For plastically yielded point, the one dimensional effective stress $\bar{\sigma}$ must be on the yield surface. Hence using the one dimensional strain hardening law given by Equation (3.9) and assuming now yield surface is a function of temperature also, we have

$$d\bar{\sigma} = H' d\bar{\varepsilon}^p + \frac{\partial \bar{\sigma}}{\partial T} dT \quad (3.50)$$

Using Equations (3.49) and (3.50), we get

$$d\bar{\varepsilon}^p = \lfloor W_1 \rfloor (\{d\varepsilon\}^t - dT \{\alpha\} - dT \frac{\partial [C]}{\partial T} \{\sigma\}) - \frac{\frac{\partial \bar{\sigma}}{\partial T} dT}{DENW_1} \quad (3.51)$$

where $\lfloor W_1 \rfloor$ is given by Equation (3.27) and

$$DENW_1 = H' + \lfloor \frac{\partial \bar{\sigma}}{\partial \sigma} \rfloor [D] \{\frac{\partial \bar{\sigma}}{\partial \sigma}\} \quad (3.52)$$

Using Equation (3.52) in Equation (3.48), we have expression for incremental stress vector as:

$$\{d\sigma\} = [D_{ep}]\{d\varepsilon\}^t - [D_{ep}]\left(dT\{\alpha\} + dT\frac{\partial[C]}{\partial T}\{\sigma\}\right) + \frac{[D]\left\{\frac{\partial \bar{\sigma}}{\partial \sigma}\right\}\frac{\partial \bar{\sigma}}{\partial T}dT}{DENW_1} \tag{3.53}$$

where $[D_{ep}]$ is given by Equation (3.29).

Comparing Equation (3.53) with general expression for $\{d\sigma\}$ given by Equation (3.13), one gets expression for $[D_{ep}]$ as given by Equation (3.29), and expression for $\{dP\}$ as

$$\{dP\} = -[D_{ep}]\left(dT\{\alpha\} + dT\frac{\partial[C]}{\partial T}\{\sigma\}\right) + \frac{[D]\left\{\frac{\partial \bar{\sigma}}{\partial \sigma}\right\}\frac{\partial \bar{\sigma}}{\partial T}dT}{DENW_1} \tag{3.54}$$

This can be noted that for thermo-plastic analysis, further load increment depends upon stress field from the previous iteration and hence it is absolutely necessary to calculate stress field very accurately.

3.7 Thermo-Plastic Analysis of Plane Strain Problems

The welding of long plates or cylinders is essentially a plane strain case, as explained in Chapter 6. In [20] this case has been simplified by postulating an expression for $d\bar{\varepsilon}^p$. Some authors, such as in [7,17], keep a separate identity of stress increment in z-direction for this case also. In present work, the elimination concept of Section 3.5 for plane strain elasto-plastic analysis has been extended for thermo-plastic analysis of plane strain problems. This again makes stiffness as well as further load increment a function of previous stress level and hence determination of stress level in every step very accurately is the must.

as small error in stress level keeps propagating and diverges through further iterations.

The total strain increment

is given by Equation (3.41), which in expanded form, is

$$\begin{Bmatrix} d\sigma_x \\ d\varepsilon_y \\ d\gamma_{xy} \\ d\varepsilon_z \end{Bmatrix}^t = \begin{Bmatrix} d\varepsilon_x \\ d\varepsilon_y \\ d\gamma_{xy} \\ d\varepsilon_z \end{Bmatrix}^e + \begin{Bmatrix} d\varepsilon_x \\ d\varepsilon_y \\ d\gamma_{xy} \\ d\varepsilon_z \end{Bmatrix}^p + \begin{Bmatrix} d\varepsilon_x \\ d\varepsilon_y \\ d\gamma_{xy} \\ d\varepsilon_z \end{Bmatrix}^{Th} + \begin{Bmatrix} d\varepsilon_x \\ d\varepsilon_y \\ d\gamma_{xy} \\ d\varepsilon_z \end{Bmatrix}^{TP} \tag{3.55}$$

For a plane strain case $d\varepsilon_z^t = 0$, hence

$$d\varepsilon_z^e + d\varepsilon_z^p + d\varepsilon_z^{Th} + d\varepsilon_z^{TP} = 0 \tag{3.56}$$

Substituting $d\varepsilon_z^e$ in terms of stresses from Hooke's law, we have

$$\frac{1}{E}\left[d\sigma_z - \nu\,(d\sigma_x + d\sigma_y)\right] + d\varepsilon_z^p + d\varepsilon_z^{Th} + d\varepsilon_z^{TP} = 0$$

$$\text{or} \quad d\sigma_z = \nu\,(d\sigma_x + d\sigma_y) - E(d\varepsilon_z^p + d\varepsilon_z^{Th} + d\varepsilon_z^{TP}) \tag{3.57}$$

Also rest of the relations of Equation (3.55) can be written in terms of stresses as

$$d\varepsilon_x^t = \frac{1}{E}\left[d\sigma_x - \nu\,(d\sigma_y + d\sigma_z)\right] + d\varepsilon_x^p + d\varepsilon_x^{Th} + d\varepsilon_x^{TP}$$

$$d\varepsilon_y^t = \frac{1}{E}\left[d\sigma_y - \nu\,(d\sigma_z + d\sigma_x)\right] + d\varepsilon_y^p + d\varepsilon_y^{Th} + d\varepsilon_y^{TP} \tag{3.58}$$

$$d\gamma_{xy}^t = \frac{1}{G}\,d\tau_{xy} + d\gamma_{xy}^p + d\gamma_{xy}^{TP} \quad (\because\ d\gamma_{xy}^{Th} = 0)$$

Substituting for $d\sigma_z$ from Equation (3.57) and solving for incremental stresses in terms of incremental strains, we get

$$\begin{Bmatrix} d\sigma_x \\ d\sigma_y \\ d\tau_{xy} \end{Bmatrix} = \frac{E}{(1+\nu)(1-2\nu)} \begin{bmatrix} 1-\nu & \nu & 0 \\ \nu & 1-\nu & 0 \\ 0 & 0 & \frac{1-2\nu}{2} \end{bmatrix}$$

$$\begin{Bmatrix} d\varepsilon_x^t - (d\varepsilon_x^p + \nu\, d\varepsilon_z^p) - d\varepsilon_x^{Th} - d\varepsilon_x^{TP} \\ d\varepsilon_y^t - (d\varepsilon_y^p + \nu\, d\varepsilon_z^p) - d\varepsilon_y^{Th} - d\varepsilon_y^{TP} \\ d\gamma_{xy}^t - d\gamma_{xy}^p - d\gamma_{xy}^{TP} \end{Bmatrix}$$

$$- \frac{E\nu}{(1+\nu)(1-2\nu)} (d\varepsilon_z^{Th} + d\varepsilon_z^{TP}) \begin{Bmatrix} 1 \\ 1 \\ 0 \end{Bmatrix} \qquad (3.59)$$

Substituting expressions for $d\varepsilon_x^p$, $d\varepsilon_y^p$ and $d\varepsilon_z^p$ from Equation (3.24), Equation (3.59) becomes

$$\begin{Bmatrix} d\sigma_x \\ d\sigma_y \\ d\tau_{xy} \end{Bmatrix} = [D] \begin{Bmatrix} d\varepsilon_x^t - \frac{3}{2\bar{\sigma}} (S_x + \nu S_z) d\bar{\varepsilon}^p - d\varepsilon_x^{Th} - d\varepsilon_x^{TP} \\ d\varepsilon_y^t - \frac{3}{2\bar{\sigma}} (S_y + \nu S_z) d\bar{\varepsilon}^p - d\varepsilon_y^{Th} - d\varepsilon_y^{TP} \\ d\gamma_{xy}^t - \frac{3}{\bar{\sigma}} \tau_{xy}\, d\bar{\varepsilon}^p - d\gamma_{xy}^{TP} \end{Bmatrix}$$

$$- \frac{E\nu}{(1+\nu)(1-2\nu)} (d\varepsilon_z^{Th} + d\varepsilon_z^{TP}) \{A\} \qquad (3.60)$$

where

$$\{A\} = \begin{Bmatrix} 1 \\ 1 \\ 0 \end{Bmatrix}$$

Using the notation defined in Equation (3.35), we have

$$\{d\sigma\} = [D]\left(\{d\varepsilon\}^t - d\bar{\varepsilon}^p \left\{\frac{\partial Q}{\partial \sigma}\right\} - \{d\varepsilon\}^{Th} - \{d\varepsilon\}^{TP}\right) - \frac{E\nu}{(1+\nu)(1-2\nu)}\left(d\varepsilon_z^{Th} + d\varepsilon_z^{TP}\right)\{A\} \tag{3.61}$$

Using Equations (3.50), (3.38) and (3.61), we have

$$d\bar{\varepsilon}^p = \lfloor W_2 \rfloor \left(\{d\varepsilon\}^t - \{d\varepsilon\}^{Th} - \{d\varepsilon\}^{TP}\right) - \frac{\left(\frac{E\nu}{(1+\nu)(1-2\nu)} \left\lfloor \frac{\partial Q}{\partial \sigma} \right\rfloor \{A\} + \frac{3}{2}\frac{S_z}{\bar{\sigma}} E\right)}{DENW_2}\left(d\varepsilon_z^{Th} + d\varepsilon_z^{TP}\right) - \frac{\frac{\partial \bar{\sigma}}{\partial T} dT}{DENW_2} \tag{3.62}$$

where $\lfloor W_2 \rfloor$ is defined by Equation (3.40) and

$$DENW_2 = H' + \left\lfloor \frac{\partial Q}{\partial \sigma} \right\rfloor [D] \left\{\frac{\partial Q}{\partial \sigma}\right\} + \frac{9}{4}\frac{S_z^2}{\bar{\sigma}^2} E \tag{3.63}$$

Using Equation (3.62) in Equation (3.61), we have

$$\{d\sigma\} = [D_{ep}]\left(\{d\varepsilon\}^t - \{d\varepsilon\}^{Th} - \{d\varepsilon\}^{TP}\right) + \frac{[D]\left\{\frac{\partial Q}{\partial \sigma}\right\}\frac{\partial \bar{\sigma}}{\partial T} dT}{DENW_2} - \frac{E}{(1+\nu)}\left[-[D]\left\lfloor \frac{\partial Q}{\partial \sigma} \right\rfloor \frac{\frac{3}{2}\frac{S_z}{\bar{\sigma}}}{DENW_2} + \frac{\nu}{(1-2\nu)}\{A\}\right]\left(d\varepsilon_z^{Th} + d\varepsilon_z^{TP}\right) \tag{3.64}$$

Again comparing Equations (3.13) and (3.64), we have expression for $[D_{ep}]$ as given by Equation (3.15) and

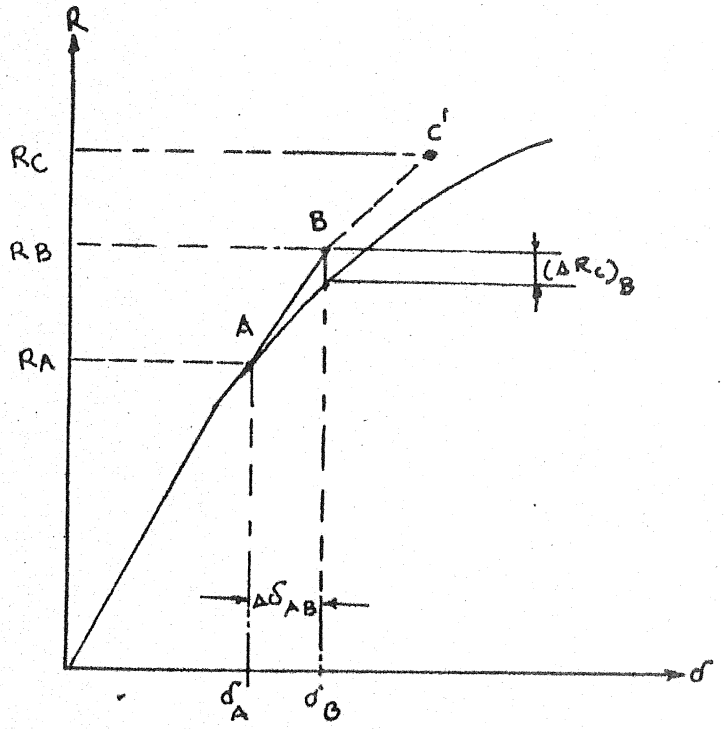

FIG. 3·5(a) LOAD VERSUS DISPLACEMENT PLOT OF SAMPLING POINT

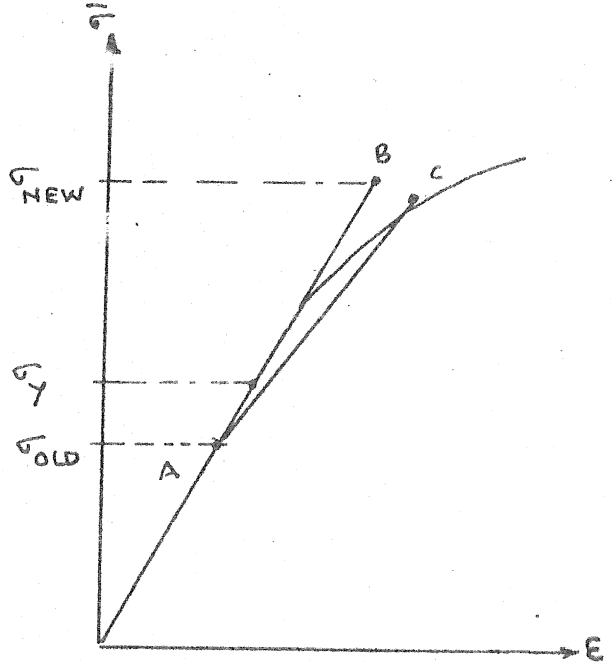

FIG. 3·5(b) ELASTIC-PLASTIC TRANSITION OF A SAMPLING POINT

FIG.- 3·5 GRAPHIC REPRESENTATION OF TIME STEPPING SOLUTION ALGORITHM

$$\{dP\} = -[D_{ep}]\left(\begin{bmatrix}1\\1\\0\end{bmatrix}^T \alpha\, dT + \frac{\partial [C]}{\partial T} dT \{\sigma\}\right) + \frac{[D]\left\{\frac{\partial Q}{\partial \sigma}\right\} \frac{\partial \bar{\sigma}}{\partial T} dT}{DENW_2}$$

$$- \frac{E}{(1+\nu)}\left[-[D]\left\{\frac{\partial Q}{\partial \sigma}\right\} \frac{\frac{3}{2}\frac{S_z}{\bar{\sigma}}}{DENW_2} + \frac{\nu}{(1-2\nu)}\{A\}\right](d\varepsilon_z^{Th} + d\varepsilon_z^{TP}) \tag{3.65}$$

3.8 An Iterative Solution Algorithm

Four sets of formulations presented in Sections 3.4 through 3.7 can be used for elasto-plastic and thermo-plastic analysis of 2-D structures. Different solution procedures are available in literatures. An iterative solution algorithm adopted in this work, for solving nonlinear equations, is presented here [6,27,33].

3.8.1 A Solution Step

A typical step of the solution is described with the aid of Figure 3.5(a), which is a single degree of freedom representation of an actual multi degree of freedom problem. Let under loads $\{R\}_A$, the correct displacements $\{\delta\}_A$ and structure tangent stiffness $[K]_A$ are known. Displacements produced by the next load increment are computed as

$$[K]_A \{\Delta\delta\}_{AB} = \{\Delta R\}_{AB} = \{R\}_B - \{R\}_A \tag{3.66}$$

and

$$\{\delta\}_B = \{\delta\}_A + \{\Delta\delta\}_{AB} \tag{3.67}$$

Stresses, strains and tangent stiffness must now be updated. Displacements $\{\Delta d\}$ of an element are extracted from $\{\Delta\delta\}_{AB}$. Then, for each sampling point in the element,

total strain increment $\{\Delta\varepsilon\}^t = [B]\ \{\Delta d\}$ is computed. Once $\{\Delta\varepsilon\}^t$ are known following quantities are computed from different expressions derived earlier.

Expressions for $d\bar{\varepsilon}^p$ for all the four cases considered in Sections 3.4 to 3.7 can be written in the form

$$d\bar{\varepsilon}^p = \lfloor f_1 \rfloor \{d\varepsilon\}^t + f_2\, dT \tag{3.68}$$

where for plane stress and axisymmetric elasto-plastic case

$$\lfloor f_1 \rfloor = \lfloor W_1 \rfloor \quad \text{and} \quad f_2 = 0 \tag{3.69}$$

for plane strain, elasto-plastic case

$$\lfloor f_1 \rfloor = \lfloor W_2 \rfloor \quad \text{and} \quad f_2 = 0 \tag{3.70}$$

for plane stress and axisymmetric thermo-plastic case

$$\lfloor f_1 \rfloor = \lfloor W_1 \rfloor$$

$$\text{and} \quad f_2 = -\lfloor W_1 \rfloor \left(\{\alpha\} + \frac{\partial [C]}{\partial T}\{\sigma\}\right) - \frac{\frac{\partial \bar{\sigma}}{\partial T}}{DENW_1} \tag{3.71}$$

for plane strain thermo-plastic case

$$\lfloor f_1 \rfloor = \lfloor W_2 \rfloor \quad \text{and}$$

$$f_2 = -\lfloor W_2 \rfloor \left(\{\alpha\} + \frac{\partial [C]}{\partial T}\{\sigma\}\right)$$

$$- \frac{\left(\frac{E\nu}{(1+\nu)(1-2\nu)} \left\lfloor \frac{\partial Q}{\partial \sigma} \right\rfloor \{A\} + \frac{3}{2}\frac{S_z}{\bar{\sigma}} E\right)}{DENW_2}$$

$$\left(\alpha - \frac{1}{E}\left(\dot{\nu} - \frac{\nu}{E}\dot{E}\right)(\sigma_x + \sigma_y) - \frac{\dot{E}}{E^2}\sigma_z^2\right) - \frac{\frac{\partial \bar{\sigma}}{\partial T}}{DENW_2} \tag{3.72}$$

Using Equation (3.68), we have

$$\Delta\bar{\varepsilon}^p = \int_a^b \lfloor f_1 \rfloor \{d\varepsilon\}^t + \int_a^b f_2 \, dT$$

$$\approx \lfloor f_1 \rfloor_a \{\Delta\varepsilon\}^t + f_{2a} \Delta T \tag{3.73}$$

Also from the flow rule given by Equation (3.24)

$$\{\Delta\varepsilon_p\} = \int_a^b \{\frac{\partial \bar{\sigma}}{\partial \sigma}\} \, d\bar{\varepsilon}^p \approx \{\frac{\partial \bar{\sigma}}{\partial \sigma}\}_a \Delta\bar{\varepsilon}_p \tag{3.74}$$

Also expression for $\{d\sigma\}$ for all the four cases considered in Sections 3.4 to 3.7 can be written in the form

$$\{d\sigma\} = [D_{ep}] \{d\varepsilon\}^t + \{f_3\} \, dT \tag{3.75}$$

where for plane stress, plane strain and axisymmetric elasto-plastic cases

$$\{f_3\} = \{0\} \tag{3.76}$$

for plane stress and axisymmetric thermo-plastic cases

$$\{f_3\} = -[D_{ep}] \left(\{\alpha\} + \frac{\partial [C]}{\partial T} \{\sigma\} \right) + \frac{[D] \{\frac{\partial \bar{\sigma}}{\partial \sigma}\} \frac{\partial \bar{\sigma}}{\partial T}}{DENW_1} \tag{3.77}$$

for plane strain thermo-plastic case

$$\{f_3\} = -[D_{ep}] \left(\{\alpha\} + \frac{\partial [C]}{\partial T} \{\sigma\} \right) + \frac{[D] \{\frac{\partial Q}{\partial \sigma}\} \frac{\partial \bar{\sigma}}{\partial T}}{DENW_2}$$

$$- \frac{E}{(1+\nu)} \left[- [D] \{\frac{\partial Q}{\partial \sigma}\} \frac{\frac{3}{2} \frac{S_z}{\bar{\sigma}}}{DENW_2} + \frac{\nu}{(1-2\nu)} \{A\} \right.$$

$$\left. (\alpha - \frac{1}{E}(\dot{\nu} - \frac{\nu}{E} \dot{E})(\sigma_x + \sigma_y) - \frac{\dot{E}}{E^2} \sigma_z^2 \right) \tag{3.78}$$

So using Equation (3.75), we have

$$\{\Delta\sigma\} = \int_a^b [D_{ep}] \{d\varepsilon\}^t + \int_a^b \{f_3\}\, dT$$

$$\cong [D_{ep}]_a \{d\varepsilon\}^t + \{f_3\}_a\, dT \qquad (3.79)$$

Then values of $\bar{\varepsilon}_p$, $\{\varepsilon_p\}$ and $\{\sigma\}$ are updated by adding corresponding increment to their previous values. The updated $\bar{\sigma}$ can be computed from the updated $\{\sigma\}$. Also from the updated $\bar{\varepsilon}_p$, H' can be calculated from the input material properties. Now for the current stress level and material properties, $[D_{ep}]$ and $\{dP\}$ are calculated from the different equations given above depending upon the case. Hence updated stiffness matrix and load increment for the point B in Figure 3.5(a) are calculated. In this solution algorithm one has to keep records of $\bar{\varepsilon}_p$, $\{\varepsilon_p\}$, $\bar{\sigma}$ and $\{\sigma\}$ at each sampling point in each element and store the updated $\{\delta\}$ if structure displacements are needed.

3.8.2 Elastic-Plastic Transition

When a sampling point makes the transition from elastic to plastic within a single load increment, one has to switch on from equations of elasticity to equations of plasticity. Hence a correction is needed. In the present work the method adopted is as suggested in [36]. In this method when a sampling point goes to plastic state in a single load increment, a factor 'm' is calculated by

$$m = \frac{\sigma_{YP} - \sigma_{old}}{\sigma_{new} - \sigma_{old}} \qquad (3.80)$$

where σ_{old} is the previous elastic stress and σ_{new} is the present elastic stress which is more than yield stress σ_{YP}. Then $[D_{ep}]$ is calculated by

$$[D_{ep}] = [D] - (1 - m)[D]\{\frac{\partial \bar{\sigma}}{\partial \sigma}\}\lfloor W_1 \rfloor \qquad (3.81)$$

for plane stress and axisymmetric cases and

$$[D_{ep}] = [D] - (1 - m)[D]\{\frac{\partial Q}{\partial \sigma}\}\lfloor W_2 \rfloor \qquad (3.82)$$

for plane strain case.

Hence (1-m) represents a fraction of partial yielding of sampling point. This $[D_{ep}]$ is used to calculate stiffness matrix. Displacements calculated by this $[D_{ep}]$, will be nearer to the yield surface, say point 'C' in Figure 3.5(b). Hence more iterations may be required to bring all the stresses on the yield surface, by perturbing value of 'm' accordingly. After the convergence, Equations (3.68) to (3.79) are used to calculate different parameters, replacing $\Delta\varepsilon^t$ by (1-m) $\Delta\varepsilon^t$ and also $\Delta\varepsilon^{Th}$ by (1-m) $\Delta\varepsilon^{Th}$. It may be noted that this replacement is different than suggested in Cook [3], where replacement $\Delta\varepsilon^t$ by (1-m) $\Delta\varepsilon^t$ is suggested only. Present author found this replacement is incorrect, since pseudo thermal strain should also be subtracted from total strain, beforemultiplying by the fraction of partial yielding. Also while calculating unbalance plastic load $\{dP\}$, this vector should be again multiplied by (1-m).

3.8.3 Calculation of Unbalance Force

A drift appears, when upper solution procedure is adopted, as shown in Figure 3.5(a). To avoid this, following method has been used.

Upon reaching R_B, the computed displacement δ_B is smaller than the true value, hence the resulting stresses are smaller too and are not adequate to resist the applied load R_B. If a corrective load ΔR_c were added to ΔR, the computed δ_B would be larger and more nearly the true value. The corrective load, which is also called unbalanced force, is the difference between applied loads and resistance produced corresponding to the calculated displacements. Hence

$$\{\Delta R\}_{cor} = \{R\} - \sum_{e} \int_{Vol} [B]^T \{\sigma\}\, dV \qquad (3.83)$$

where the summation extends overall elements of the structure. Forces $\{R\}$ and stresses $\{\sigma\}$ are those at the end of a step. Correction $\{\Delta R\}_{cor}$ is applied in the subsequent step and hence equilibrium equations for step B to C is

$$[K]_B \{\Delta\delta\}_{BC} = \{\Delta R\}_{BC} + \{\Delta R\}_{cor,B}$$

There are other methods available such as Newton Raphson and modified Newton Raphson, to avoid drifts. These methods ask for more number of internal iterations, within a load increment. But in the present work it is seen that just by adding unbalance force to the next iteration, it is possible to follow yield surface closely, provided load increment is kept below a particular value. For example, in case of thermal load, temperature increment of a sampling

point should not be more than 50°C in one load increment step. But it is necessary to do internal iterations to bring a sampling point on the yield surface, whenever there is a transition from elastic to plastic stage, as explained in Section 3.6.2.

3.9 A Computer Program and Check Out Problems

Depending upon the formulation presented in Section 3.4, present author developed a computer program PLSTIC before this work and was reported along with the check out problems in [27]. During the course of this work same program was modified for elastic-plastic plane strain case (formulation 3.5), thermo-plastic plane stress and axisymmetric case (formulation 3.6) and thermo-plastic plane strain case (formulation 3.7). This computer program THESIS (THErmo-plastic analySIS) was tested for number of sample problems to check its capability. Some of these sample problems are presented here to demonstrate some of the analysis capabilities of the program THESIS and to show the accuracy of the solutions and hence comparisons are made with the results of other authors, wherever available.

3.9.1 Thick Cylinder Under Internal Pressure (A Plane Strain Case)

This problem was solved to test elasto-plastic plane strain analysis capability (corresponds to formulation 3.5) of THESIS. For this a cylinder under internal pressure was solved for plane strain elasto-plastic case. The cylinder

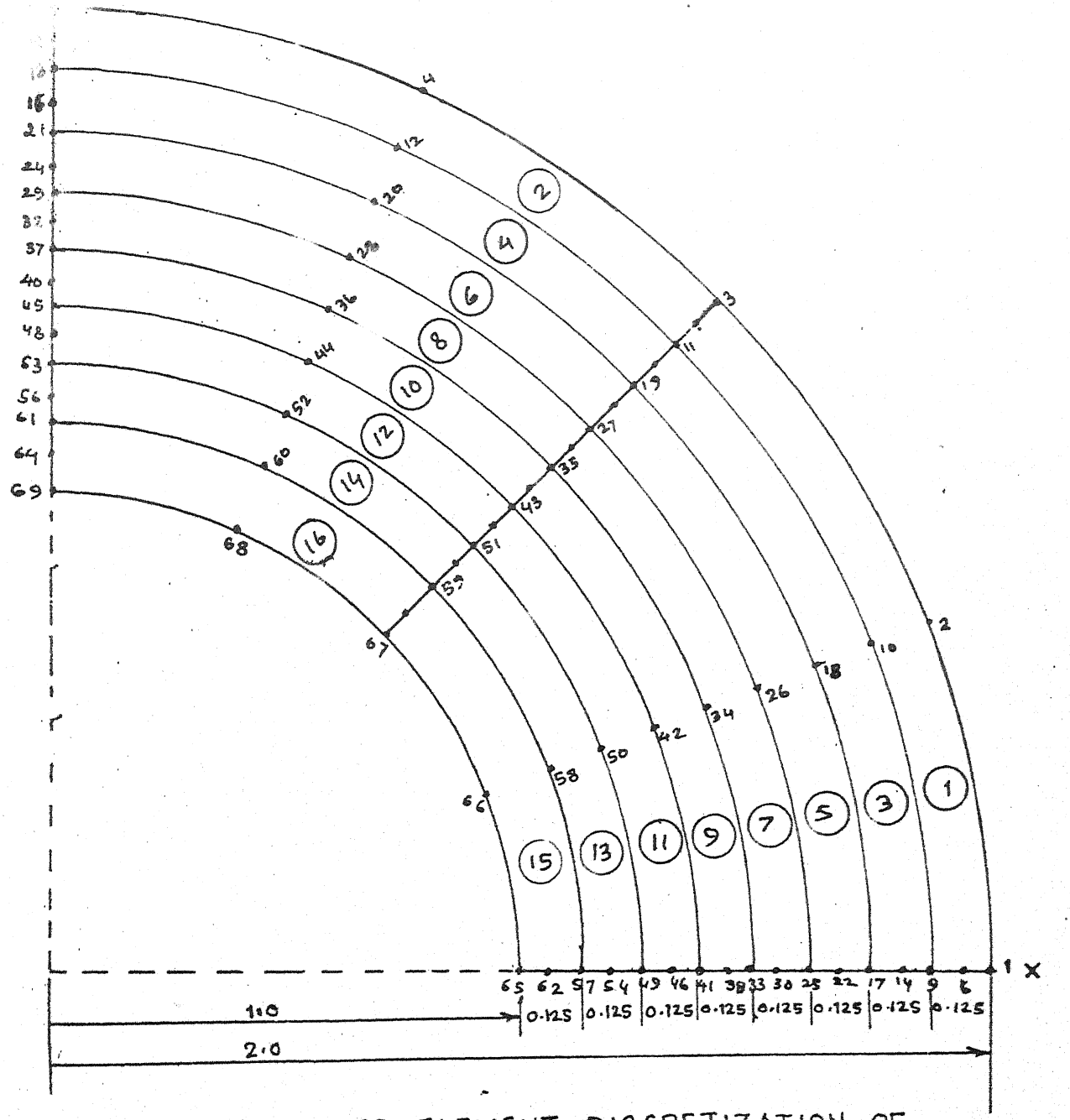

FIG.-3·6 FINITE ELEMENT DISCRETIZATION OF CYLINDER FOR ELASTIC-PLASTIC ANALYSIS (A PLANE STRAIN CASE)

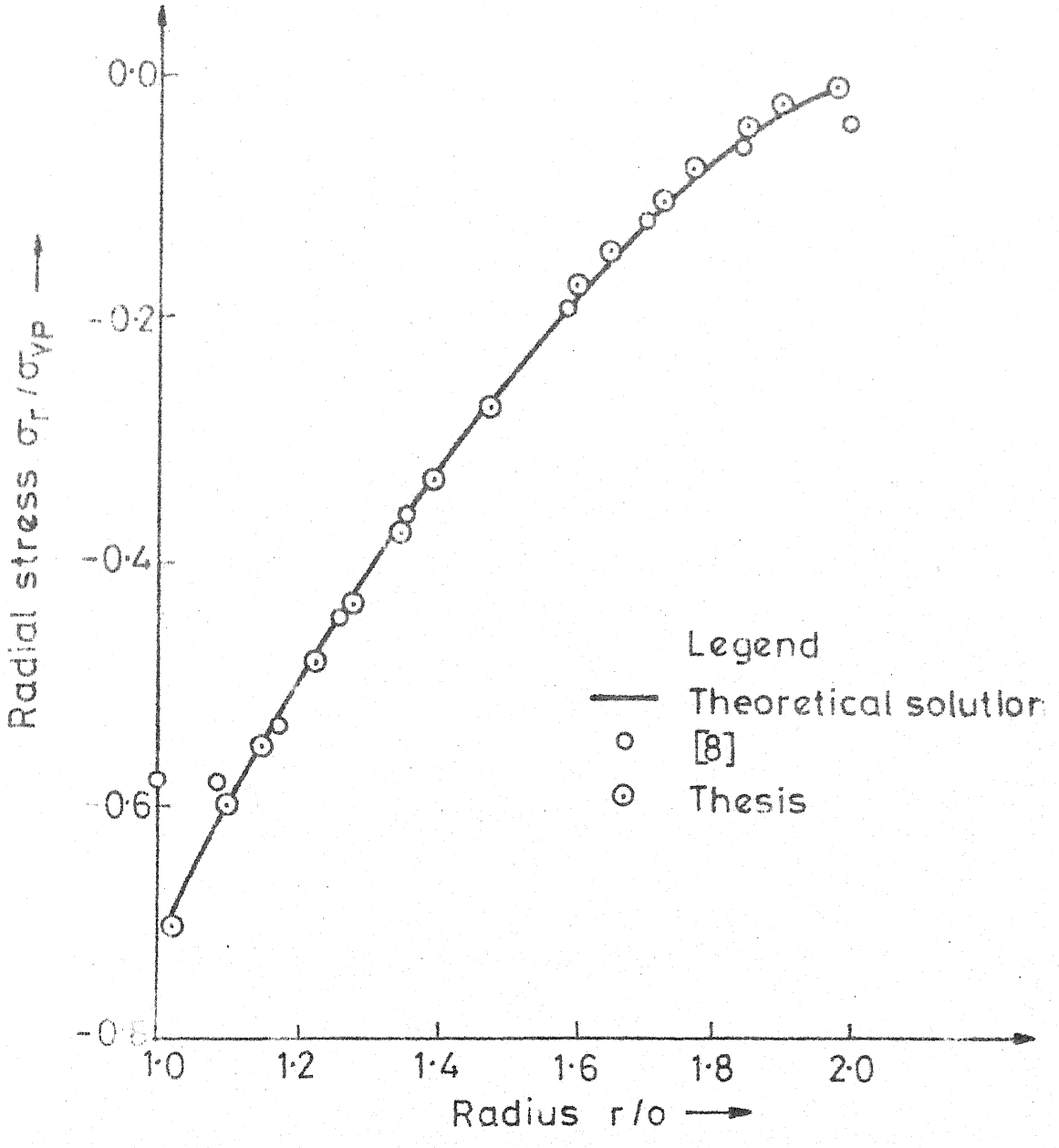

FIG. 3·7 RADIAL STRESS VARIATION OF ELASTO-PLASTIC PLANE STRAIN CYLINDER

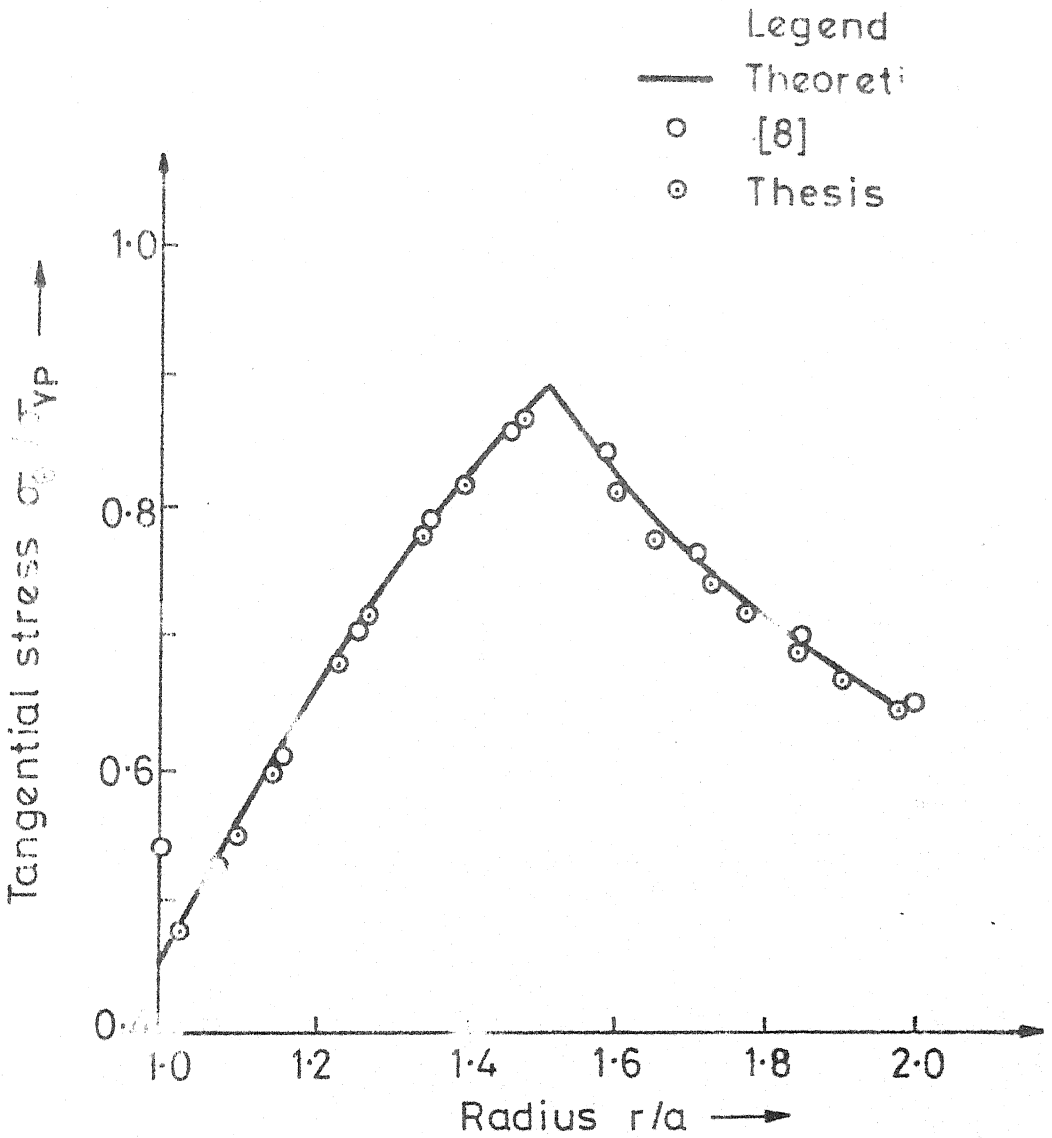

FIG·3·8 TANGENTIAL STRESS VARIATION OF ELASTO-PLASTIC PLANE STRAIN CYLINDER

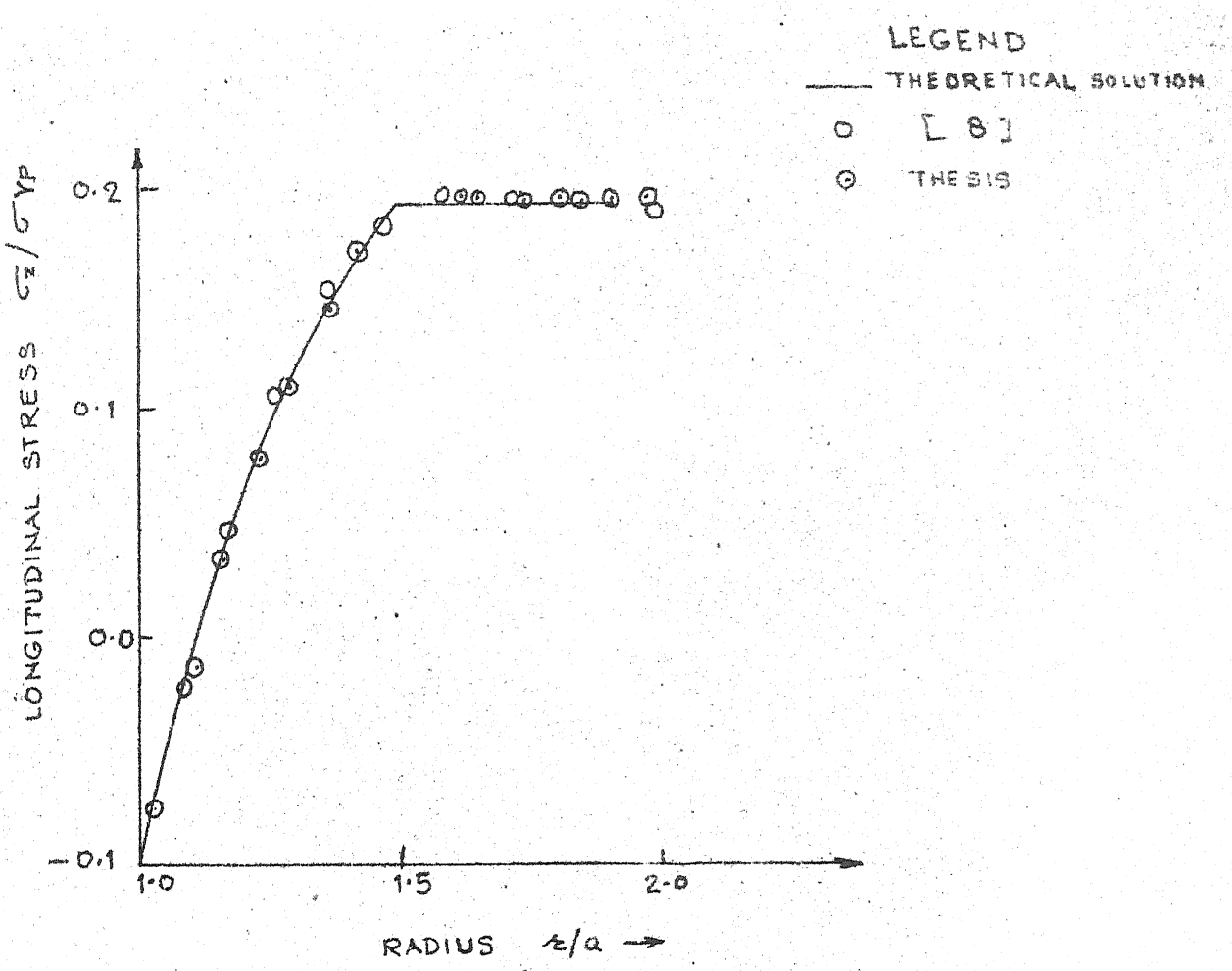

FIG.– 3.9. LONGITUDINAL STRESS VARIATION OF ELASTO-PLASTIC PLANE STRAIN CYLINDER

was characterized by the following non-dimensional parameters:

$$\text{outer radius/inner radius} = 2$$

$$\nu = 0.3$$

$$\text{yield stress/E} = 0.002$$

In Figure 3.6 finite element discretization is shown for this geometry and Figures 3.7 to 3.9 show the variations of σ_r, σ_θ and σ_z with radius, when plastic zone radius is equal to 1.5 times the inner radius. In the same figures, a comparison has been made with the results quoted for the same problem in [8]. Figures show a good agreement of different parameters except near to the inner radius, where present program computes a much better results than in [8]. This can judged from the variation of σ_r, where σ_r must be equal to -p at the inner surface to satisfy natural boundary condition. Ref. [8] failed to reproduce this boundary condition, whereas present program followed this condition with smooth variations of σ_r, σ_θ and σ_z.

3.9.2 Thick Cylinder Under Radial Temperature Gradient (Plane Stress as well as Axisymmetric Case)

The results for this problem are presented here to show the solving capability of program THESIS for thermo-plastic analysis of plane stress and axisymmetric bodies.

Theoretical solution of this problem is quoted in [2]. The problem is characterised as a thick cylinder of 2.25 inner to outer radii ratio, is under radial temperature gradient. The radial temperature drop is increased from 0°C to a value for which $\frac{E \alpha \Delta T}{2 \sigma_{yp}} = 6.0$.

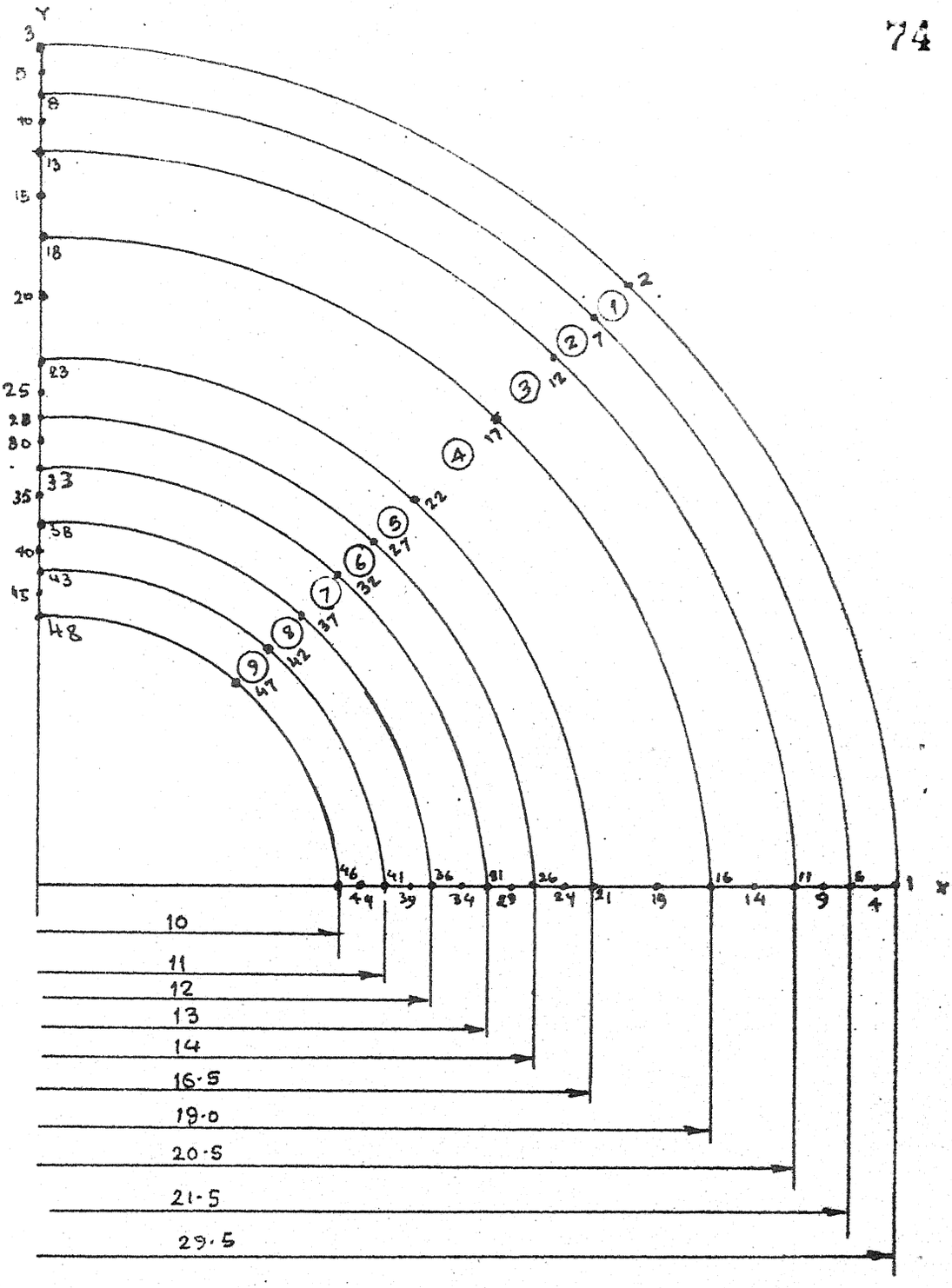

FIG. - 3·10 DISCRETIZATION OF CYLINDER FOR PLANE STRESS THERMO-PLASTIC ANALYSIS

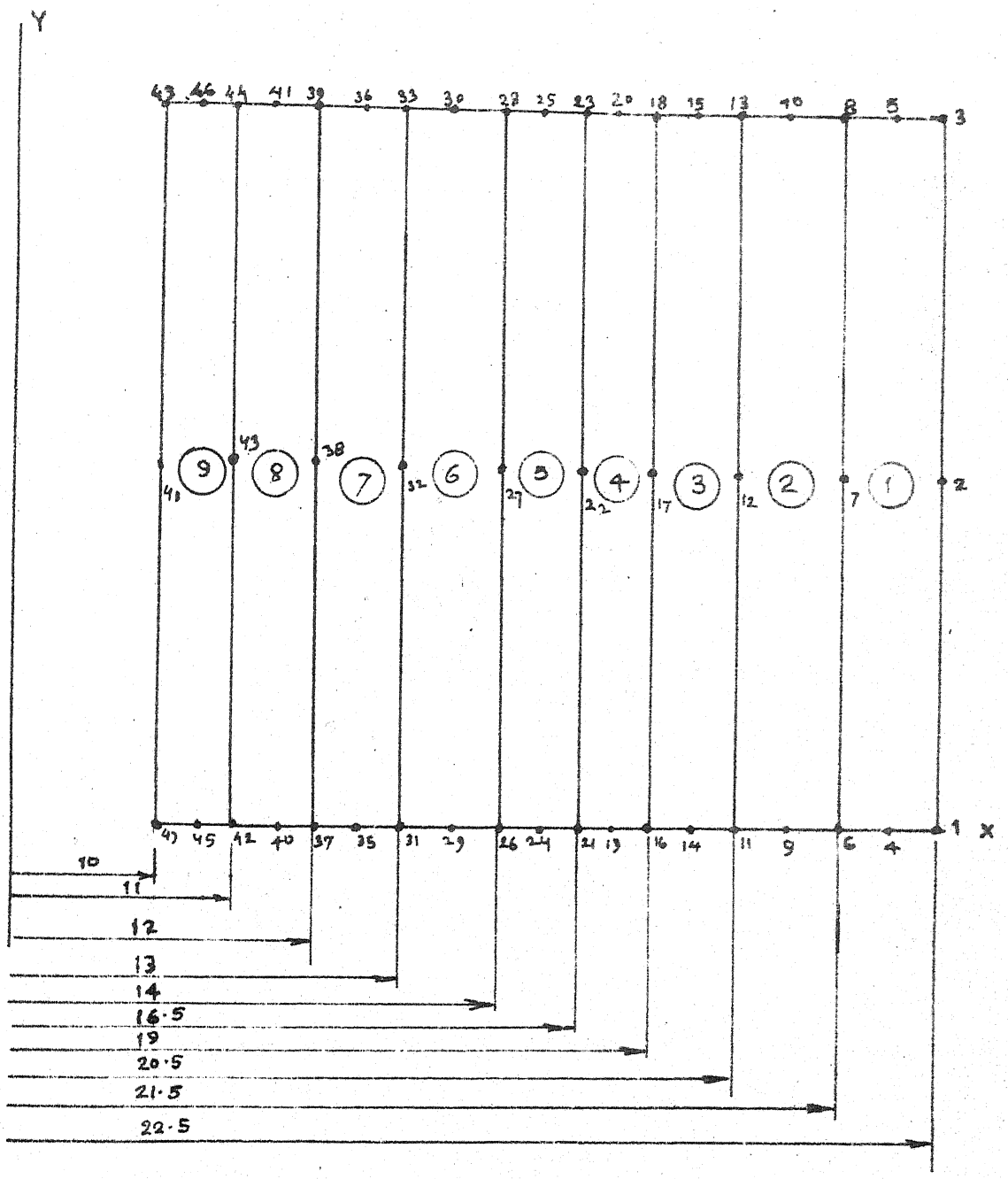

FIG.-3·11 DISCRETIZATION OF CYLINDER FOR AXISYMMETRIC THERMO-PLASTIC ANALYSIS

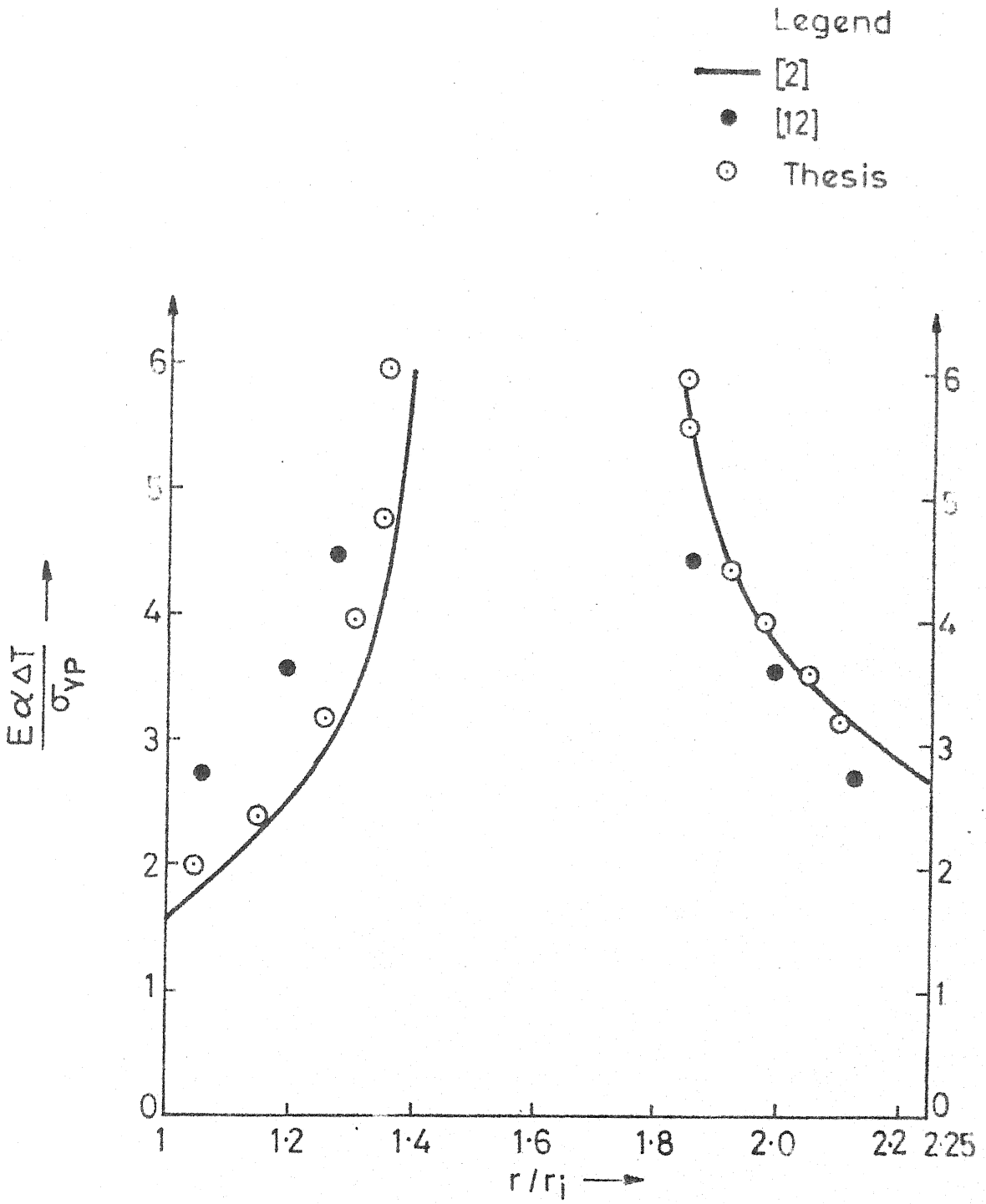

FIG.3·12 THE GROWTH OF PLASTIC ZONES IN [illegible]ISC WITH A VERY SLOWLY INCREASING R[illegible]L HEAT FLOW

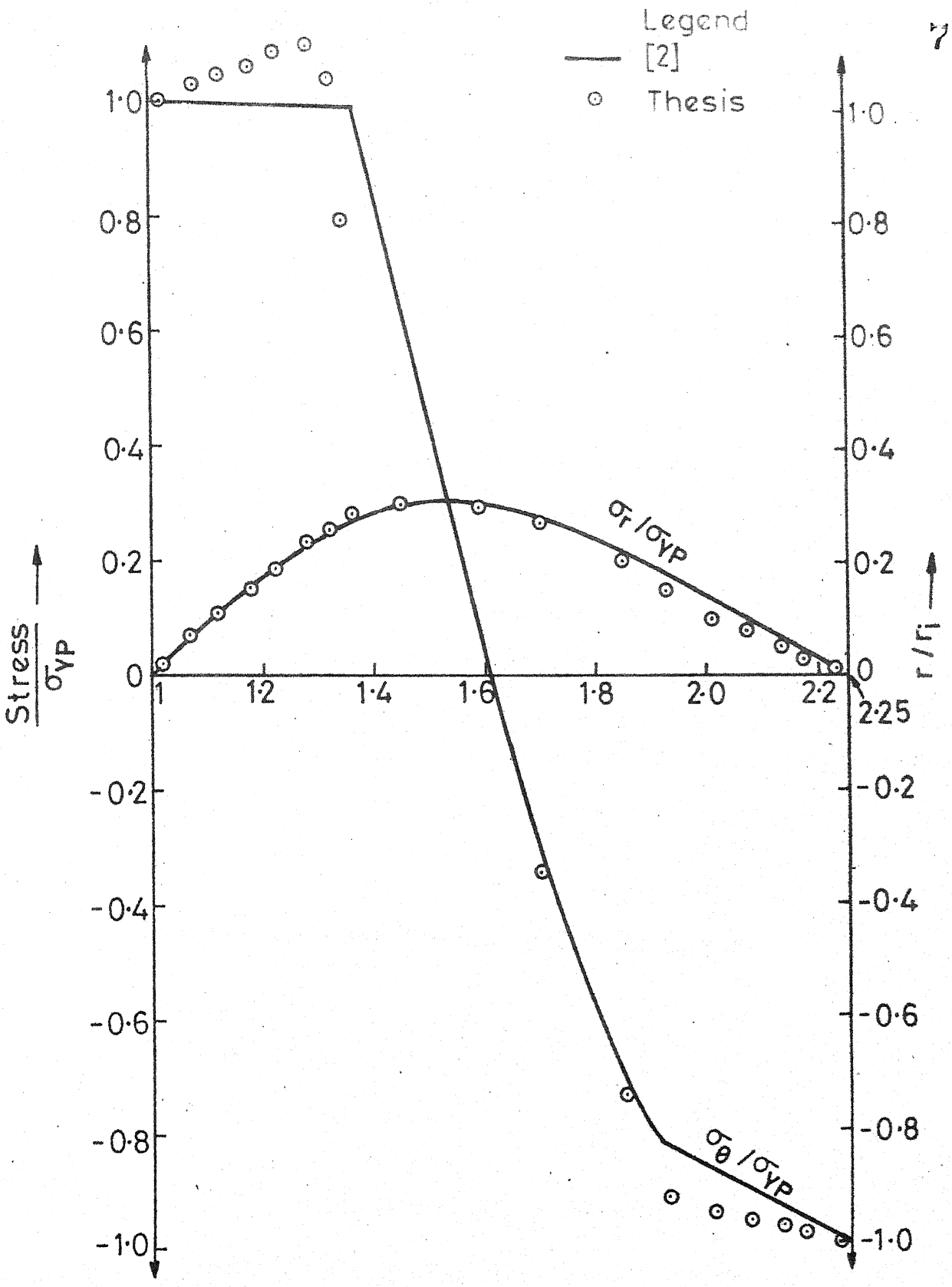

FIG.3·13 VARIATION OF RADIAL AND TANGENTIAL STRESSES FOR THERMO PLASTIC CYLINDER UNDER RADIAL TEMPERATURE GRADIENT

Since essentially this problem is a one dimensional case, hence it has been solved by THESIS as a plane stress as well as axisymmetric case. Figures 3.10 and 3.11 show the plane stress and axisymmetric finite element discretization of this problem respectively. Results obtained from both the analysis are similar.

In Figure 3.12, progress of plastic front is shown as a function of $\frac{E \alpha \Delta T}{\sigma_{YP}}$, upto the value of $\frac{E \alpha \Delta T}{\sigma_{YP}} = 6.0$, for which results are quoted in [2]. Same problem is solved in [12] and Figure 3.12 also shows results from [12]. It is seen results from present program are in better agreement with theoretical result, than quoted in [12]. In Figure 3.13, variations of σ_r and σ_θ along radius are shown for $\frac{E \alpha \Delta T}{\sigma_{YP}} = 4.525$ and a comparison has also been made with theoretical results from [2].

3.9.3 Thick Cylinder Under Radial Temperature Gradient (A Plane Strain Case)

Lastly to check the thermo-plastic analysis capability for plane strain problems of THESIS, solution of thick cylinder under radial temperature gradient, considered as plane strain case is presented here. Same problem is solved in [35] and those results are also shown for a comparisons.

The problem is characterised as follows:

inner radius/outer radius = 4

$E = 31$

$\nu = 0.25$

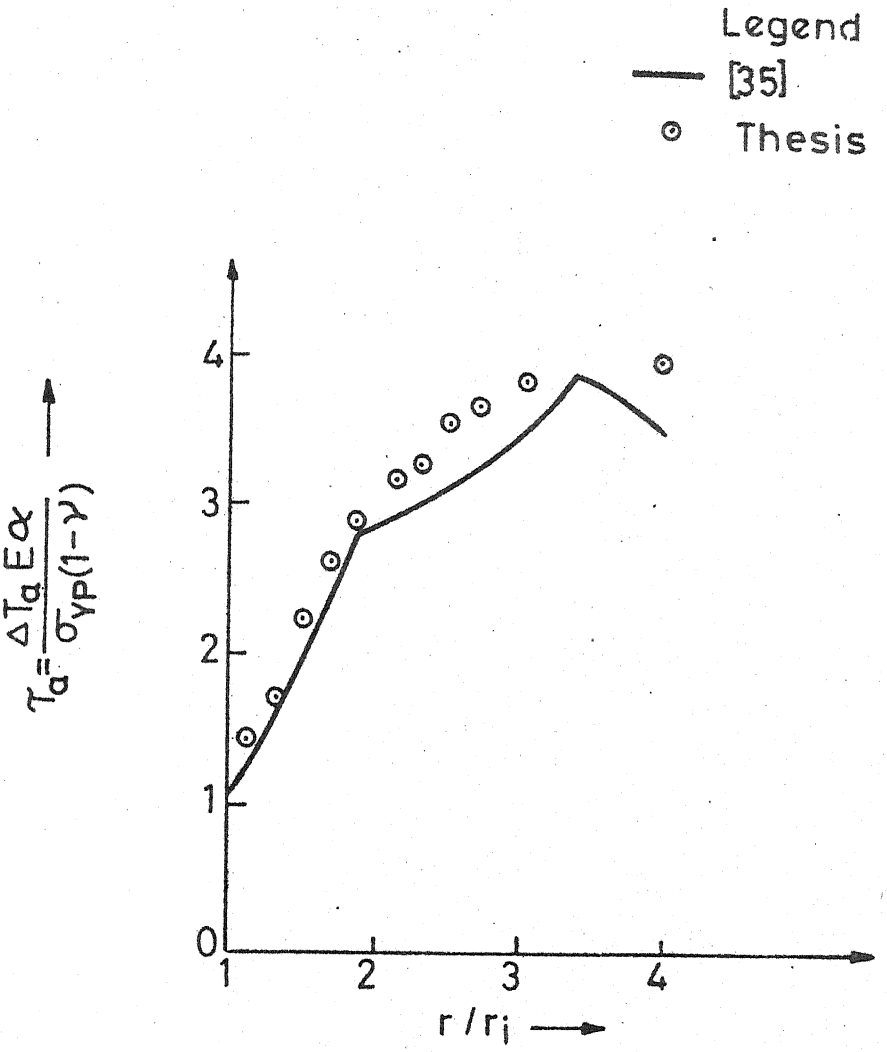

FIG.3.14 THE GROWTH OF PLASTIC ZONES IN A PLANE STRAIN CYLINDER UNDER RADIAL TEMPERATURE GRADIENT

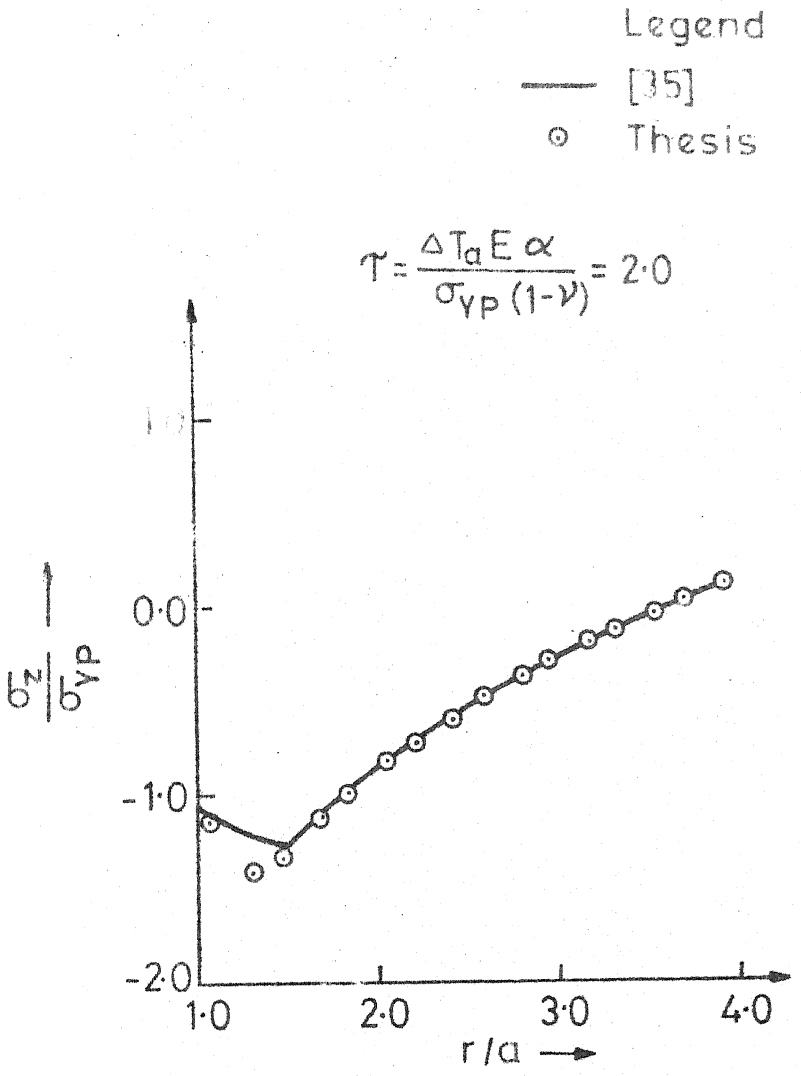

FIG.3·15 VARIATION OF σ_z FOR A PLANE STRAIN CYLINDER UNDER RADIAL TEMPERATURE GRADIENT

Progress of plastic front is shown in Figure 3.14. A comparison with [35] shows both results are not in good agreement. Present author feels this is essentially because, yield criteria used in [35] is Tresca and in THESIS yield criteria is Von-Mises. Similar differences in progress of plastic front because of different yield criteria are reported in [6] for only elasto-plastic analysis.

In Figure 3.15, variation of σ_z along radius is shown, when plastic front progressed upto 1.5 times inner radius.

CHAPTER 4

THERMO-MECHANICAL ANALYSIS OF 2-D STRUCTURES WITH CREEP

4.1 Introduction

In order to investigate stress annealing behaviors of welded structures, the effect of creep strain should be included in the theory presented in Chapter 3. To consider creep strain Cyr and Tete[28] suggested separation of creep strain from elastic and plastic strains in the formulation. In [18] authors adopted this way of including creep strain in existing elastic-plastic formulations of tangent stiffness method. They derived incremental stress-strain relations for several creep laws, such as power, exponential, time-hardening and strain-hardening. These incremental stress-strain relations are used here for analysing annealing of welded structures.

These four creep laws are given in Section 4.2. Derivations of incremental strain, as done in [18], are presented in Section 4.3. A modification for plane strain case including creep strain, as done for thermo-mechanical analysis in Chapter 3, has been done by the present author and is presented in Section 4.4. In Section 4.5 solutions of some sample problems are shown for verification of this formulation.

4.2 Creep Laws and Representative Incremental Creep Strain Form

Many mathematical relations are used to represent creep behavior of a material. But four creep laws, such as power, exponential, time-hardening and strain-hardening seem to be popular and a combination of these laws can represent the creep behavior of a material for entire range of annealing temperature of a welded structure successfully. Hence

all these creep laws are used in the formulation adopted in this work and any of these laws can be used for any temperature range depending upon the user's choice.

In one-dimensional stress state, these four laws can be represented mathematically as

$$\dot{\varepsilon}^c = \beta\sigma^n \quad : \text{power-creep law} \qquad (4.1)$$

$$\dot{\varepsilon}^c = A \exp(B\sigma) \quad : \text{exponential-creep law} \qquad (4.2)$$

$$\dot{\varepsilon}^c = m\, a\, \sigma^{\gamma}\, t^{m-1} \quad : \text{time-hardening-creep law} \qquad (4.3)$$

$$\dot{\varepsilon}^c = m\, a^{1/m}\, \sigma^{\gamma/m}\, (\varepsilon^c)^{1-\frac{1}{m}} \quad : \text{strain-hardening-creep law} \qquad (4.4)$$

where

σ = axial stress; ε^c = creep axial strain; $\dot{\varepsilon}^c$ = creep strain rate i.e. $\frac{d\varepsilon^c}{dt}$

β, n, A, B, m, a, γ are all constants and functions of material properties.

In three-dimensional stress state, assuming that the creep behavior is described by the theory of incremental strain of plasticity, the component of the creep strain rate is proportional to deviatoric stress. Hence

$$\{\dot{\varepsilon}^c\} = \frac{3}{2\bar{\sigma}}\, \bar{\dot{\varepsilon}}^c\, \{S\} \qquad (4.5)$$

where $\bar{\dot{\varepsilon}}^c$: proportionality factor, called equivalent creep strain rate

$\bar{\sigma}$: equivalent stress as defined earlier

$\lfloor S \rfloor : \lfloor S_x \; S_y \; 2\tau_{xy} \; S_z \rfloor$

Taking account of the effect of variation in the state of stress and creep properties, the general form of creep strain increment $\{d\varepsilon\}^{cr}$ during a time increment dt is given by

$$\{d\varepsilon\}^{cr} = [C_c]\{d\sigma\} + \{d\hat{\varepsilon}^c\} \qquad (4.6)$$

Hence for different creep laws matrices $[C_c]$ and $\{d\hat{\varepsilon}^c\}$ should be derived in terms of state of stress and creep properties.

4.3 Derivations of $[C_c]$ and $\{d\hat{\varepsilon}^c\}$ Matrices for Different Creep Laws

Comparing Equations (4.1) and (4.3), we find that if

$$\gamma \equiv n \; ; \qquad a \equiv \beta \qquad \text{and} \qquad m \equiv 1 \qquad (4.7)$$

then Equation (4.3) reduces to (4.1). Hence it can be said that power-creep law is a particular case of time-hardening creep law. So form of $[C_c]$ and $\{d\hat{\varepsilon}^c\}$ for time-hardening creep law can be used by substituting equivalence given in Equation (4.7) for power-creep law.

4.3.1 Time-Hardening Creep Law

Substituting for 1-D creep strain rate in Equation (4.5) from Equation (4.3), we have

$$\{\dot{\varepsilon}^c\} = \frac{3}{2} m a \bar{\sigma}^{\gamma-1} t^{m-1} \{S\} \qquad (4.8)$$

Using the notations

$$b = m a \qquad \text{and} \qquad \mu = m - 1 \qquad (4.9)$$

We have

$$\{\dot{\varepsilon}^c\} = \frac{3}{2} b \bar{\sigma}^{\gamma-1} t^{\mu} \{S\} \tag{4.10}$$

Assuming that b, $\bar{\sigma}$ and {S} in Equation (4.10) vary linearly and μ, γ are constants over the time interval dt, and integrating this creep strain rate during the time interval $t_1 \leq t \leq t_1 + dt$, where t_1 is real time, the vector $\{d\hat{\varepsilon}^c\}$ and matrix $[C_c]$ can be expressed as follows

$$\{d\hat{\varepsilon}^c\} = \frac{3}{2} (K_1 b + K_2\, db)\, \bar{\sigma}^{\gamma-1} \{S\} \tag{4.11}$$

and

$$[C_c] = (K_1 b + K_2\, db)\, \bar{\sigma}^{\gamma-1} [C_{ij}] \tag{4.12}$$

where

$$K_1 = \{(t_1 + dt)^{\mu+1} - (t_1)^{\mu+1}\}/(\mu + 1) \tag{4.13}$$

$$K_2 = (t_1 + dt)^{\mu+1}/(\mu + 1) - \{(t_1 + dt)^{\mu+2} - (t_1)^{\mu+2}\}/\{(\mu + 1)(\mu + 2)\, dt\} \tag{4.14}$$

$$K_3 = (t_1 + dt)^{\mu+1}/(\mu + 1) - 2(t_1 + dt)^{\mu+2}/\{(\mu + 1)(\mu + 2)dt\} + 2\{(t_1 + dt)^{\mu+3} - (t_1)^{\mu+3}\}/\{(\mu + 1)(\mu + 2)(\mu + 3)(dt)^2\} \tag{4.15}$$

Also

$$C_{11} = F S_x S_x + 1 \qquad C_{12} = F S_x S_y - 0.5$$

$$C_{13} = 2F S_x \tau_{xy} \qquad C_{14} = F S_x S_z - 0.5$$

$$C_{22} = F S_y S_y + 1 \qquad C_{23} = 2F S_y \tau_{xy} \tag{4.16}$$

$$C_{24} = F S_y S_z - 0.5 \qquad C_{33} = 4F \tau_{xy} \tau_{xy} + 3$$

$$C_{34} = 2F S_z \tau_{xy} \qquad C_{44} = F S_z S_z + 1$$

where

$$C_{ij} = C_{ji} \quad (i,j = 1 \sim 4) \quad \text{and} \quad F = 9(\gamma - 1)/(4\bar{\sigma}^2)$$

4.3.2 Power-Creep Law

It is apparent that for the power creep law, the creep strain increment is obtained by putting b, γ and μ in Equations (4.11) through (4.16) equal to β, n and zero, respectively.

4.3.3 Exponential-Creep Law

Substituting for one-dimensional creep strain rate from Equation (4.2) into Equation (4.5), we have

$$\{\dot{\varepsilon}^c\} = \frac{3}{2\bar{\sigma}} A \exp(B\bar{\sigma}) \{S\} \tag{4.17}$$

Again assuming variations of A, $\bar{\sigma}$ and {S} as linear and no variation of B, over the interval dt, we have

$$\{d\hat{\varepsilon}^c\} = \frac{3dt}{2\bar{\sigma}} (A + \frac{dA}{2}) \exp(B\bar{\sigma}) \{S\} \tag{4.18}$$

$$[C_c] = dt \, (\frac{A}{2} + \frac{dA}{3}) \frac{\exp(B\bar{\sigma})}{\bar{\sigma}} [C'_{ij}] \tag{4.19}$$

Such that

$$\begin{aligned}
C'_{11} &= G S_x S_x + 1 & C'_{12} &= G S_x S_y - 0.5 \\
C'_{13} &= 2G S_x \tau_{xy} & C'_{14} &= G S_x S_z - 0.5 \\
C'_{22} &= G S_y S_y + 1 & C'_{23} &= 2G S_y \tau_{xy} \\
C'_{24} &= G S_y S_z - 0.5 & C'_{33} &= 4G \tau_{xy} \tau_{xy} + 3 \\
C'_{34} &= 2G S_z \tau_{xy} & C'_{44} &= G S_z S_z + 1
\end{aligned} \tag{4.20}$$

also $C_{ij} = C_{ji}$ $(i,j = 1 \sim 4)$;

$G = 9(B\bar{\sigma} - 1)/(4\bar{\sigma}^2)$

and dA is the change in A due to temperature increment in time dt.

When Equations (4.18) to (4.20) are used for analysis, a time increment dt should be chosen to satisfy the inequality $B\, d\bar{\sigma} \leq 1$, as an exponential function is approximated by a series of polynomials in the process of derivations of these expressions.

4.3.4 Strain-Hardening Creep Law

In case of strain-hardening creep law, given by Equation (4.4), material constant m is generally less than unity. Since at the beginning of the iterations creep strain ε^c is zero, hence from Equation (4.4), creep strain rate $\dot{\varepsilon}^c$ is infinity. So, direct application of this equation is not possible for computation. A method suggested in [18], has been used in the present work for this creep law implementation.

In [18], a new creep law, called total-strain creep law, has been defined and is given by

$$\varepsilon^c = a\, \sigma^{\gamma} t^m \qquad (4.21)$$

Hence strain-hardening creep law (Equation 4.4) is now a solution of simultaneous equations of Equations (4.3) and (4.21) for parameter t. In such a case where the stresses in a continuum do not change in a specified period of time $(t_1 \leq t \leq t_2)$, the following method is completely

equivalent to the direct application of Equation (4.4) to evaluate the creep strain. The creep strains are calculated by integrating Equation (4.3) for the specified interval ($t_{eq} \leq t \leq t_{eq} + (t_2 - t_1)$), in which the equivalent time t_{eq} is calculated by Equation (4.21) of a function of stresses and creep strains at the real time t_1. In actual stress relief annealing, the stresses in a structure vary during the treatment. The changes of the stresses during a small time interval can be regarded as invariant. In this case, the creep strain increment under the strain-hardening creep law can be evaluated by the above-mentioned method.

In the three-dimensional stress state, the equivalent time t_{eq} is given by the equation

$$t_{eq} = \{ \bar{\varepsilon}^c / (a \bar{\sigma}^\gamma) \}^{1/m} \qquad (4.22)$$

Hence Equation (4.3) must be integrated for analysis during a time increment $dt (t_{eq} \leq t \leq t_{eq} + dt)$. So, the results given by Equations (4.11) through (4.16) can be used by replacing t_1 by t_{eq}. Also at the first incremental step, t_{eq} is equal to zero because there is no creep strain.

4.4 Thermo-Mechanical Analysis of Plane Strain Case with Creep

In case of elasto-plastic and thermo-plastic analysis of plane-stress and axisymmetric structures with creep, formulations presented in Sections (3.2) and (3.4) can be used, after adding one more strain terms corresponding to creep, given by Equation (4.6). Hence no attempt has been made to rederive those formulations. But in case of plane

strain structures, an attempt being made here to rederive the formulations presented in (3.3) and (3.5), as many new vectors appear in the final expressions if creep is considered. Derivation given below is essentially for thermo-mechanical analysis, which of course is a generalisation of elasto-plastic case. This conversion can be done by dropping. The components of $\{d\hat{\varepsilon}_c\}$, $\{d\varepsilon\}^{Th}$ and $\{d\varepsilon\}^{TP}$ from the final expressions.

Total strain increment is given by (considering creep also)

$$\{d\varepsilon\}^t = \{d\varepsilon\}^e + \{d\varepsilon\}^p + \{d\varepsilon\}^{Th} + \{d\varepsilon\}^{TP} + \{d\varepsilon\}^{cr} \quad (4.23)$$

Substituting $\{d\varepsilon\}^e$ in terms of stress increments from Hooke's law and $\{d\varepsilon\}^{cr}$ from Equation (4.6) in Equation (4.23), we have

$$\{d\varepsilon\}^t = \frac{1}{E}\begin{bmatrix} 1 & -\nu & 0 & -\nu \\ -\nu & 1 & 0 & -\nu \\ 0 & 0 & \frac{E}{G} & 0 \\ -\nu & -\nu & 0 & 1 \end{bmatrix} \{d\sigma\} + \{d\varepsilon\}^p + \{d\varepsilon\}^{Th} + \{d\varepsilon\}^{TP} + [C_c]\{d\sigma\} + \{d\hat{\varepsilon}^c\} \quad (4.24)$$

Denoting components of matrix $[C_c]$ as C_{11}, C_{12} etc., we rewrite Equation (4.24) as

$$\{d\varepsilon\}^t = \begin{bmatrix} \frac{1}{E}+C_{11} & \frac{-\nu}{E}+C_{12} & C_{13} & \frac{-\nu}{E}+C_{14} \\ \frac{-\nu}{E}+C_{21} & \frac{1}{E}+C_{22} & C_{23} & \frac{-\nu}{E}+C_{24} \\ C_{31} & C_{32} & \frac{1}{G}+C_{33} & C_{34} \\ \frac{-\nu}{E}+C_{41} & \frac{-\nu}{E}+C_{42} & C_{43} & \frac{1}{E}+C_{44} \end{bmatrix}$$

$$\{d\sigma\} + \{d\varepsilon\}^P + \{d\varepsilon\}^{Th} + \{d\varepsilon\}^{TP} + \{d\hat{\varepsilon}^c\} \qquad (4.25)$$

Since for plane strain case $d\varepsilon_z^t = 0$, hence from last equation of Equation (4.25), we have

$$(\frac{-\nu}{E} + C_{41})d\sigma_x + (\frac{-\nu}{E} + C_{42})d\sigma_y + C_{43}\, d\tau_{xy} + (\frac{1}{E} + C_{44})d\sigma_z + d\varepsilon_z^p + d\varepsilon_z^{Th} + d\varepsilon_z^{TP} + d\hat{\varepsilon}_z^c = 0 \qquad (4.26)$$

or

$$d\sigma_z = \frac{1}{(1 + E\, C_{44})} \{(\nu - E\, C_{41})d\sigma_x + (\nu - E\, C_{42})d\sigma_y - E\, C_{43}\, d\tau_{xy} - E(d\varepsilon_z^p + d\varepsilon_z^{Th} + d\varepsilon_z^{TP} + d\hat{\varepsilon}_z^c)\} \qquad (4.27)$$

Hence eliminating $d\sigma_z$ from first three equations of Equation (4.25) and also using flow rule

$$\{d\varepsilon\}^p = \frac{3}{2}\frac{d^{-p}}{\bar{\sigma}} \begin{Bmatrix} S_x \\ S_y \\ 2\tau_{xy} \\ S_z \end{Bmatrix} \qquad (4.28)$$

We have

$$\{d\varepsilon\}^t = [C]\{d\sigma\} + d\bar{\varepsilon}^p \{\frac{\partial \bar{Q}}{\partial \sigma}\} + \{d\varepsilon\}^{Th} + \{d\varepsilon\}^{TP} + \{d\hat{\varepsilon}^c\} + \{H\}(d\varepsilon_z^{Th} + d\varepsilon_z^{TP} + d\hat{\varepsilon}_z^c) \quad (4.29)$$

where

$$[C] = \begin{bmatrix} (\frac{1+EC_{11}}{E}) + (\frac{\nu - EC_{41}}{1+EC_{44}})^* & (\frac{-\nu+EC_{12}}{E}) + (\frac{\nu-EC_{42}}{1+EC_{44}})^* & C_{13} - (\frac{C_{43}}{1+EC_{44}})^* \\ (\frac{-\nu+EC_{14}}{E}) & (\frac{-\nu+EC_{14}}{E}) & (-\nu+EC_{14}) \\ & (\frac{1+EC_{22}}{E}) + (\frac{\nu-EC_{42}}{1+EC_{44}})^* & C_{23} - (\frac{C_{43}}{1+EC_{44}})^* \\ & (\frac{-\nu+EC_{24}}{E}) & (-\nu+EC_{24}) \\ \text{Symmetric} & & \frac{1}{G} + C_{33} - C_{34}^* \\ & & \frac{EC_{43}}{1+EC_{44}} \end{bmatrix} \quad (4.30)$$

$$\{\frac{\partial \bar{Q}}{\partial \sigma}\} = \begin{Bmatrix} \frac{3}{2}(S_x + \frac{\nu - E\,C_{14}}{1 + E\,C_{44}} S_z) \\ \frac{3}{2\bar{\sigma}}(S_y + \frac{\nu - E\,C_{24}}{1 + E\,C_{44}} S_z) \\ \frac{3}{\bar{\sigma}}(\tau_{xy} - \frac{E\,C_{34}}{(1 + E\,C_{44})} \frac{S_z}{2} \end{Bmatrix} \quad (4.31)$$

and

$$\{H\} = \begin{Bmatrix} \dfrac{\nu - C_{14}\, E}{1 + E\, C_{44}} \\ \dfrac{\nu - C_{24}\, E}{1 + E\, C_{44}} \\ \dfrac{-E\, C_{34}}{1 + E\, C_{44}} \end{Bmatrix} \qquad (4.32)$$

Denoting $[C]^{-1} = [\bar{D}]$, we have from Equation (4.29)

$$\{d\sigma\} = [\bar{D}]\,(\{d\varepsilon\}^t - d\bar{\varepsilon}^p \{\frac{\partial \bar{Q}}{\partial \sigma}\} - \{d\varepsilon\}^{Th} - \{d\varepsilon\}^{TP} - \{d\hat{\varepsilon}^c\}) - [\bar{D}]\{H\}\,(d\varepsilon_z^{Th} + d\varepsilon_z^{TP} + d\hat{\varepsilon}_z^c) \qquad (4.33)$$

Using Von-Mises yield criteria, we have

$$\bar{\sigma} = \frac{1}{\sqrt{2}} [(\sigma_x - \sigma_y)^2 + (\sigma_z - \sigma_x)^2 + (\sigma_y - \sigma_z)^2 + 6\tau_{xy}^2]^{1/2}$$

Hence

$$d\bar{\sigma} = \frac{3}{2}\frac{S_x}{\bar{\sigma}} d\sigma_x + \frac{3}{2}\frac{S_y}{\bar{\sigma}} d\sigma_y + \frac{3S_z}{2\bar{\sigma}} d\sigma_z + \frac{3\tau_{xy}}{\bar{\sigma}} d\tau_{xy} \qquad (4.34)$$

Using expression for $d\sigma_z$ from Equation (4.27) in (4.34) we have (also noting Equation (4.31) and Equation (3.50))

$$d\bar{\sigma} = H'\, d\bar{\varepsilon}^p + \frac{\partial \bar{\sigma}}{\partial T} dT = \lfloor \frac{\partial \bar{Q}}{\partial \sigma} \rfloor \{d\sigma\} - \frac{3}{2}\frac{S_z}{\bar{\sigma}} \frac{E}{(1 + E\, C_{44})} (d\varepsilon_z^p + d\varepsilon_z^{Th} + d\varepsilon_z^{TP} + d\hat{\varepsilon}_z^c) \qquad (4.35)$$

Solving for $d\bar{\varepsilon}^p$ from Equation (4.35), we have

$$d\bar{\varepsilon}^p = \lfloor \bar{W} \rfloor (\{d\varepsilon\}^t - \{d\varepsilon\}^{Th} - \{d\varepsilon\}^{TP} - \{d\hat{\varepsilon}^c\})$$

$$- \frac{\left\{ \left\{ \frac{\partial \bar{Q}}{\partial \bar{\sigma}} \right\} [\bar{D}] \{H\} + \frac{3}{2} \frac{S_z}{\bar{\sigma}} \frac{E}{(1 + E\, C_{44})} \right\}}{DEN\bar{W}} (d\varepsilon_z^{Th} + d\varepsilon_z^{TP} + d\hat{\varepsilon}_z^{c})$$

$$- \frac{\frac{\partial \bar{\sigma}}{\partial T} dT}{DEN\bar{W}} \qquad (4.36)$$

where

$$\left\{ \left[\frac{\partial \bar{Q}}{\partial \bar{\sigma}} \right] [\bar{D}] \left(\{d\varepsilon\}^t - \{d\varepsilon\}^{Th} - \{d\varepsilon\}^{TP} - \{d\hat{\varepsilon}^c\} \right) - \right.$$

$$\left. \left[\frac{\partial \bar{Q}}{\partial \bar{\sigma}} \right] [\bar{D}] \{H\} (d\varepsilon_z^{Th} + d\varepsilon_z^{TP} + d\hat{\varepsilon}_z^{c}) - \frac{3}{2} \frac{S_z}{\bar{\sigma}} \frac{E}{(1 + E\, C_{44})} \right\} *$$

$$\left[\bar{W} \right] = \frac{(d\varepsilon_z^{Th} + d\varepsilon_z^{TP} + d\hat{\varepsilon}_z^{c}) - \frac{\partial \bar{\sigma}}{\partial T} dT\}}{DEN\bar{W}} \qquad (4.37)$$

and

$$DEN\bar{W} = H' + \left[\frac{\partial \bar{Q}}{\partial \bar{\sigma}} \right] [\bar{D}] \left\{ \frac{\partial \bar{Q}}{\partial \bar{\sigma}} \right\} + \frac{9}{4} \frac{S_z^2}{\bar{\sigma}^2} \frac{E}{(1 + E\, C_{44})} \qquad (4.38)$$

Substituting expression for $d\bar{\varepsilon}^p$ from Equation (4.36) into Equation (4.33), we have

$$\{d\sigma\} = [\bar{D}_{ep}] \left(\{d\varepsilon\}^t - \{d\varepsilon\}^{Th} - \{d\varepsilon\}^{TP} - \{d\hat{\varepsilon}^c\} \right) +$$

$$[\bar{D}] \left\{ \frac{\partial \bar{Q}}{\partial \bar{\sigma}} \right\} \frac{\frac{\partial \bar{\sigma}}{\partial T} dT}{DEN\bar{W}} + [\bar{D}] \left(\left\{ \frac{\partial \bar{Q}}{\partial \bar{\sigma}} \right\} \left[\bar{W} \right] \{H\} \right.$$

$$\left. + \left\{ \frac{\partial \bar{Q}}{\partial \bar{\sigma}} \right\} \frac{\frac{3}{2} \frac{S_z}{\bar{\sigma}} \frac{E}{1 + E\, C_{44}}}{DEN\bar{W}} - \{H\} \right) (d\varepsilon_z^{Th} + d\varepsilon_z^{TP} + d\hat{\varepsilon}_z^{c}) \qquad (4.39)$$

where

$$[\bar{D}_{ep}] = [\bar{D}] - [\bar{D}]\{\frac{\partial \bar{Q}}{\partial \sigma}\}[\bar{W}] \qquad (4.40)$$

Hence in Equation (3.13), we have $[D_{ep}] \equiv [\bar{D}_{ep}]$ and

$$\{dP\} = [\bar{D}_{ep}]\ (\{d\varepsilon\}^{Th} + \{d\varepsilon\}^{TP} + \{d\hat{\varepsilon}^{c}\}) - \frac{\frac{\partial \bar{\sigma}}{\partial T}\, dT}{DEN\bar{W}}[\bar{D}]\{\frac{\partial \bar{Q}}{\partial \sigma}\} - [\bar{D}]\ (\{\frac{\partial \bar{Q}}{\partial \sigma}\}[\bar{W}]\{H\} + \{\frac{\partial \bar{Q}}{\partial \sigma}\}\frac{\frac{3}{2}\frac{S_z}{\bar{\sigma}}\frac{E}{1 + E\, C_{44}}}{DEN\bar{W}} - \{H\})\ (d\varepsilon_z^{Th} + d\varepsilon_z^{TP} + d\hat{\varepsilon}_z^{c}) \qquad (4.41)$$

It can be seen here explicit expression for $[\bar{D}]$ is very difficult to find, and hence one has to compute matrix $[C]$ from Equation (4.30) and then invert it numerically for all gauss points for every iteration. This inversion is likely to be easier from numerical point of view, as $[C]$ matrix will be a diagonally dominated matrix.

4.5 Solved Examples

Program THESIS described in Chapter 3, is then modified for taking into consideration creep effect, depending upon the formulation presented in Section (4.4). This program is then tested for different sample problems. Some of these are presented here, also to show the accuracy a comparison is made with the results of same problems from [18].

4.5.1 A Note on Material Properties

Material properties used to solve different sample problems are same as given in [18], which are essentially

E ; YOUNG MODULUS

σ_{YP} ; YIELD STRESS

H' ; RATIO OF STRAIN HARDENING

σ_U ; ULT. TENSILE STRESS

α ; INST. LINEAR EXP. COEFF.

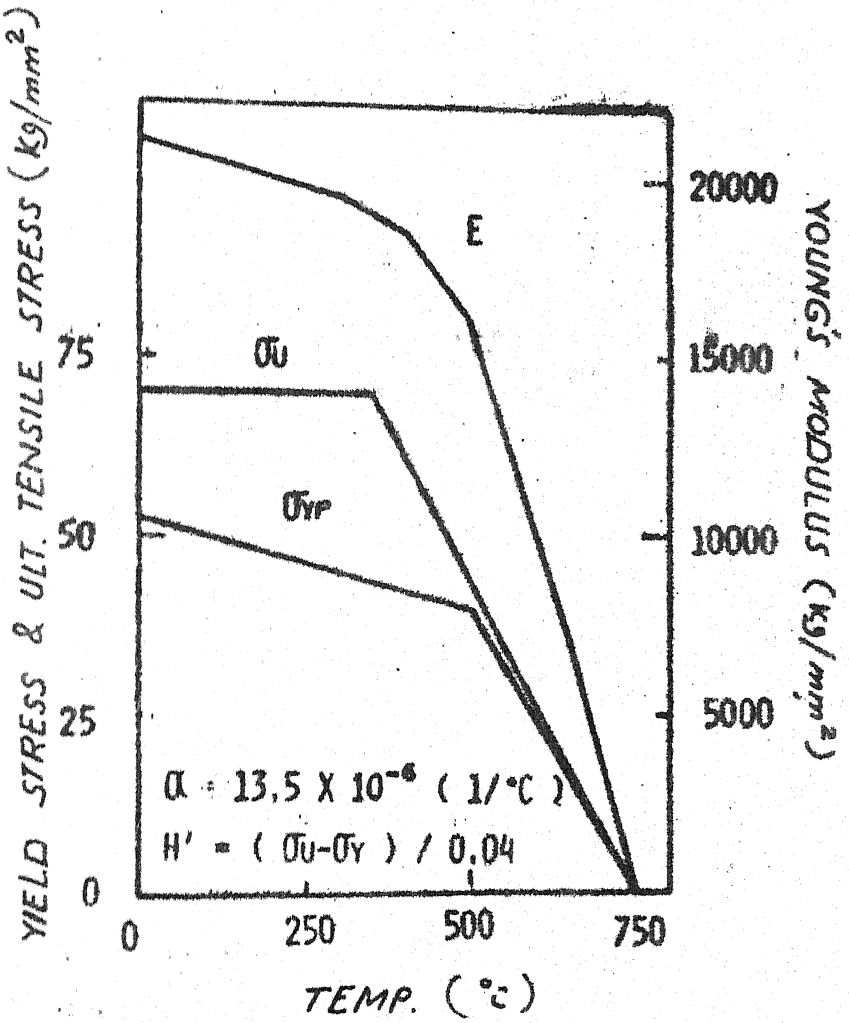

FIG. 4.1 TEMPERATURE DEPENDENCY OF MECHANICAL PROPERTIES.

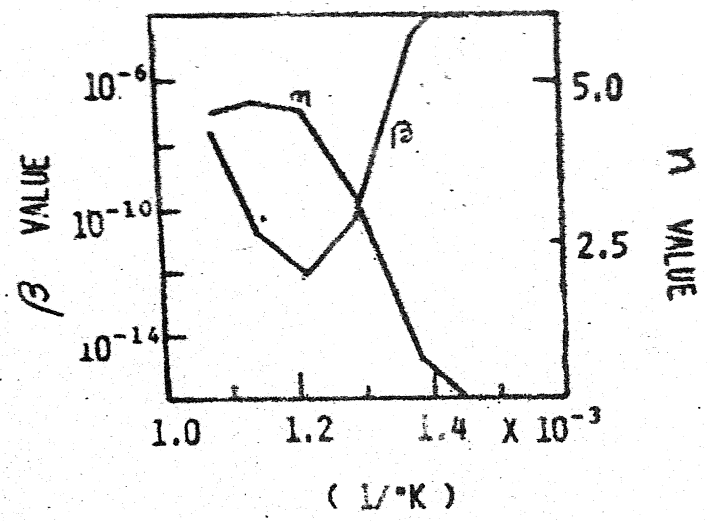

a) POWER CREEP LAW

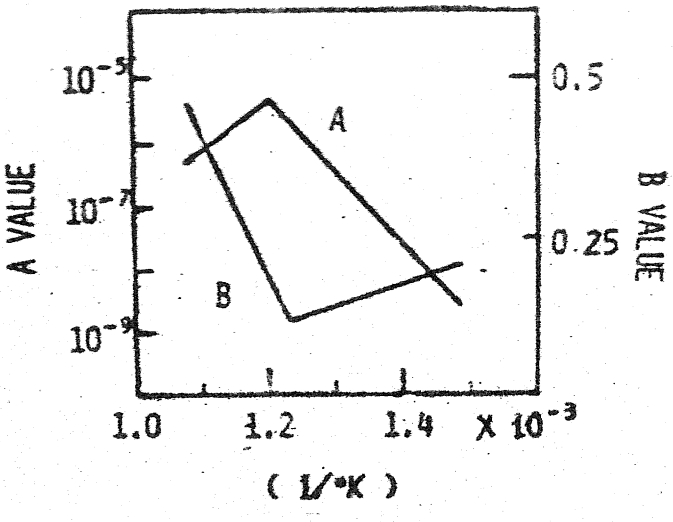

b) EXPONENTIAL CREEP LAW

FIG. 4.2 TEMPERATURE DEPENDENCY OF CREEP PROPERTIES (FOR HEATING STAGE)

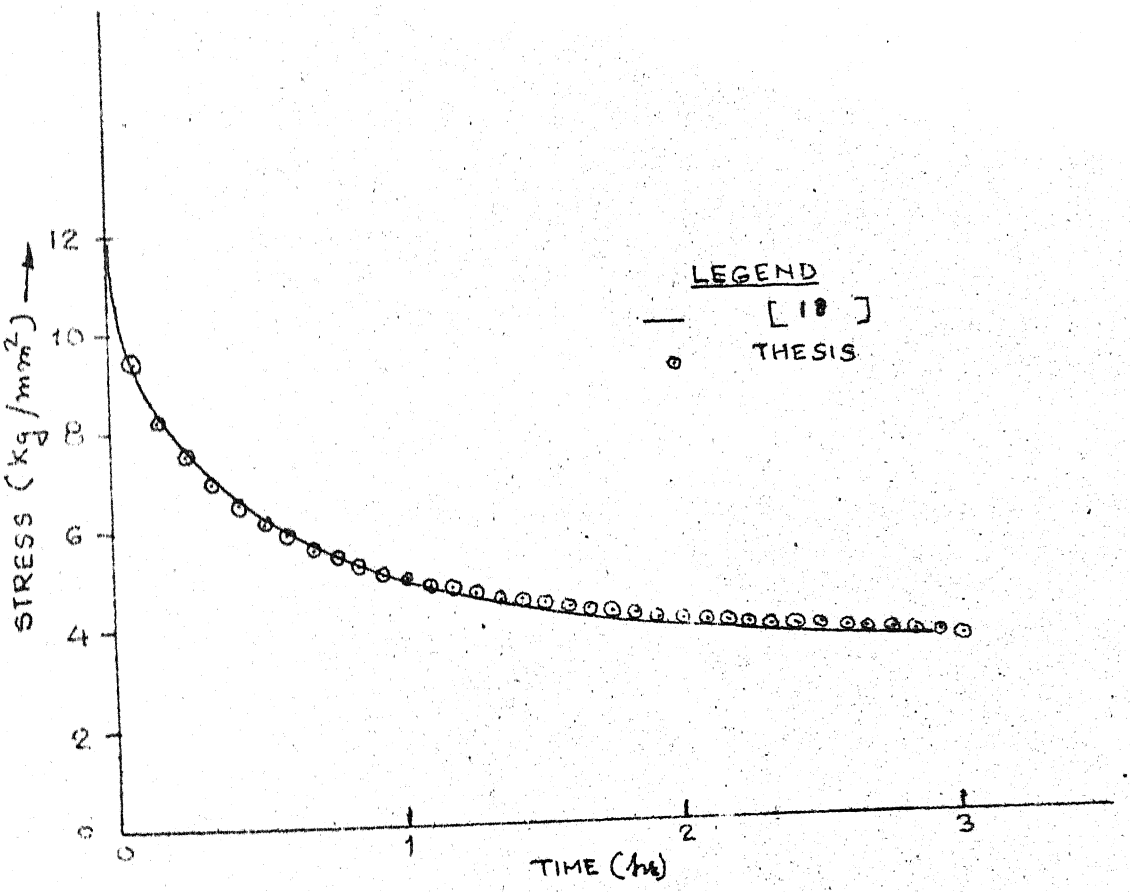

FIG.- 4.3 STRESS VARIATION FOR 1-D BAR DUE TO CREEP

for quenched and tempered high strength steel H.T. 60. These properties are shown in Figures 4.1 and 4.2. This material seems to obey power creep law above 550°C and exponential creep law below 550°C.

4.5.2 One-Dimensional Creep Stress Relaxation at Constant Temperature

The problem consists of a 1-D bar, carrying axial initial stress of 12 Kg/mm^2. Bar is fixed from both the sides and kept at a constant temperature of 600°C, for 3 hours.

Since temperature of the bar is above 550°C, hence as per the material properties described here, it follows power creep law. Using the properties as

$$n = 4.2 \quad \text{and} \quad \beta = 2.7 \times 10^{-9}$$

Since program THESIS is essentially for 2-D structures, hence present problem is treated as plane stress case. The results are shown in Figure 4.3. A comparison has been made with results shown in [18] and found in excellent agreement.

4.5.3 One-Dimensional Creep Stress Relaxation for Varying Temperatures

In conventional stress relief annealing, it is a common process that the structure is gradually heated up to a holding temperature. So, the initial stress decreases during the heating stage by reduction of Young's modulus and the yield stress, and also due to increase in creep strain.

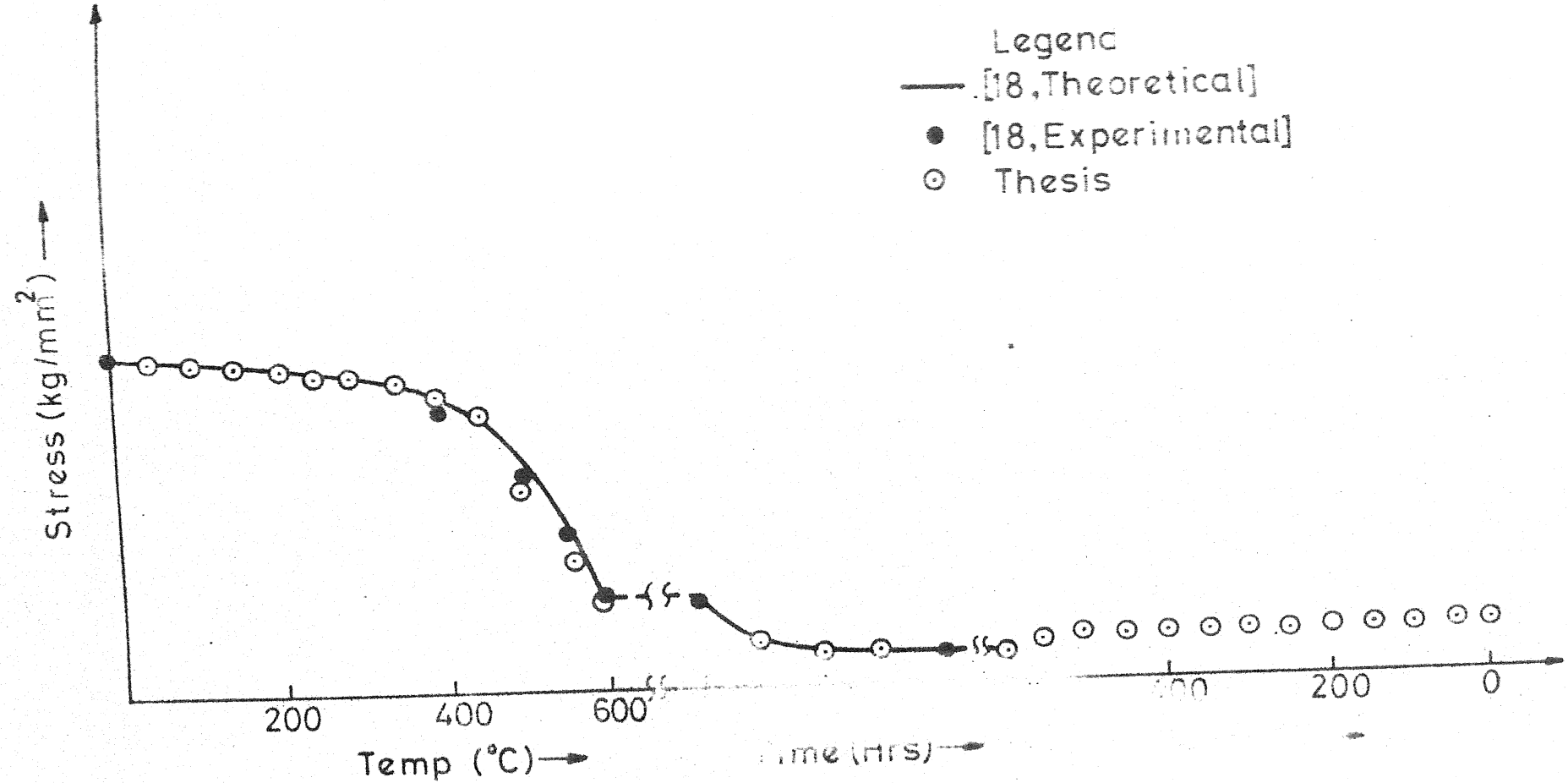

FIG.4-4 STRESS VARIATIONS DURING HEATING AND COOLING OF [illegible]
(A PLANE STRESS CASE)

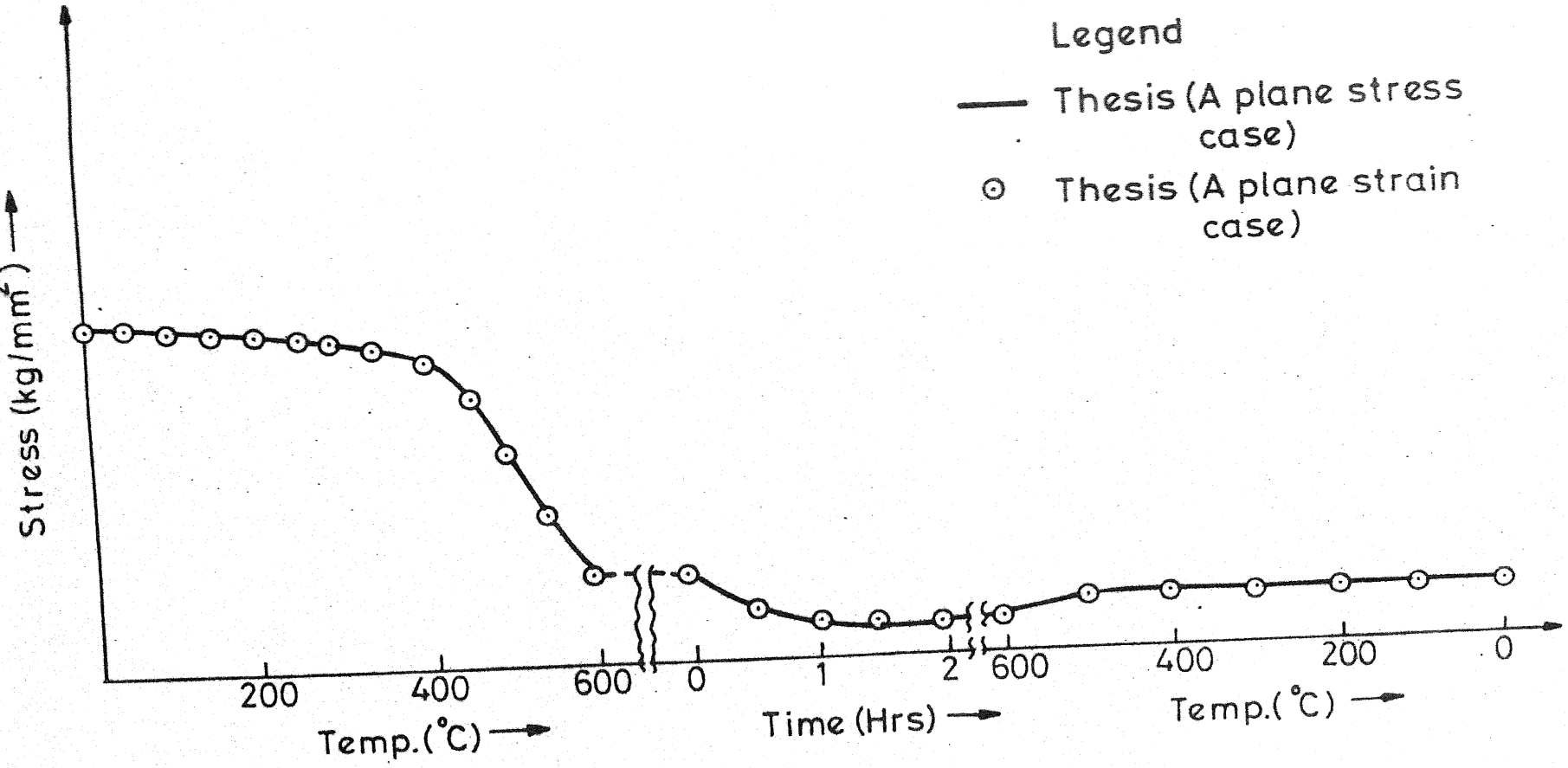

FIG.4·5 STRESS VARIATIONS DURING HEATING AND COOLING OF 1-D BAR (A PLANE STRAIN CASE)

To study this, problem defined in Section 4.5.2, is solved for a heating rate of 600°C/hr for one hour and then holding at this temperature for 2 hours and then cooled down to room temperature at 600°C/hr.

The material properties used are as defined in Section 4.5.1. The results are shown in Figure 4.4 and also compared for first 3 hours with results quoted in [18] and found in good agreement. Results show at the range below 400°C, stress decreases due to decrease in Young's modulus and at the range above 400°C the stress indicates lower value than one estimates from only the change of Young's modulus. In this case, the stress is in the elastic range even if high temperature is held. Then, it decreases not only due to decrease in yield stress but also because of generation of creep strain.

4.5.4 One-Dimensional Creep Stress Relaxation for a Plane Strain Case

Example solved in Section 4.5.3, is also solved as a plane strain case for initial σ_z = 12 Kg/mm^2 and no inplane stresses. Though results of this problem is not available in literature, but author expects to obtain a similar variation of stresses as was in Section 4.5.3, since problem essentially is 1-D. Also since while solving as a plane stress case, bar is assumed to be of small and constant length, and hence also can be solved as a plane strain case, assuming strain is zero along the length of the bar. Results of this example are shown in Figure 4.5, and found as per the expectation.

CHAPTER 5

THERMAL RESPONSE ANALYSIS FOR NONLINEAR HEAT TRANSFER PROBLEM

5.1 Introduction

Calculation of residual stresses during different mechanical processes, such as welding, casting, grinding etc., necessitates prediction of temperature distribution with a high degree of accuracy. Since present work is aimed to determine residual stresses during mechanical processes, a computer program is required to calculate temperature distribution for nonlinear heat transfer problems. A computer program WELTEM was developed by the present author, as a part of this integrated work, before joining the present institute. This program was reported in [29,30]. A brief description of the theory used in this program is presented here for the sake of completeness. A modification developed during this work over the existing method to consider phase change effectively, is also explained in Section 5.4.3.

This program has been used for computing temperature distribution during longitudinal welding of cylinder, as described in Chapter 6.

5.2 Theory of Two Dimensional Linear Heat Transfer

The governing differential equation for two dimensional time dependent heat conduction is given below. For an axisymmetric geometry the equation gets slightly modified and is also given below.

For 2-D Case

$$\frac{\partial}{\partial X}\left(K_X \frac{\partial T}{\partial X}\right) + \frac{\partial}{\partial Y}\left(K_Y \frac{\partial T}{\partial Y}\right) + \tilde{Q} = \rho C \frac{\partial T}{\partial t} \qquad (5.1)$$

Boundary Conditions

Constant temperature $T = T(x, y, t)$ on $S1$, $t > 0$

(5.2)

Convective heat loss

$$K_X \frac{\partial T}{\partial X} n_X + K_Y \frac{\partial T}{\partial Y} n_Y + q + h(T - T_\infty) = 0 \quad \text{on} \quad S_2, \; t > 0 \tag{5.3}$$

Initial temperature

$$T = T_o(X, Y) \quad \text{in} \quad D, \; t = 0 \tag{5.4}$$

For Axisymmetric Case

$$\frac{\partial}{\partial r}\left(K_r \, r \frac{\partial T}{\partial r}\right) + \frac{\partial}{\partial Z}\left(K_Z \, r \frac{\partial T}{\partial Z}\right) + r \tilde{Q} = \rho C \frac{\partial T}{\partial t} \tag{5.5}$$

Boundary Conditions

Constant temperature $T = T(r, z, t)$ on $S1$, $t > 0$

(5.6)

Convective heat loss

$$K_r \, r \frac{\partial T}{\partial r} n_r + K_Z \, r \frac{\partial T}{\partial Z} n_Z + r \, h(T - T_\infty) = 0 \quad \text{on} \quad S_Z, \; t > 0 \tag{5.7}$$

Initial temperature

$$T = T_o(r, z) \quad \text{in} \quad D, \; t = 0 \tag{5.8}$$

The temperature distribution over an element 'e' is assumed as

$$T^{(e)}(X, Y, t) = \sum_{i=1}^{n} N_i(X, Y) \, T_i(t) = [N] \{T\}^{(ne)} \tag{5.9}$$

Substituting Equation (5.9) in differential Equations (5.1) or (5.5) and using Galerkin's method, we get

$$[K_t]^e \{T\}^e = \{Q\}^e - \{q\}^e - [K_h]^e \{T\}^e + \{K_{T_\infty}\}^e - [K_c] \left\{\frac{\partial T}{\partial t}\right\}^e \tag{5.10}$$

where

$$K_{t_{ij}} = \iint_{D^e} \left[K_X \frac{\partial N_i}{\partial X} \frac{\partial N_j}{\partial Y} + K_Y \frac{\partial N_j}{\partial X} \frac{\partial N_i}{\partial Y}\right] dX\, dY \tag{5.11}$$

$$Q_i = \int_{D^e} \tilde{Q}\, N_i\, dX\, dY \tag{5.12}$$

$$q_i = \int_{S_2^e} q\, N_i\, d\Sigma^e \tag{5.13}$$

$$K_{h_{ij}} = \int_{S_2^e} h\, N_i\, N_j\, d\Sigma^e \tag{5.14}$$

$$K_{T_\infty} = \int_{S_2^e} h\, T_\infty\, N_i\, d\Sigma^e \tag{5.15}$$

$$K_{c_{ij}} = \int_{D^e} \rho\, C\, N_i\, N_j\, dX\, dY \tag{5.16}$$

Combining $[K_t]^e$ and $[K_h]^e$ and all the load vectors, the equation appears as

$$[K]^{(e)} \{T\}^{(ne)} + [C]^e \left\{\frac{\partial T}{\partial t}\right\}^{(ne)} = \{F\}^{(ne)}$$

The elements are assembled into global matrices and the final system of equations is obtained as

$$[K] \{T\} + [C] \left\{\frac{\partial T}{\partial t}\right\} = \{F\} \tag{5.17}$$

This procedure is same for the axisymmetric geometry except that $2\pi\, r\, dr\, dZ$ replaces $dX\, dY$ and $2\pi\, r\, d\Sigma$ replaces $d\Sigma$. The final set of equations have the same form.

5.3 Solutions of Differential Equations for Transient Analysis

The set of differential equations for time dependent heat conduction are given by Equation (5.17).

Two procedures for solution of these equations are popular, namely direct integration and modal superposition. Since modal superposition method is not useful for nonlinear heat transfer problems, direct integration methods are discussed here.

In direct integration, time dependent heat conduction equations are integrated using a numerical step by step procedure without applying any transformation prior to integration. The heat balance is carried out only at discrete time intervals Δt apart over a time interval Δt, a certain variation of $\{\frac{\partial T}{\partial t}\}$ is assumed.

Here finite difference approach is discussed in details since this has been used in the present work.

5.3.1 Finite Difference

The time derivative of temperature is approximated using finite difference. It is assumed constant over the time step. Let the superscripts i and i+1 denote beginning and end of the time step. Depending on what constant value is assumed, three schemes are possible, which are listed as follows:

Scheme	Constant value of $\{\frac{\partial T}{\partial t}\}$ over Δ^t	
1. Euler's/Explicit scheme	$\{\frac{\partial T}{\partial t}\}^i$	(5.18)
2. Implicit scheme	$\{\frac{\partial T}{\partial t}\}^{i+1}$	(5.19)
3. Crank-Nicholson's scheme	$\frac{1}{2}[\{\frac{\partial T}{\partial t}\}^i + \{\frac{\partial T}{\partial t}\}^{i+1}]$	(5.20)

Of the three, only Crank-Nicholson's scheme is described here because it allows for larger time steps and produces stable oscillations in case the stability criterion is violated [13]. In this scheme

$$\{T\}^{i+1} = \{T\}^i + \frac{\Delta t}{2}[\{\frac{\partial T}{\partial t}\}^i + \{\frac{\partial T}{\partial t}\}^{i+1}] \tag{5.21}$$

Using Equation (5.21) in Equation (5.17), we have after simplifications:

$$[[C] + \frac{\Delta t}{2}[K]]\{T\}^{i+1} = [[C] - \frac{\Delta t}{2}[K]]\{T\}^i + \frac{1}{2}[\{R\}^i + \{R\}^{i+1}] \tag{5.22}$$

or $$[A]\{T\}^{i+1} = [B]\{T\}^i + \{R\} \tag{5.23}$$

where

$$[A] = [C] + \frac{\Delta t}{2}[K] \tag{5.24}$$

$$[B] = [C] - \frac{\Delta t}{2}[K]\ ;\ \{R\}^i = \Delta t\{F\}^i \tag{5.25}$$

and $$\{R\} = \frac{1}{2}\{\{R\}^i + \{R\}^{i+1}\} \tag{5.26}$$

These equations form the time stepping algorithm.

There is a modified version of Crank-Nicholson's scheme called modified Crank-Nicholson's method [13]. If

average temperature of a time interval is defined as

$$\{T_a\} = \{\{T\}^i + \{T\}^{i+1}\}/2 \tag{5.27}$$

then

$$\{T\}^{i+1} = 2\{T_a\} - \{T\}^i \tag{5.28}$$

So above equation can be written as

$$[[C] + \frac{\Delta t}{2}[K]]\{2\{T_a\} - \{T\}^i\} = [[C] - \frac{\Delta t}{2}[K]]\{T\}^i + \frac{1}{2}\{\{R\}^i + \{R\}^{i+1}\} \tag{5.29}$$

or

$$[\frac{2}{\Delta t}[C] + [K]]\{T_a\} + \{R\}^a + \frac{2}{\Delta t}[C]\{T\}^i \tag{5.30}$$

Once $\{T_a\}$ is calculated for every step, $\{T\}^{i+1}$ is calculated by

$$\{T\}^{i+1} = 2\{T_a\} - \{T\}^i \tag{5.31}$$

Present program WELTEM for nonlinear heat transfer, uses this solution procedure.

5.4 Nonlinearity in Heat Transfer

5.4.1 Change of Material Properties with Temperature

Material properties such as heat capacitance, thermal conductivity. density etc. are in general temperature dependent. Many a times their temperature dependency can be neglected. But many mechanical processes such as welding, rolling etc. involve large range of temperature change and hence one cannot neglect change of material properties with temperature.

The easiest way of considering property changes with temperature is, by supplying values of properties at different temperatures. During transient calculation one can linearly interpolate values of properties for a particular element depending upon its average temperature, before every time step and compute its capacitance and conductivity matrices.

Interpolation of properties may be done depending upon the temperature of every gauss point or depending upon the average temperature of element. Former gives better result in terms of accuracy but involves more amount of computations.

5.4.2 Consideration of Thermal Radiation

Heat loss due to thermal radiation is very significant when high temperature boundaries are dealt with, such as during welding, casting etc. This is essentially a non-linear problem, because of explicit temperature dependency of heat loss on boundary temperatures.

For taking into consideration heat loss due to radiation one can define a factor h_r (coefficient of radiation heat transfer) similar to h_c (coefficient of convective heat transfer) such that heat loss due to radiation is equal to [14]

$$h_r (T - T_{at}) = \varepsilon_r \sigma_r (T^4 - T_{at}^4) \qquad (5.32)$$

where ε_r is emissivity, σ_r is Stefan-Boltzmann constant, T is the boundary temperature and T_{at} is the atmospheric

temperature. Hence

$$h_r = \varepsilon_r \sigma_r (T^2 + T_{at}^2)(T + T_{at}) \qquad (5.33)$$

To evaluate value of h_r, if one assumes linear temperature distribution within the interval $t - \Delta t$ to $t + \Delta t$, then

$$h_r = \frac{1}{2\Delta t} \int_{t-\Delta t}^{t+\Delta t} \varepsilon_r \sigma_r (T^2 + T_{at}^2)(T + T_{at})\, dt$$

$$\simeq \varepsilon_r \sigma_r \left[(T(t)^2 + T_{at}^2)(T(t) + T_{at}) + (T(t) - T(t - \Delta t))^2 \left(T(t) + \tfrac{1}{3} T_{at}\right)\right] \qquad (5.34)$$

Here T_{at} is assumed to be constant. Since right hand side of Equation (5.34) involves only known values of temperature, hence it can be calculated at every time step. ε_r is a material properties and hence may be a function of temperature also.

5.4.3 Phase Change

In different mechanical processes such as welding, casting etc., materials change phase during heating and cooling. This in turn affects the temperature distribution calculations during change of phase.

The mathematical model of liquidification or solidification alloys is complicated by the fact that there is a moving boundary, which is the interface between the solid phase and the liquid phase. In pure metals the phase change occurs at one freezing temperature. In case of alloys,

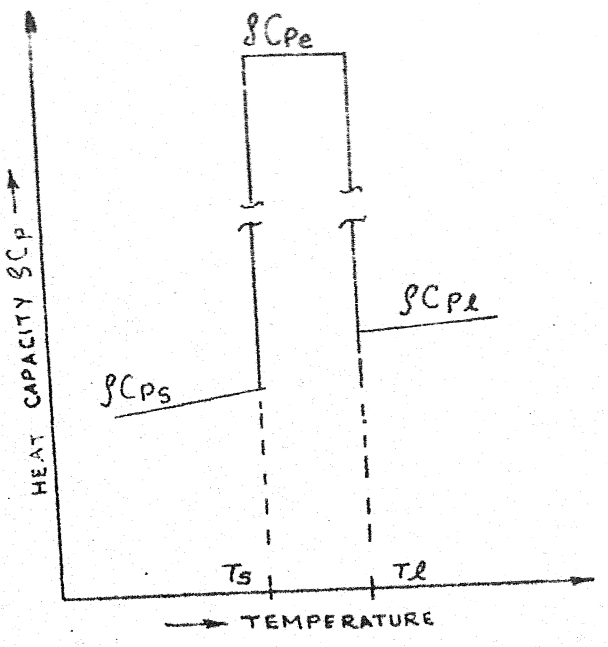

FIG. 5·1 DEFINITION OF ρCpe FOR PHASE CHANGE CONSIDERATION

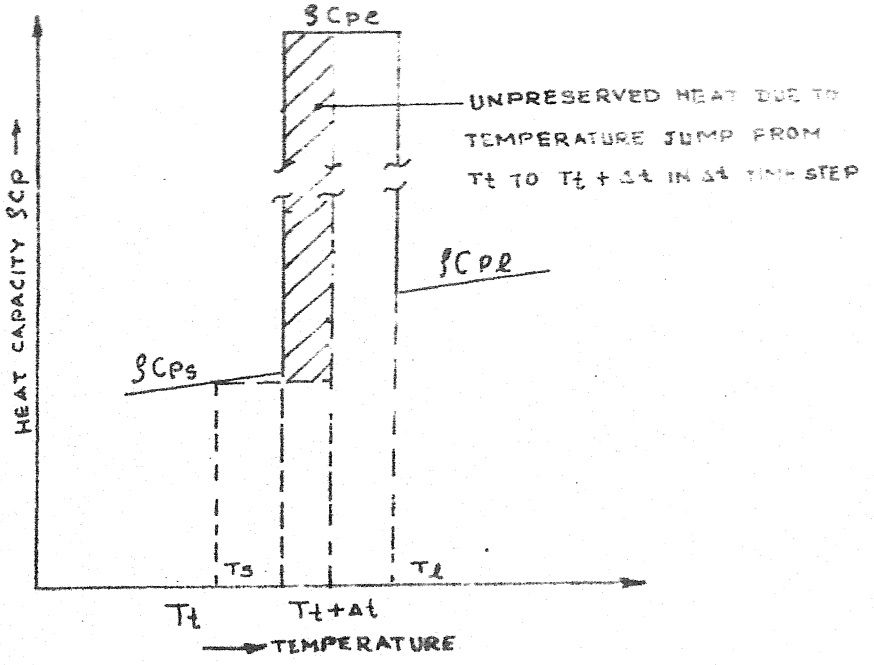

FIG. 5·2 SCHEMATIC DIAGRAM OF UNPRESERVED HEAT DUE TO DISCRETE TEMPERATURE JUMP

however, the phase change occurs between two temperature levels called the solidus and the liquidus temperatures. Above the liquidus the alloy is completely liquid, below the solidus it is completely solid, and in between the alloy consists of a mixture of solid and liquid. Hence, two moving boundaries, one at solidus temperature and the other at the liquidus temperature, exist during the solidification of an alloy. Keeping track of these boundaries in the finite element model, is very cumbersome. Therefore, in this work the concept of equivalent specific heat is used to approximate the solidification process.

This concept is from the facts that during phase change alloys either release or absorb large amount of heat without appreciable temperature change. This phenomena can be viewed in other way that during phase change apparent specific heat of alloys is very high and hence even for small temperature change large amount of heat is released or absorbed whatever the case may be. This apparent high specific heat C_{Pe} is found as follows.

As shown in Figure 5.1, C_{Ps} is the specific heat at solidus temperature and C_{Pl} is specific heat at liquidus temperature. L_H is latent heat of solidification and T_l and T_s are liquidus and solidus temperatures respectively. Then C_{Pe} can be approximated by

$$C_{Pe} = \frac{C_{Ps} + C_{Pl}}{2} + \frac{L_H}{(T_l - T_s)} \qquad (5.35)$$

The equivalent specific heat value calculated above can be used whenever the average temperature of the element

is between the liquidus and solidus temperatures. By this means, the effect of latent heat released during the alloy solidification is taken into account, and the overall heat balance is maintained.

But in this method, the greatest drawback is that, there is a tendency of either jumping the melting temperature range or entering the range leaving a gap between solidus temperature and average temperature of the element, as shown in Figure 5.2, and hence not preserving full latent heat, associated to that element.

Different methods are suggested to consider the phase change, to avoid upper mentioned drawbacks [22,40]. But all these methods are iterative and hence requires more computer time. To avoid this and also to make use of upper simple method, during the course of the present work, a modification was implemented in WELTEM, which was found very effective.

This modification is explained as follows for different cases:

Different notations used are:

$\bar{T}$ - temperature at the end of current iteration

T_1 - an estimated temperature for the next iteration, considering heat capacity $\overline{\rho c}$ corresponds to $\bar{T}$, shows a change of region. It is estimated from $\bar{T}$ by adding temperature increment of the previous iteration.

T_2 - an improved estimation to temperature for next iteration, considering a better approximation to heat capacity $(\rho c)_{av}$.

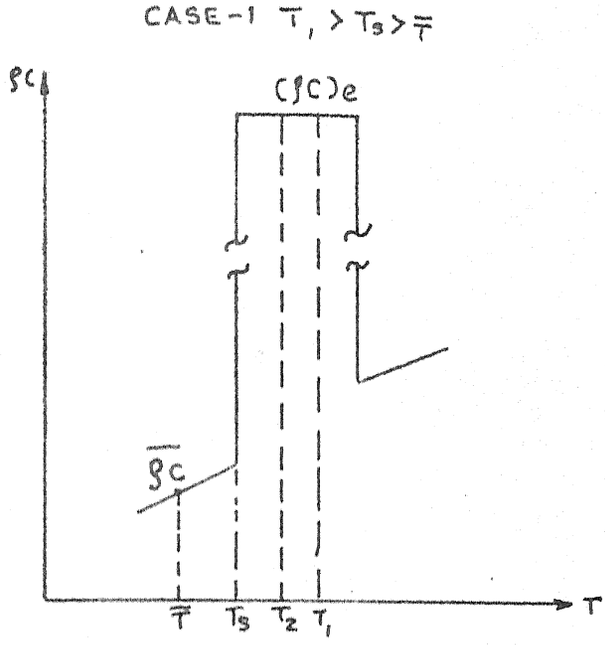

FIG. 5·3 (a)

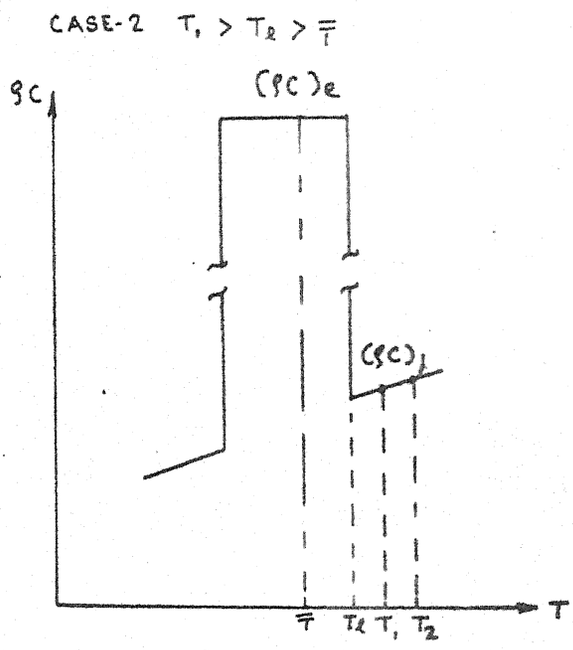

FIG. 5·3 (b)

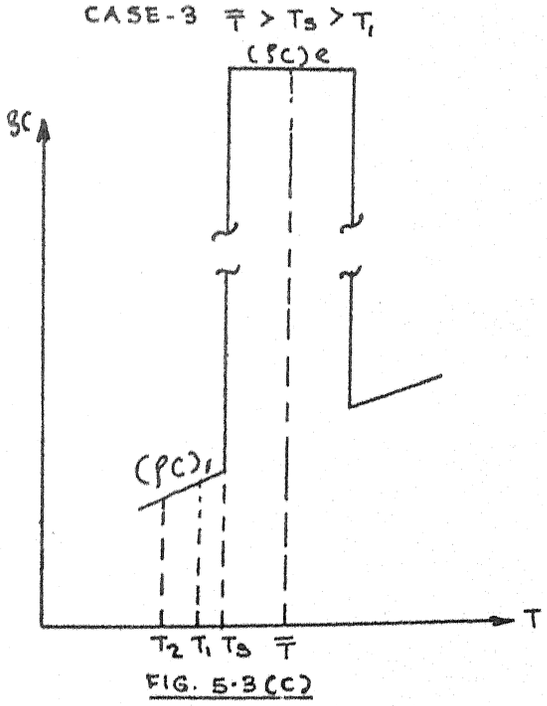

FIG. 5·3 (c)

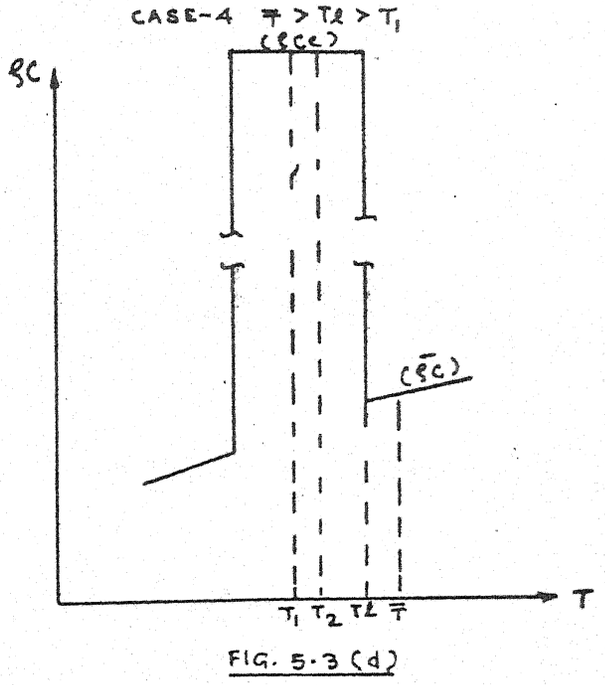

FIG. 5·3 (d)

FIG.-5·3 SCHEMATIC REPRESENTATIONS OF MODIFICATION IN PHASE CHANGE CALCULATIONS

Case 1 - $T_1 > T_s > \bar{T}$ (Ref.: Figure 5.3(a))

Heat absorbed from T_1 to $\bar{T}$ (considering heat capacity as $\overline{\rho c}$)

$$= \overline{\rho c}\,(T_1 - \bar{T}) \tag{5.36}$$

Let this heat to the element undergoing change of region be a constant. This assumption is justified as very few elements undergo a change of region in one iteration.

Since T_2 is a better estimation to T_1, hence by heat balance, we have

$$\overline{\rho c}\,(T_1 - \bar{T}) = \overline{\rho c}\,(T_s - \bar{T}) + (\rho c)_e\,(T_2 - T_s)$$

or $$T_2 = T_s + \frac{\overline{\rho c}}{(\rho c)_e}\,(T_1 - T_s) \tag{5.37}$$

Equation (5.37) is independent of $\bar{T}$ explicitly. Hence defining $(\rho c)_{av}$ as

$$(\rho c)_{av}\,(T_2 - \bar{T}) = \overline{\rho c}\,(T_s - \bar{T}) + (\rho c)_e\,(T_2 - T_s)$$

or $$(\rho c)_{av} = \frac{\overline{\rho c}\,(T_1 - \bar{T})}{(T_2 - \bar{T})} \tag{5.38}$$

Hence a better approximation to $\overline{\rho c}$ is $(\rho c)_{av}$, calculated by Equation (5.38).

For other cases, proceeding in a similar way, the expressions for T_2 and $(\rho c)_{av}$ are determined as follows.

Case 2 - $T_1 > T_1 > \bar{T}$ (Ref.: Figure 5.3(b))

$$T_2 = T_1 + \frac{(\rho c)_e\,(T_1 - T_1)}{(\rho c)_1} \tag{5.39}$$

and $$(\rho c)_{av} = \frac{\overline{\rho c}\,(T_1 - \bar{T})}{(T_2 - \bar{T})} \tag{5.40}$$

Case 3 - $\bar{T} > T_s > T_1$ (Ref.: Figure 5.3(c))

$$T_2 = T_s + \frac{(\rho c)_e}{(\rho c)_1} (T_1 - T_s) \tag{5.41}$$

$$(\rho c)_{av} = (\rho c)_e \frac{(T_1 - \bar{T})}{(T_2 - \bar{T})} \tag{5.42}$$

Case 4 - $\bar{T} > T_1 > T_1$ (Ref.: Figure 5.3(d))

$$T_2 = T_1 + \frac{\overline{\rho c}}{(\rho c)_e} (T_1 - T_1) \tag{5.43}$$

$$(\rho c)_{av} = \overline{\rho c} \left(\frac{T_1 - \bar{T}}{T_2 - \bar{T}}\right) \tag{5.44}$$

Any of the one pair of equations from Equations (5.37) to (5.44) can be used to calculate T_2 and $(\rho c)_{av}$, depending upon the case.

PART II

APPLICATIONS

CHAPTER 6

ANALYSIS OF WELDED STRUCTURES FOR RESIDUAL STRESSES

6.1 Introduction

The welding of metal structures is aimed at providing a means of joining together a number of components in such a way as to minimise the impairment of the properties of those components. Considerable effort has been expended on developing effective welding techniques for a large number of metals and alloys. Concurrent with these developments have been efforts aimed at identifying the various problems that results from welding processes, determining the strength of welded joints and structures subject to specified loading conditions, and establishing guidelines and criteria for most effective joint design. The information accumulated in these areas over the years has been overwhelmingly experimental. More recently, efforts have been directed toward developing analytical models to predict the thermal-mechanical response of welded structures.

Analytical formulations for predicting temperature distribution during welding are frequently obtained by assuming that the thermal energy supplied by the weld process can be idealized as a point or line heat source. Early work in this area focussed on quasi-stationary, transient temperature distributions resulting from a point heat source travelling at a constant speed along a line on an infinitely plate. The line heat source and moving point heat source have been used to obtain good correlation with temperature measurements for welding conditions. As an alternative to the analytical approach, numerical techniques like finite difference and finite element methods have also been used.

Analytical models for calculating stresses during welding have been developed based on the line heat source and moving point heat source. These techniques generally show good agreement between residual stresses of the model and experimental data but are often limited to single pass welds. The complexities inherent in performing analytical studies of welding stresses and distortions for various weld configurations - in particular, irregular geometries, inelastic material response and material loading and reloading - suggest the use of numerical methods to calculate residual stresses and distortions. Because of its generality, finite element method has been applied to study the behavior of the welded structures.

To show analysis capability of program THESIS, which has been developed during the present work, depending upon the theory presented in Chapters 3 and 4, stress transients during butt welding of two plates and longitudinal welding of a cylinder are presented here. In fact programs WELTEM and THESIS combined provide a complete set to compute temperature and stress transients during welding, casting, annealing etc.

6.2 Thermal Model

6.2.1 Quasi-Stationary Theory

Calculation of the transient temperature distribution is based on the attainment of quasi-stationary conditions, which are developed when the welding heat source is moving at constant speed on a regular path, and also end

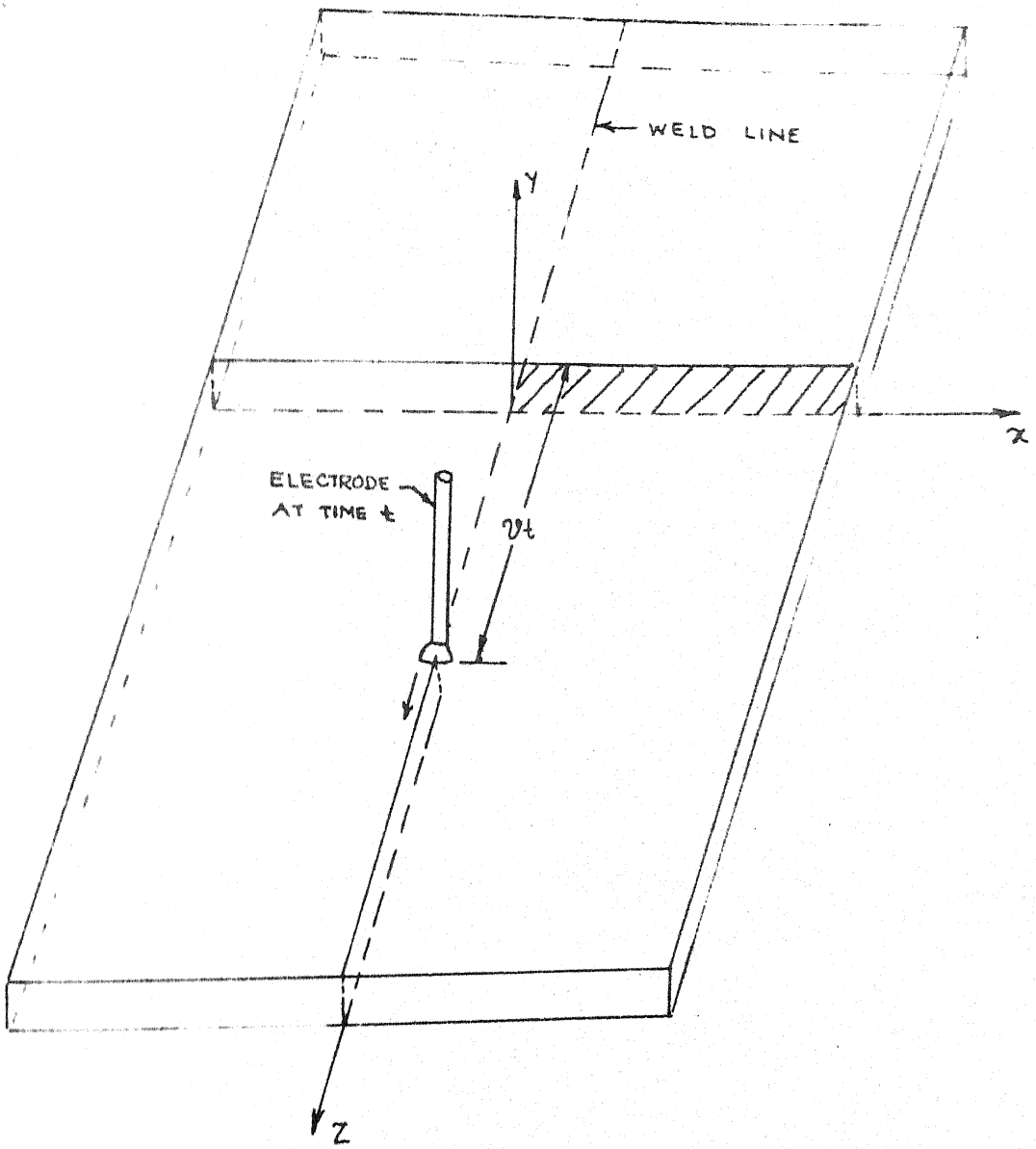

FIG. 6·1 WELDMENT CONFIGURATION

effects resulting from either initiation or termination of the heat source are neglected. The temperature distribution is then stationary with respect to a moving coordinate system whose origin coincides with the point of application of the heat source.

Considering the planar weld shown in Figure 6.1. The temperature at any point in the weldment is expressed functionally as:

$$T(x, y, z, t) = T(x, y, z, -vt) \tag{6.1}$$

where v is the welding speed. Thus, given the transient temperature distribution at any one section of the weldment defined, say, by z = 0, the temperature at any other section is determined by an appropriate shift of the time scale as follows:

$$T(x, y, z, t) = T(x, y, o, t - z/v) \tag{6.2}$$

The problem is therefore, reduced to finding the two dimensional, unsteady temperature field at a section normal to the weld line. A planar analysis may be used for this purpose when the weld speed, relative to a characteristics diffusion rate for the material, is sufficiently high so that the amount of heat conducted ahead of the weld torch is very small relative to the total heat input. In this case, the net heat flow across any infinitesimally thin slice of the weldment normal to the weld line is assumed to be negligible relative to the heat being diffused within the slice itself, that is, the term $\frac{\partial}{\partial Z}\left(K_Z(T)\,\frac{\partial T}{\partial Z}\right)$ is neglected in the heat conduction equation. Two dimensional

thermal analysis at the section Z = 0, normal to the direction of welding, is thus treated in the present work.

6.2.2 Heat Input and Distribution Calculations

Perhaps the most critical input data required for welding thermal analysis are the parameters necessary to describe the heat input to the weldment from the arc. Not only the magnitude, but the distribution of heat input will influence the dimensions of the weld metal and heat-affected zones, the cooling rates, and the peak temperature distribution, as well as the temperature gradients necessary to calculate stresses and distortions. The welding parameters required to formulate the heat flux boundary conditions are the magnitude of heat input from the arc Q, the distribution of the heat input, characterized by a length parameter , and the weld speed v. Introducing the arc efficiency η, Q is found simply from the formula

$$Q = \eta E I \tag{6.3}$$

where E and I are the arc voltage and current, respectively. The heat deposited per unit length of weld is merely Q/v. It must be recognized that a priori determination of the magnitude and distribution of heat input cannot, in general, be made due to the lack of knowledge regarding energy transfer from the arc to the workpiece. Investigations of the physics of the welding arc are required to shed light on this area.

The heat from the welding arc is, at any given time, assumed to be deposited on the surface of the weldment as a

radially symmetric normal distribution function [11].
Letting r be the distance from the center of the heat source, which is coincident with the axis of the electrode, the heat flux q is given by

$$q(r) = q_o e^{-c r^2} \tag{6.4}$$

where q_o and c are constants determined by the magnitude and distribution of the heat input.

The heat input parameters Q and $\bar{r}$ are defined by [11]

$$Q = 2\pi \int_0^\infty q(r)\, r\, dr \tag{6.5}$$

and

$$q(\bar{r}) = 0.05\, q_o \tag{6.6}$$

Then Equation (6.4) becomes

$$q(r) = \frac{3Q}{\pi \bar{r}^2} e^{-\left[3\left(\frac{r}{\bar{r}}\right)^2\right]} \tag{6.7}$$

Here $\bar{r}$ defines the region in which 95 percent of the heat flux is deposited. Let x be the distance from the weld line in the section Z = 0 and t = 0 is the time at which the centre of the heat source (electrode) passes over this section. The heat flux distribution on the surface of the weldments, directed parallel to the electrode, is given by [11]

$$q(x, t) = \frac{3Q}{\pi \bar{r}^2} e^{-\left[3\left(\frac{r}{\bar{r}}\right)^2\right]} e^{-\left[3\left(\frac{vt}{\bar{r}}\right)^2\right]} \tag{6.8}$$

The three welding parameters Q, $\bar{r}$ and v are all embodied in this formula.

6.3 Stress and Distortion Model

6.3.1 2-D Simulation of Welding Process for Stress Calculations

A complete thorough determination of the mechanical response due to the welding thermal cycle, as determined by the quasi-stationary temperature analysis, would require a full three dimensional incremental plasticity analysis with, at the least, recalculation of the stiffness coefficients at each time step. Computer run times would be very large and the cost, therefore, will be prohibitive. Hence in the present work, the section normal to the weld direction, is analysed. This implies that all sections normal to the weld line remain plane during the entire welding process. Though this assumption is probably adequate in regions somewhat removed from the weld puddle, it may not be valid in the neighborhood of the molten metal. The approach employed at present therefore prevents calculation of distortions ahead of the welding arc, and may inhibit accurate computations of deformations in the immediate vicinity of the weld puddle. It nevertheless enables the essential features of the mechanical response during cool down to be modelled, and the resultant residual stresses and distortions to be calculated.

6.3.2 A Model for Simulating Melted Domain

The stiffness becomes negligible as the melting range is approached, but the material also is relatively incompressible in the molten state. In order to model this behavior and, at the same time, to avoid possible ill-behavior

of the solution process and thus facilitate convergence, the elastic modulus approaches zero and the poisson's ratio one half, in such a way that the bulk modulus is maintained at its room temperature value through the entire high temperature range, including the phase transition and the liquid state.

For illustration, since for plane strain case stress-strain matrix [D] is given by

$$[D] = \frac{E}{(1+\nu)(1-2\nu)} \begin{bmatrix} 1-\nu & \nu & 0 \\ \nu & 1 & 0 \\ 0 & & \frac{1-2\nu}{2} \end{bmatrix}$$

for melted region enforcing the conditions $E \to 0$, $\nu \to 0.5$ such that $\frac{E}{3(1-2\nu)} \to B_m$. Hence

$$[D] = B_m \begin{bmatrix} 1 & 1 & 0 \\ 1 & 1 & 0 \\ 0 & 0 & 0 \end{bmatrix} \qquad (6.9)$$

Since compressibility has no effect on the generalized plastic strain, no plastic strain is, as expected, accumulated in the weld puddle.

6.3.3 Stress Calculations by Finite Element Method

Stress transient computations during welding of a plane stress or plane strain or axisymmetric structure can be done by computer program THESIS. Theory of isoparametric finite element is given in Appendix 1 and calculations of material matrix and load vector are shown for a

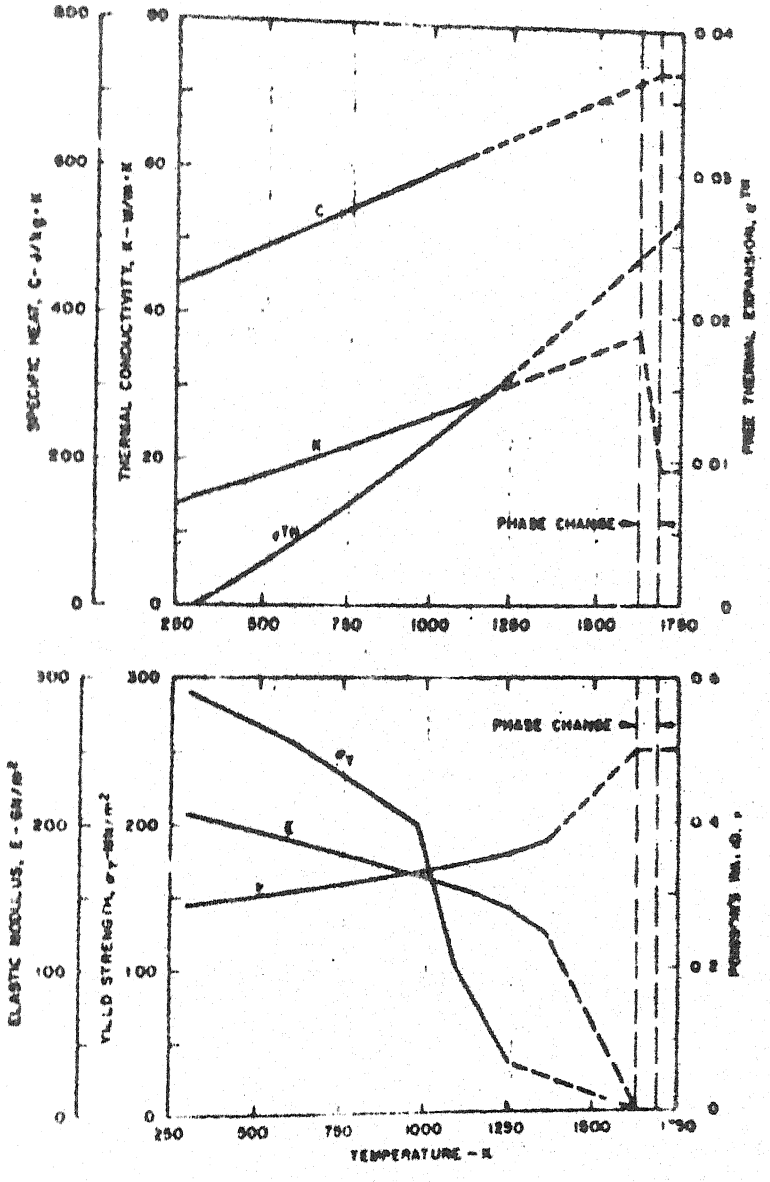

FIG. 6.2 MATERIAL PROPERTIES

2-D thermoplastic structure in Chapter 3. Solution procedure along with elastic-plastic transient calculations adopted by program THESIS are also shown in Chapter 3.

6.4 Solved Examples

6.4.1 A Note on Material Properties

The weldment material properties employed are those as used by Friedman [20], which are essentially for Inconel alloy 600, an alloy of nickel, chromium and iron.

Variation of Material Properties with Temperature - Variations of $E, \nu, \sigma_y, c_p, K, \varepsilon^{Th}$ with temperature are shown in Figure 6.2, taken from [20].

Density and Latent Heat - Density is taken as 8430 Kg/m^3 and latent heat as 309 kJ/Kg. The solidus and liquidus temperatures are taken 1630°K and 1690°K respectively.

Hardening Rule - Isotropic strain hardening of the yield surface is assumed, with the rule

$$\bar{\sigma} = \sigma_y \left(\bar{\varepsilon}^{PL}/0.002\right)^{\frac{1}{11}} \tag{6.10}$$

Effect of Recrystallization - Following empirical expression is used to approximate the reduction of previously accumulated plastic strain at high temperatures

$$\varepsilon_{ij}^{PL} \rightarrow f(T)\, \varepsilon_{ij}^{PL} \tag{6.11}$$

where
$$f(T) = e^{0.02(T-T_m)} \quad \text{if } T \leq T_m$$
$$= 0 \quad \text{if } T \geq T_m \tag{6.12}$$

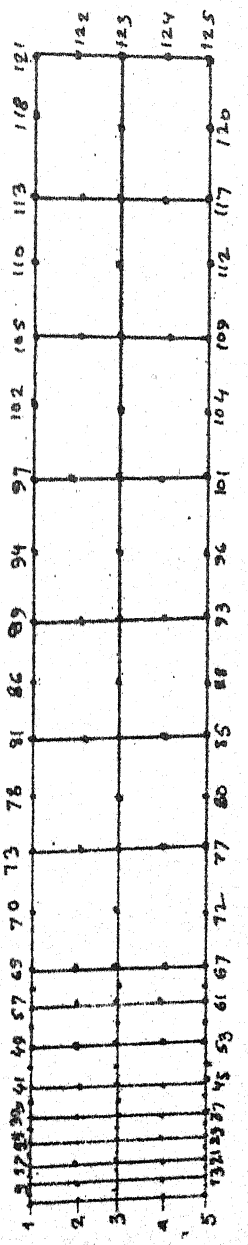

FIG. - 6·3 DISCRETIZATION OF PLATE FOR WELDING ANALYSIS

where T_m = melting temperature = 1630°K.

6.4.2 Analysis of Butt Weld of Two Plates

Aim to analyse this case here is to compare the results of THESIS and by other authors [20] using different analysis procedure.

Problem consists of a 2.54 mm thick flat plate of width 150 mm. The section is assumed in a plane strain condition, with the heat input data as (Ref.: Equation (6.8))

$$Q = 703 \text{ W}$$

$$\bar{r} = 5.08 \text{ mm}$$

$$v = 2.12 \text{ mm/sec}$$

Other material properties are taken, as explained in Section 6.4.1. Temperature transient analysis of this case was done by WELTEM and was reported in [30] by the present author. Since object of the analysis of this case, during the present work, is to test the formulation given in Chapter 3, hence temperature distribution was used from Figure 4 of [20], instead of solving by WELTEM, to avoid any incompatibility in temperature distribution during the analysis.

In the present analysis only 50 mm from the line of welding is considered for finite element discretization, as no stresses are developed after this length, as shown in Figure 7 of [20]. There are 30 elements and 125 nodes with two degrees of freedom per node used for the finite element model. Figure 6.3 shows this discretization as plotted by computer.

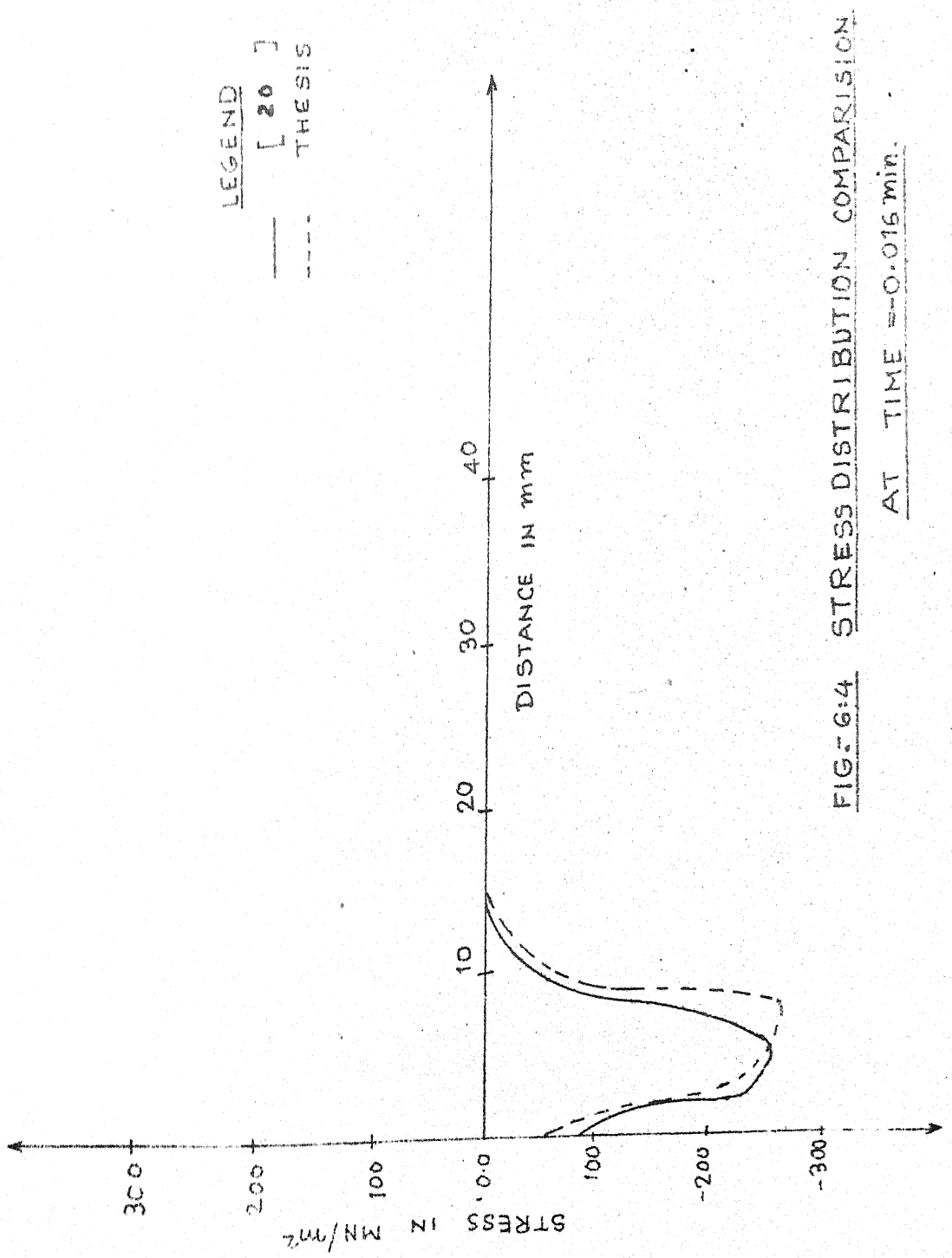

FIG.- 6:4 STRESS DISTRIBUTION COMPARISION AT TIME =-0.016 min.

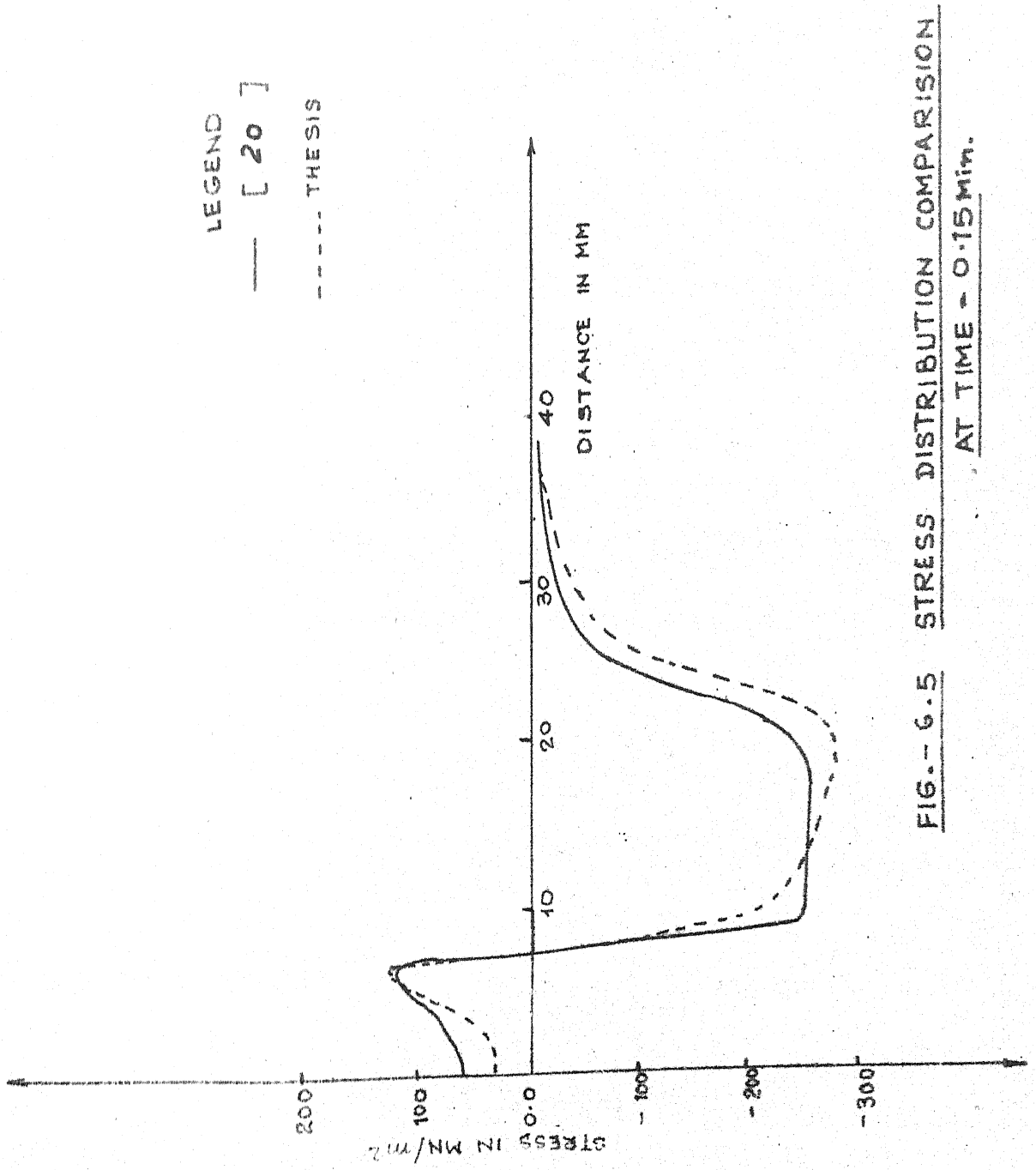

FIG.- 6.5 STRESS DISTRIBUTION COMPARISION AT TIME = 0.15 Min.

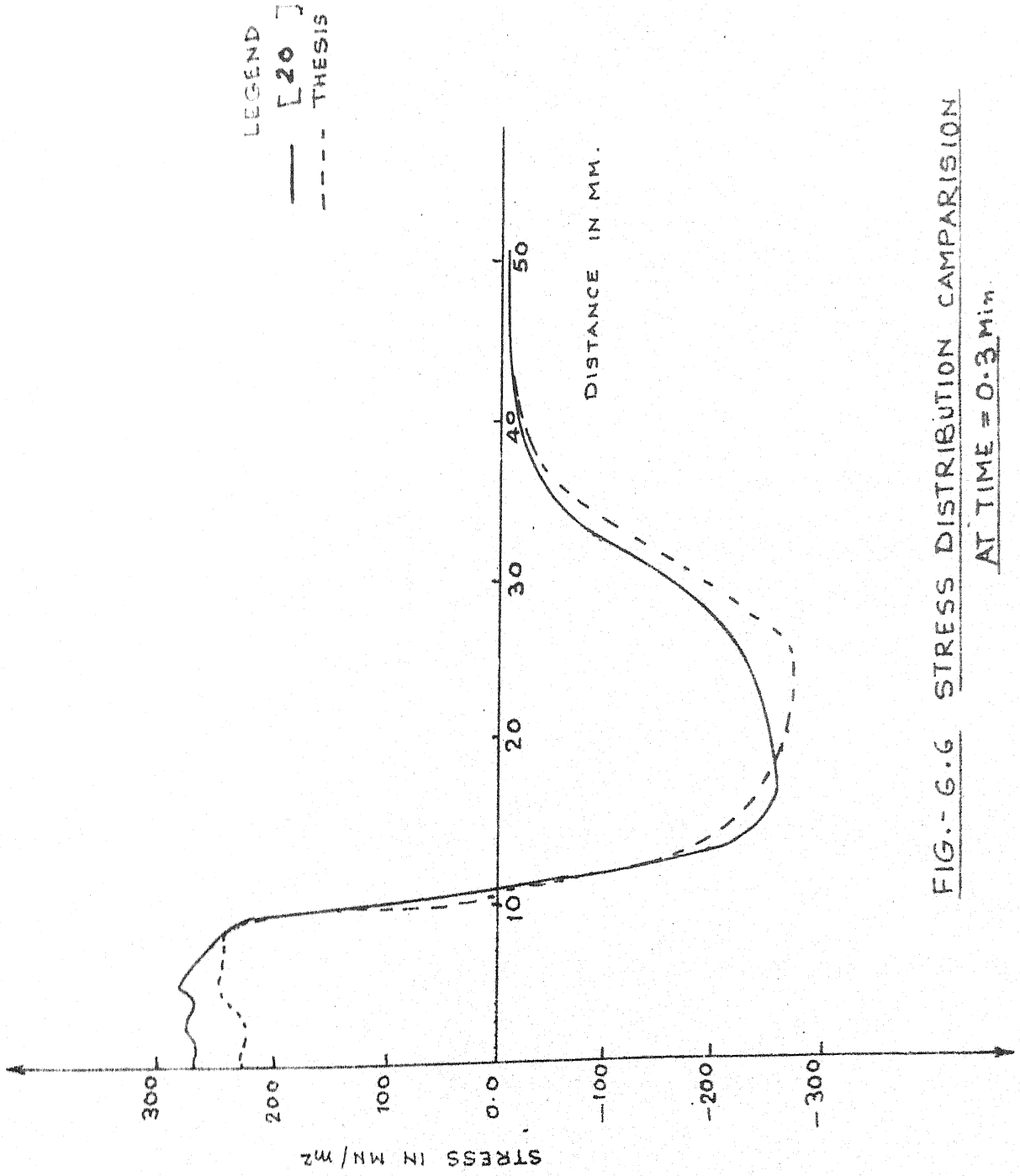

FIG.- 6.6 STRESS DISTRIBUTION CAMPARISION AT TIME = 0.3 Min.

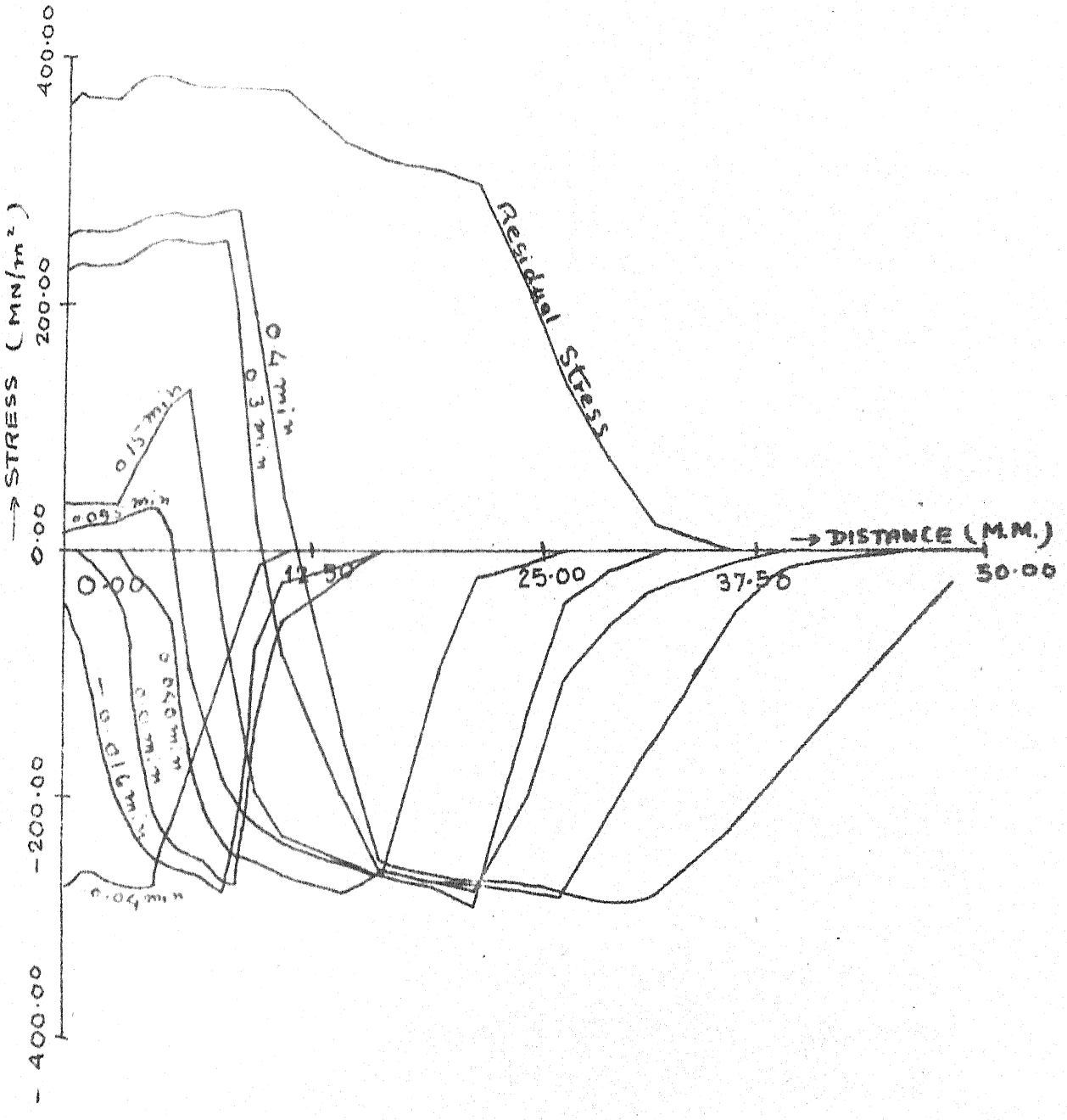

FIG. 6·7 STRESS TRANSIENTS DURING PLATE WELDING

Figures 6.4 to 6.6 show the mid surface Z direction stress variation at times -0.016 min, 0.15 min and 0.3 min respectively. Comparison with [20] shows, a close agreement, though the formulations used in both cases are entirely different. A careful comparison reveals that stresses calculated by THESIS in heat affected zone are lower than shown in [20]. This difference of stresses is reported, without giving any proof, by Rybicki et al in their paper 'A Finite Element Model for Residual Stresses in Girth Butt Welded Pipes' published in [7]. Figure 6.7 shows complete mid surface σ_z variations at different timings.

6.4.3 Analysis of Longitudinal Welding of a Cylinder

Program WELTEM and THESIS have been used to analyse longitudinal welding of a cylinder for temperature and stress transients.

For this, a cylinder of 50 mm radius is discretized with 50 finite elements and 205 nodes. Material properties and heat input data are again taken as given in Section 6.4.1.

Figure 6.8 shows the finite element model of the cross-section of cylinder, assumed in a plane strain condition. Figures 6.9 and 6.10 show temperature transient and mid surface stress σ_z variation along the circumference for different time intervals.

Stress transients show that upon initial heat up, the localization of severe temperature gradients in the immediate vicinity of the weld line produces compressive yielding in this region. A temperature increases, the

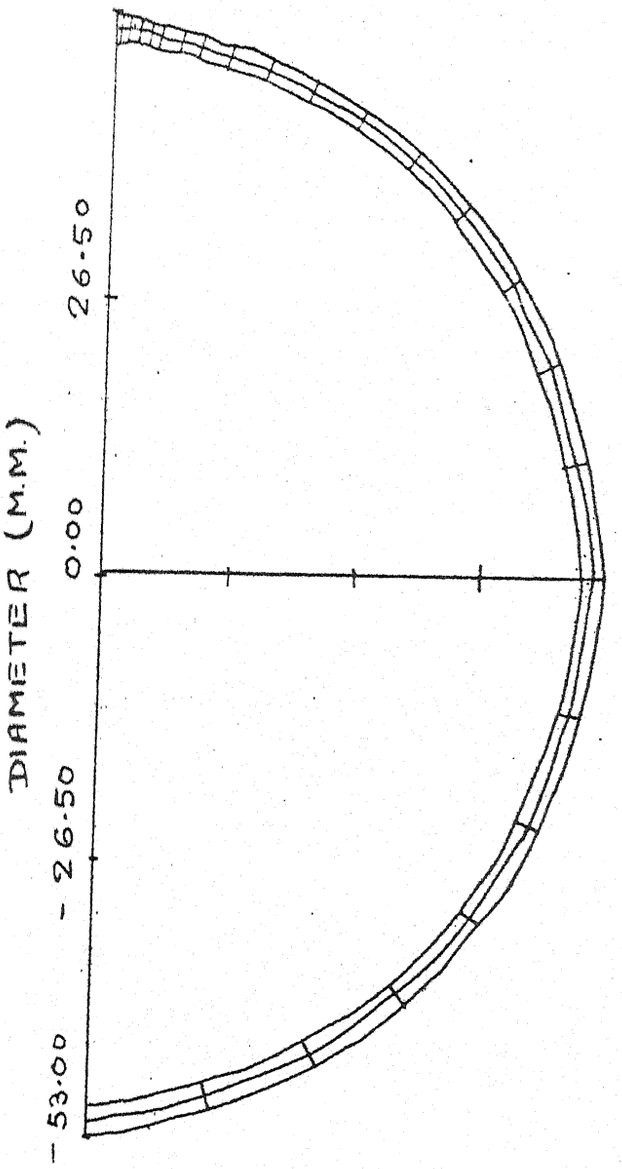

FIG.- G:8 DISCRETIZATION OF CYLINDER FOR LONGITUDINAL WELDING ANALYSIS

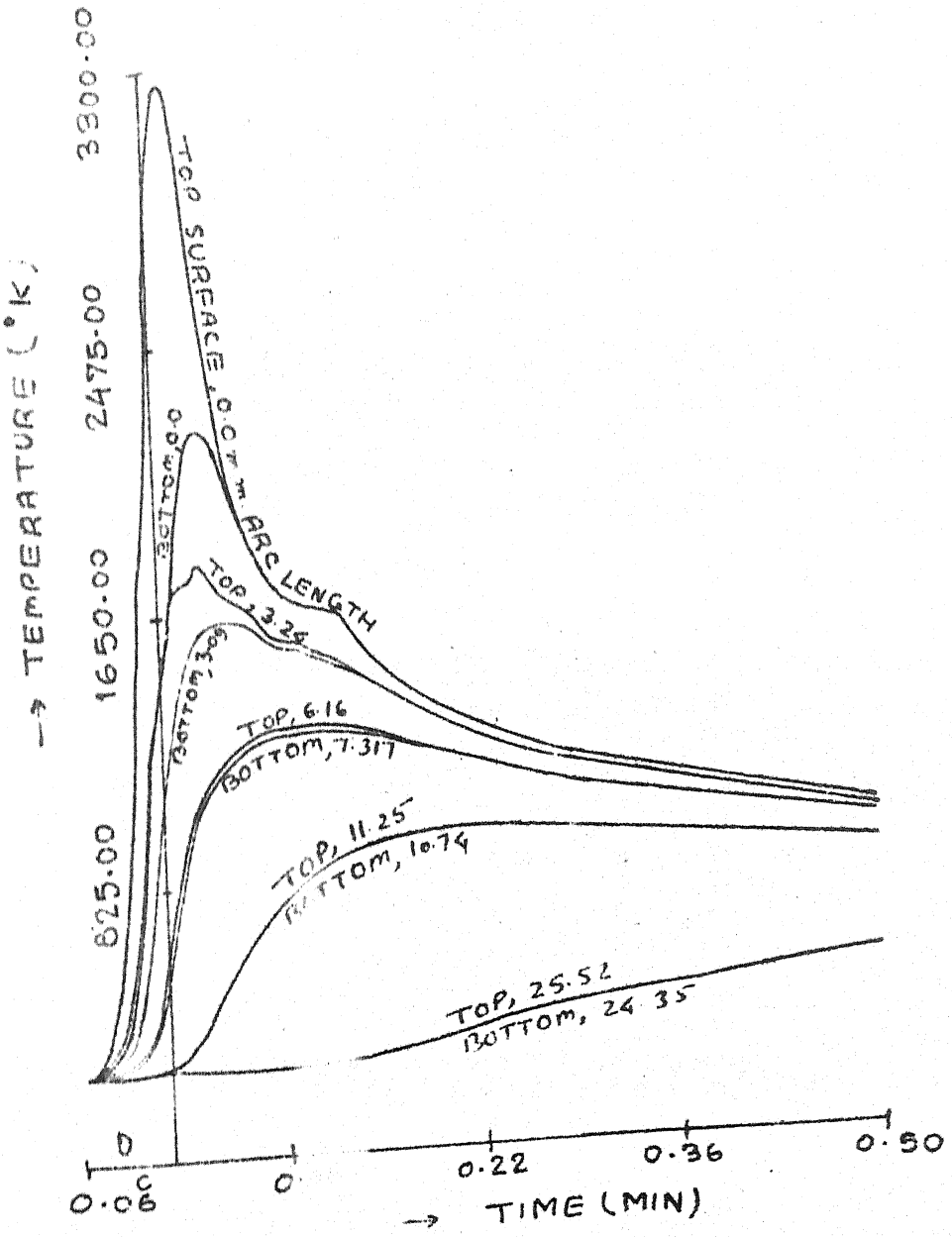

FIG. 6. TEMPERATURE DISTRIBUTION DURING CYLINDER WELDING

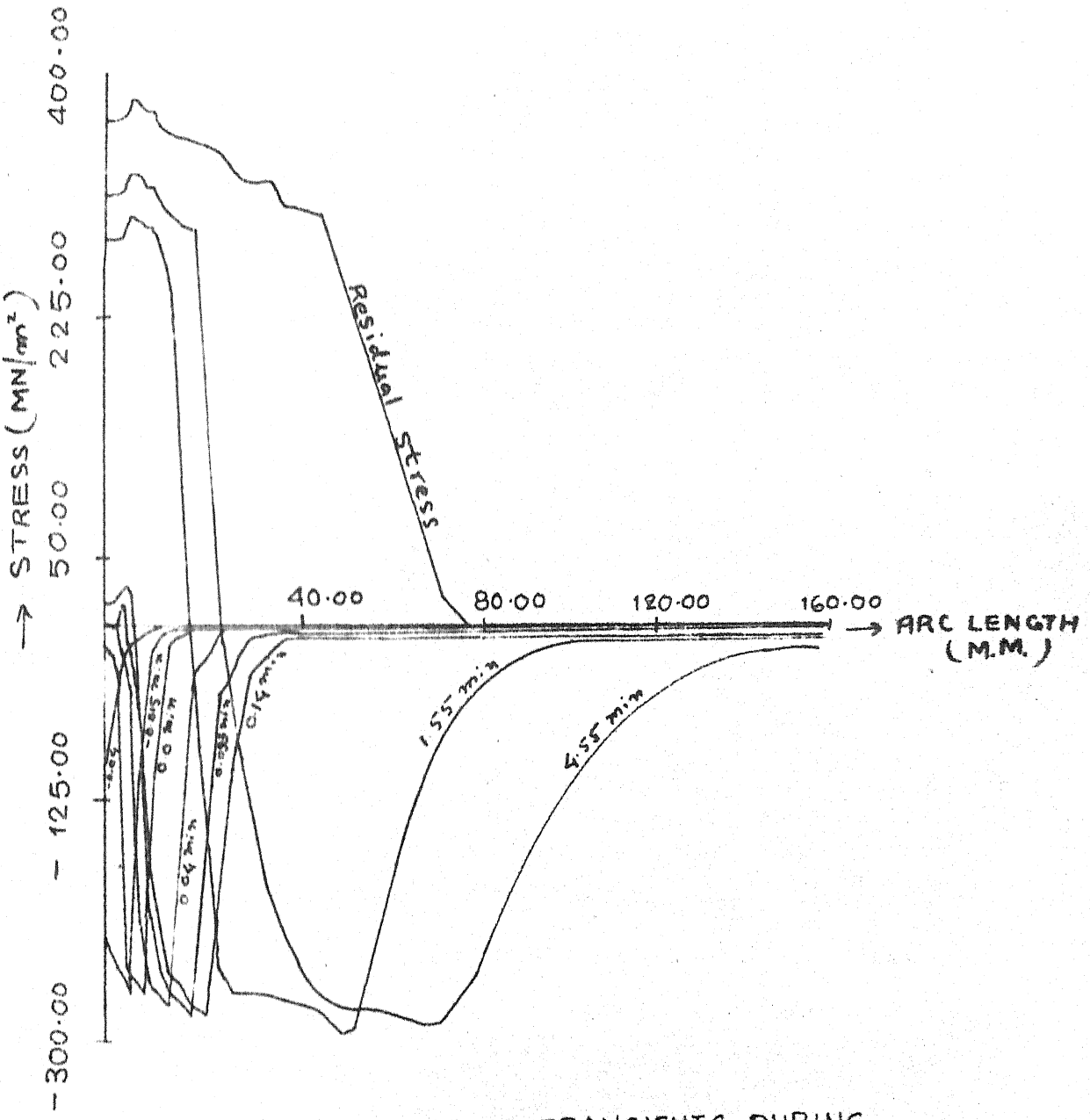

FIG.-6.10 STRESS TRANSIENTS DURING CYLINDER WELDING

yield strength quickly decreases untill, at the melting point, it is negligible. During the time period prior to solidification of the weld metal, all material outside the puddle is in compression with that region immediately adjacent to the molten zone in a plastic state of stress. Upon solidification, the fusion zone material yields initially in compression at rather low stress levels. Upon further cooling tensile stresses are produced after unloading at heat affected zone. Hence, as cooldown proceeds, that portion of the weldment that is in tension longitudinally grows steadily until, at final cool-down, the residual longitudinal stresses, which are appreciable only in the region within about 80 mm of the weld centerline, are completely tensile. This is due to the plane strain restrictions placed on the analysis. The residual stresses in the plastic region exceed the room temperature yield strength because of material strain hardening, which is such that the initial short time compressive yielding produces an expansion of the yield surface followed, during cool-down, by yielding in tension at a stress level higher than the room temperature yield strength.

CHAPTER 7

ANNEALING OF WELDED STRUCTURES

7.1 Introduction

It has been shown in Chapter 6, that the residual stresses at the welded joint are generally above the yield point at room temperature. These high residual stresses reduce the life of the component. Therefore it is necessary to releive these stresses either by heat treatment or by some other mechanical method such as vibratory stress relief. Annealing is a type of popular heat treatment process, in which welded structure is heated below recrystallisation temperature slowly and is kept for a long time at that temperature and then cooled down to room temperature slowly.

Relaxation of residual stresses occurs initially during heating due to the decrease of yield point and Young's modulus and then due to generation of creep strain.

The program THESIS can be used to predict stress transient in the welded structure during annealing. To show the capability of THESIS, results of annealing of two structures are presented here. In both cases creep properties are taken as described in Section 4.5.1.

7.2 Annealing of Butt Welded Plate

Butt weld of two plates, as described in Section 6.4.2, is solved for annealing. The plates were assumed to be heated up to 600°C at the rate of 600°C/hr and held at this temperature for 2 hrs and then cooled to room temperature at the rate of 600°C/hr.

The residual stress obtained from the analysis of Section 6.4.2 was used as input for annealing analysis. The

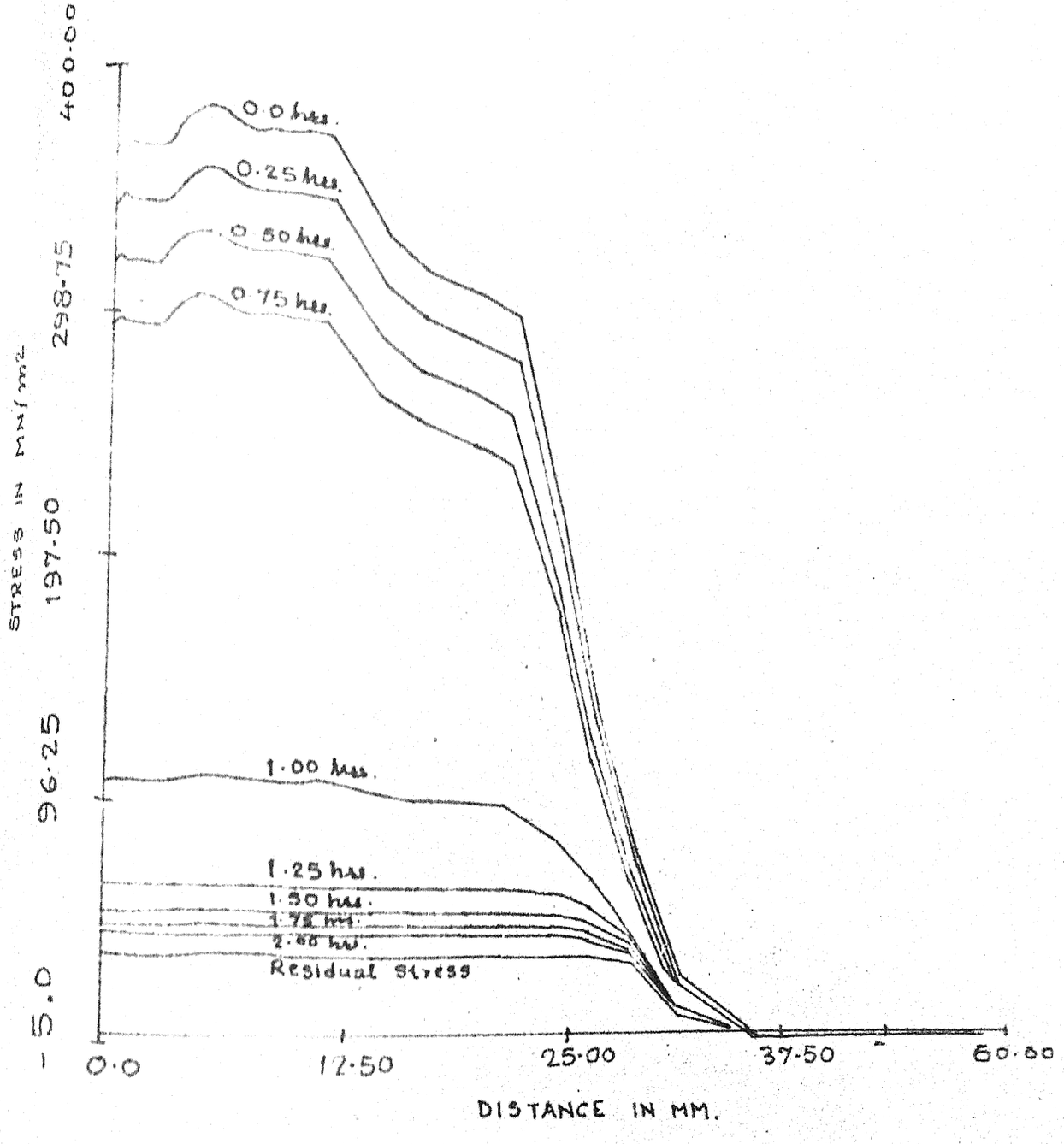

FIG. - 7·1 ANNELING OF WELDED PLATE

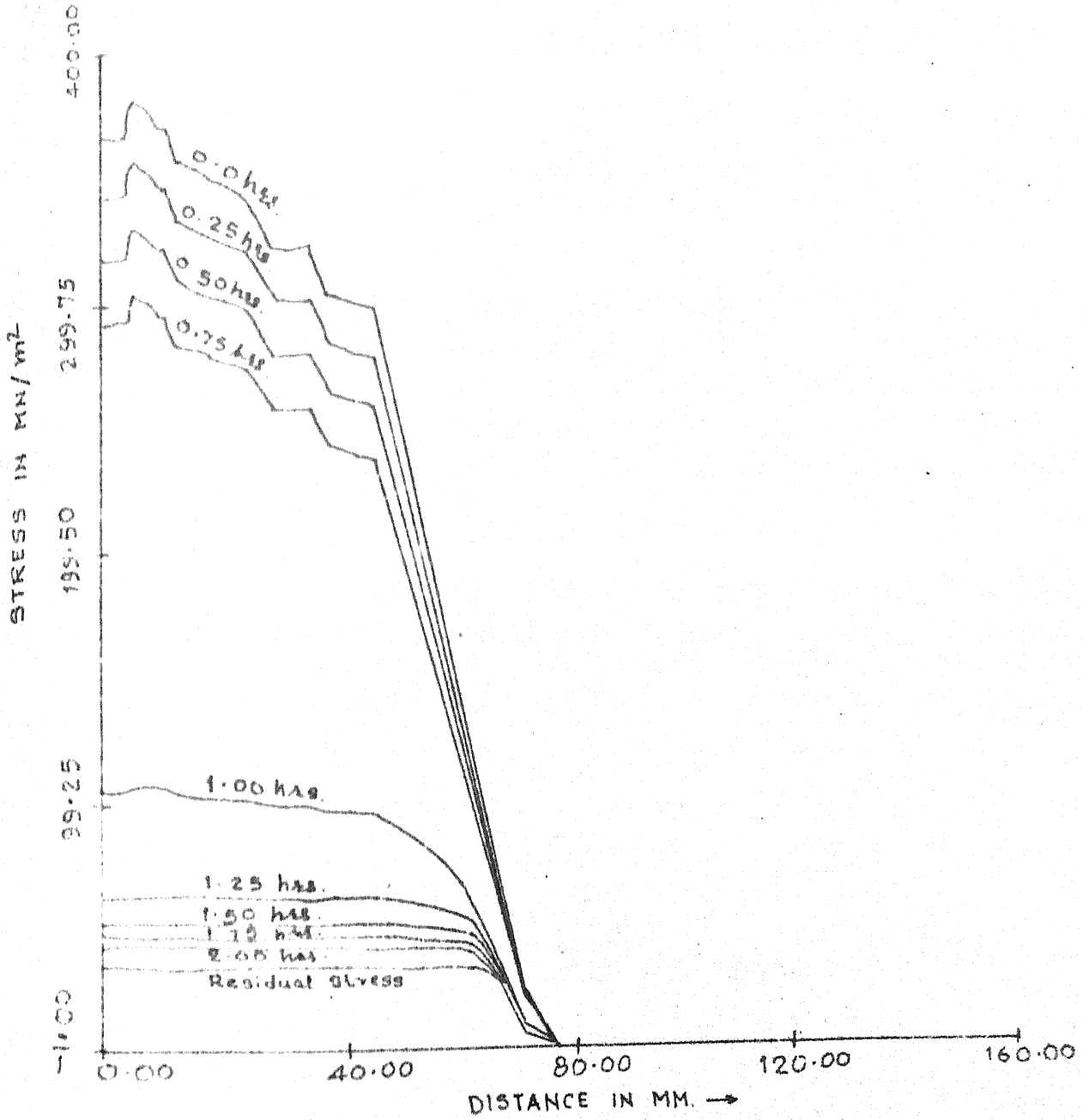

FIG. - 7.2 ANN LING OF WELDED CYLINDER

stress transients during complete annealing at different time intervals are shown in Figure 7.1, as plotted by computer.

7.3 Annealing of Butt Welded Cylinder

The example of longitudinal weld of a cylinder, described in Section 6.4.3, was then analysed for annealing. For this, again the cylinder is heated to a 600°C temperature in one hour and then held at this temperature for two hours and is then cooled to room temperature in one hour time. The stress transients during this annealing cycle is plotted by computer for different time intervals are shown in Figure 7.2.

In both the above analysis, it is seen that residual stress decreases slowly till 400°C and decreases rapidly afterwards because of the generation of creep strain. No significant increase in residual stress is obtained while cooling the structure, though yield point and Young's modulus increase. This is because of the generation of large creep strain during the two hours of holding time at constant temperature which completely dominates the process of stress relief.

CHAPTER 8

CONCLUSIONS AND FUTURE WORK

8.1 Conclusions

8.2 Future Work

8.1 Conclusions

A thermo-plastic formulation with creep for plane strain case is derived and used to solve different problems, along with welding and annealing.

Finite element technique is used to solve the whole structure and found to be very useful for nonlinear problems also. Tangent stiffness solution procedure is used for time stepping algorithm. It is seen that drift from yield surface can be made very small provided load increment in every iteration is kept low and remaining unbalance force is added to the load vector of the next iteration. This way internal iterations can be avoided and hence less computer time. Since in plane-strain formulation, stiffness as well as load vector are functions of stress field of the previous iteration, it is necessary to compute stress field very accurately, as small error diverges through further iterations. This precaution is more valid whenever there is elastic-plastic or plastic-elastic transition. Hence internal iterations should be done to bring the stress of a transition point to the yield surface.

Though the thermo-plastic formulation and solution procedure for the butt welding of two plates adopted in program THESIS and in [20] are entirely different, a close agreement of the temporal stresses distribution computed by both methods is obtained. Stresses at the heat affected zone calculated of THESIS is found lower than reported in [20].

Stress transients during annealing of butt welded plates or cylinder show slow decrease of residual stresses during initial heat up till 400°C. After this, stresses decrease rapidly due to the generation of creep strain. When the structure is kept at 600°C for two hours and then cooled to room temperature, a negligible increase in stresses occur. This is due to the generation of large creep strain during holding time, which dominates the while stress distribution.

8.2 Future Work

Present computer program THESIS can be modified for taking into consideration multipass welding of structures. Also since during the entire range of temperature, there is phase transformation of iron, coefficient of thermal expansion changes significantly within phase transformation temperature range. Present computer program can also be modified to take into account change in coefficient of thermal expansion due to this factor.

Experimental verifications of residual stress distribution during butt welding should be done to test validity of the theory and solution procedure used. Though some efforts have been put by different authors [10,11,19,21] to measure residual stresses during butt welding, but present author intends to do experiments for electron beam welding. Because of less radiation heat loss, good control on heat input data, less heat affected zone, a better mathematical simulation is obtained for electron beam welding and hence

a better comparison of stress and temperature variations is expected.

Though present computer program has only been used to solve welding and annealing problems, stress transients during casting can also be computed by this program. With little modifications, capability of the present program can be extended to predict stress transients during other mechanical processes such as grinding etc.

REFERENCES

1) Zienkiewicz O.C., 'The Finite Element Method', McGraw Hill, Third Edition, 1977.

2) Benham P.P. and Hoyle R., 'Thermal Stress', Pitman & Sons, 1964.

3) Cook R.D., 'Concepts and Applications of Finite Element Method', John Wiley & Sons, Second Edition, 1981.

4) Masubuchi K., 'Analysis of Welded Structures', Pergamon Press, First Edition, 1980.

5) Timoshenko S.P., Goodier J.N., 'Theory of Elasticity', McGraw Hill, International Student Edition, 1970.

6) Nayak G.C., 'Plasticity and Large Deformation Problems by Finite Element Method', Ph.D. Thesis, University College of Swansea, 1971.

7) Jones R., Armen H., Fong J.T., 'Numerical Modeling of Manufacturing Processes', ASME, Atlanta, Georgia, Nov. 27-Dec. 2, 1977.

8) Hargegard G., Larsson S.G., 'On the Finite Element Analysis of Elastic-Plastic Structures Under Plane Strain Conditions', Institutionen fur hallfasthetslara, Kungl Tekniska Hagskolan, Stockholm, 1972.

9) Han T.R., Too J.J.M., 'Analysis of Residual Stresses/Strains in Pressure Vessels Due to Cyclic Thermomechanical Loads', Internal Report, Atomic Energy of Canada Ltd.

10) Masubuchi K., 'Transient Thermal Stresses and Distortion During Welding', NASA Report, 1970.

11) Hibbitt H.D., 'Thermo-mechanical Analysis of Welded Joints and Structures', Report prepared for presentation at the Fourth Army Materials Technology Conference, Boston, Massachusetts, Sept. 16-19, 1975.

12) Beer G., Meek J.L., 'The Analysis of Thermal Stress Involving Non-Linear Material Behavior', Research Report No. CE10, University of Queensland, April 1980.

13) Orivuori Seppo, 'Efficient Method for Solution of Nonlinear Heat Conduction Problems', IJNME, Vol. 14, 1461-1476 (1979).

14) Comini G., Guidice S.D., Lewis R.W., Zienkiewicz O.C., 'Finite Element Solution of Non-Linear Heat Conduction

Problems with Special Reference to Phase Change', IJNME, Vol. 8, 613-624 (1974).

15) Chang T.Y., Chu S.C., 'Elastic-Plastic Deformation of Cylindrical Pressure Vessels Under Cyclic Loading', NED 27, 228-237 (1974).

16) Bathe K.J., Khoshgoftaar M.R., 'Finite Element Formulation and Solution of Nonlinear Heat Transfer', NED 51, 389-401 (1979).

17) Ueda Y., Yamakawa T., 'Thermal Stress Analysis of Metals with Temperature Dependent Mechanical Properties', Proc. International Conf. on Mechanical Behavior of Materials', Vol. III, 1972.

18) Ueda Y., Fukuda K., 'Application of Finite Element Method for Analysis on Process of Stress Relief Annealing', Trans. Japan Welding Society, Vol. 8, No. 1, 1977.

19) Ueda Y., Yamakawa T., 'Analysis of Thermal Elastic-Plastic Stress and Strain During Welding by Finite Element Method', Trans. Japan Welding Society, Vol. 2, No. 2, 1971.

20) Friedman E., 'Thermomechanical Analysis of the Welding Process Using the Finite Element Method', JPVT, Vol. 97, Aug. 1975.

21) Friedman E., 'Numerical Simulation of the Gas Tungsten-Arc Welding Process', Numerical Modeling of Manufacturing Processes, PVP-PB-025, 1977.

22) Friedman E., 'An Iterative Procedure for Including Phase Change in Transient Heat Conduction Programs and its Incorporation into the Finite Element Method', Proc. of the 17th National Heat Transfer Conference, AIChE, Salt Lake, Utah, Aug. 1977.

23) Friedman E., 'Analysis of Weld Puddle Distortion and its Effect on Penetration', Welding Journal, June 1978.

24) Friedman E., 'Investigation of Alloy 600 Welding Parameters', Welding Journal, April 1975.

25) Owen D.R.J., Hinton E., 'Finite Element in Plasticity: Theory and Practice', Pineridge Press Ltd., Swansea, U.K., 1980.

26) 'Refresher Course on Engineering Design by Finite Element Method', Lecture Notes, Component Analysis Section, RED, BARC, 1981.

27) Dutta B.K., Kushwaha H.S., Kakodkar A., 'Elasto-Plastic Analysis of Plane Stress/Plane Strain and Axisymmetric Bodies by Finite Element Method', Internal Report No. 1146, BARC (1982).

28) Dutta B.K., Kushwaha H.S., Kakodkar A., 'Geometric Nonlinear Problems in Structures and a Computer Code (NLISA) for Static and Dynamic Nonlinear Analysis of Plane Stress/Strain and Axisymmetric Structures by Finite Element Technique', Internal Report No. I-669, BARC (1981).

29) Dutta B.K., Kushwaha H.S., Kakodkar, A., 'Computer Program WELTEM (Analysis of Two Dimensional Heat Transfer Problems by Finite Element Technique) Theory and User's Manual', Internal Report No. I-671, BARC (1981).

30) Dutta B.K., Kushwaha, H.S., Kakodkar A., 'Thermal Response Analysis for Nonlinear Heat Transfer Problem by Finite Element Method', 6th National Heat and Mass Transfer Conference, E-23 (1981).

31) Johnson W., Mellor P.B., 'Engineering Plasticity', Van Nostrand Reinhold Company, 1973.

32) Yamada Y., Yoshimura N., Sakurai T., 'Plastic Stress-Strain Matrix and Its Application for the Solution of Elastic-Plastic Problems by the Finite Element Method', IJM Sci., Vol. 10, No. 5, 343-354 (1968).

33) Marcal P.V., King I.P., 'Elastic-Plastic Analysis of Two Dimensional Stress Systems by the Finite Element Method', IJM Sci., 9, 143-155 (1967).

34) Venkatraman B., Patel S.A., 'Structural Mechanics with Introduction to Elasticity and Plasticity', McGraw Hill Book Company, 1970.

35) Corradi L., 'An Analysis Procedure for Plane Strain Contained Plastic Deformation Problems', IJNME, Vol. 15, No. 7, 1053-1074 (1980).

36) Marcal P.V., 'Large Deflection Analysis of Elastic-Plastic Shells of Revolution', AIAAJ, Vol. 8, No. 9, 1627-1633, 1970.

37) Bathe K.J., Wilson E.L., 'Numerical Methods in Finite Element Analysis', Prentice-Hall, Englewood Cliffs, 1976.

38) Zienkiewicz O.C., Valliappan S., King I.P., 'Elasto-Plastic Solutions of Engineering Problems Initial Stress, Finite Element Approach', IJNME, 1, 75-100 (1969).

39) Nickell R.E., Hibbit H.D., 'Thermal and Mechanical Analysis of Welded Structures', NED, Vol. 32, No. 1, 110-120 (1975).

40) Lemmon E.C., 'Phase-Change Techniques for Finite Element Conduction Codes', Journal of Thermal Stress, 1982.

BIBLIOGRAPHY

(1) Turner M.J., Clough R.W., Martin H.C., Topp L.J. - 'Stiffness and deflection analysis of complex structures', J. Aero. Sci., 23, 805-23, 1956.

(2) Argyris J.H. - 'Energy theorems and structural analysis', Butterworth, London, 1960.

(3) Clough R.W. - 'The finite element in plane stress analysis', Proc. 2nd A.S.C.E. Conf. on Electronic Computation, Pittsburgh, Pa., Sept. 1960.

(4) Melosh R.J. - 'Basis for the derivation of matrices in matrix structural analysis', AIAA Journal, 1, 1631-1637, 1963.

(5) Fraeijs de Veubeke B. - 'Upper and lower bounds in matrix structural analysis', AGAR Dograph 72, 165-201, Pergamon Press, London, 1964.

(6) Pian T.H.H. - 'Derivation of element stiffness matrix', AIAA Journal, 2, 576-577, 1964.

(7) Argyris J.H. - 'Continua and discontinuous', Proc. of Conf. on Matrix Methods in Struct. Mechanics, AFIT, Wright Patterson A.F. Base, Ohio, 151-169, Oct. 1965 (1966).

(8) Zienkiewicz O.C., Cheung Y.K. - 'The finite element in structural and continuum mechanics', McGraw Hill, 1967.

(9) Przemieniecki J.S. - 'Theory of matrix structural analysis', McGraw Hill, 1968.

(10) Szabo B.A. and Lee G.C. - 'Derivation of stiffness matrices for problems in plane elasticity by Galerkin method', IJNME, 1, 301-10 (1969).

(11) Oden J.T. - 'A general theory of finite elements'
I 'Topological considerations' 205-21,
II 'Application' 247-60, IJNME, 1, 1969.

(12) Irons B.M. - 'Numerical integration applied to finite element methods', Conf. on Use of Digital Computers in Structural Engineering, New Castle-Upon-Tyne, July 1966.

(13) Armen H., Isakson G., Pifko A. - 'Discrete element methods for the plastic analysis of structures subjected to cyclic loading', IJNME, 2, 2, 189-206, 1970.

(14) Lee C.H., Kobayashi Shiro - 'Elasto-plastic analysis of plane-strain and axisymmetric flat punch indentation by the finite element method', IJMS, 12, 349-370, April 1970.

(15) Marcal P.V. - 'A stiffness method for elastic-plastic problems', IJMS, 7, 229-238, 1965.

(16) Popov E.P., Khojesteh-Bakht M., Yaghmai S. - 'Analysis of elastic-plastic circular plates', Jr. Engg. Mech. Div., 49-65, 1967.

(17) Argyris J.H. - 'Elasto-plastic matrix displacement analysis of three dimensional continua', Jn. Royal Aero. Soc., 633-635, 1965.

(18) Gallagher R.H., Padlog J., Bijlaard P.B. - 'Stress analysis of heated complex shapes', J. Am. Rocket Soc., 32, 700-707, 1962.

(19) Zienkiewicz O.C., Valliappan S., King I.P. - 'Elasto-plastic solutions of engineering problems; Initial stress finite element approach', IJNME, 1, 75-100, 1969.

(20) Nayak G.C., Zienkiewicz O.C. - 'A note on 'alpha' constant stiffness method for the analysis of non-linear problems', IJNME, 4, 579-82, 1972.

(21) Boulton N.S., Lance-Martin H.E. - 'Residual stresses in arc welded plates', Proc. of the Institution of Mechanical Engineers, 133, 295-339 (1936).

(22) Tall L. - 'The strength of welded built-up columns', Ph.D. Dissertation, Lehigh University (1961).

(23) Tall L. - 'Residual stresses in welded plates - a theoretical study', Welding Journal, 43 (1), Research Supplement, 10-23 (1964).

(24) Masubuchi K., Simmons F.B., Monroe R.E. - 'Analysis of thermal stresses and metal movement during welding', RSIC-820, Redstone Scientific Information Center, Redstone Arsenal, Alabama, July 1968.

(25) Masubuchi K. - 'Report on current knowledge of numerical analysis of stresses, strains and other effects produced by welding', Welding in the World, 13 (11/12), 271-288 (1975).

(26) Hibbit H.D., Marcal P.V. - 'A numerical, thermo-mechanical model for the welding and subsequent loading of a fabricated structure', I. J. Comp. Struct., Vol. 3, No. 5, 1145-1174 (1973).

(27) Buyukozturk O., Hibbit H.D. - 'Prediction of residual stresses and distortion in large multi-pass welds', MARC Analysis Research Corporation, Report TR75-3 (1975).

(28) Cyr N.A., Teter R.D. - 'Finite element elastic-plastic creep analysis of two-dimensional continuum with temperature dependent material properties', Computer and Structure, 3, 849-63 (1973).

APPENDIX 1

ISOPARAMETRIC FINITE ELEMENT 2-D FORMULATIONS

Element stiffness matrix of a finite element is given by

$$[K]^{(e)} = \int_V [B]^T [D] [B] \, dV$$

where $[B]$ is called strain-displacement matrix and $[D]$ is called stress-strain matrix.

Strains at a point in finite element is given by

$$\{\varepsilon\} = [\bar{B}] \{d\}$$

where $\{\varepsilon\}$ for plane stress case and plane strain case, is given by

$$\lfloor \varepsilon \rfloor = \lfloor \varepsilon_x \quad \varepsilon_y \quad \varepsilon_{xy} \rfloor$$

and for axisymmetric case

$$\lfloor \varepsilon \rfloor = \lfloor \varepsilon_x \quad \varepsilon_y \quad \varepsilon_{xy} \quad \varepsilon_\theta \rfloor$$

$\{d\}$ is the vector of displacements at a point, hence $\{d\} = \begin{Bmatrix} u \\ v \end{Bmatrix}$. So matrix $[\bar{B}]$ for plane stress case and plane strain case is given by

$$[\bar{B}] = \begin{bmatrix} \frac{\partial}{\partial x} & 0 \\ 0 & \frac{\partial}{\partial y} \\ \frac{\partial}{\partial y} & \frac{\partial}{\partial x} \end{bmatrix}$$

and for axisymmetric case

$$[\bar{B}] = \begin{bmatrix} \frac{\partial}{\partial x} & 0 \\ 0 & \frac{\partial}{\partial y} \\ \frac{\partial}{\partial y} & \frac{\partial}{\partial x} \\ \frac{1}{r} & 0 \end{bmatrix}$$

where r is the radius of the point under consideration.

In case of isoparametric formulation

$$u = \sum_{i=1}^{n} N_i u_i \; ; \quad v = \sum_{i=1}^{n} N_i v_i \; ; \quad x = \sum_{i=1}^{n} N_i x_i$$

and $$y = \sum_{i=1}^{n} N_i y_i$$

where n is the number of nodes per element and N_i is the nodal shape function. Also u_i, v_i, x_i, y_i are the corresponding nodal values.

Using these interpolations for equations for strains, we have for plane stress and plane strain case

$$\begin{Bmatrix} \varepsilon_x \\ \varepsilon_y \\ \varepsilon_{xy} \end{Bmatrix} = \begin{bmatrix} \frac{\partial N_1}{\partial x} & 0 & \frac{\partial N_2}{\partial x} & 0 & \cdots \\ 0 & \frac{\partial N_1}{\partial y} & 0 & \frac{\partial N_2}{\partial y} & \cdots \\ \frac{\partial N_1}{\partial y} & \frac{\partial N_1}{\partial x} & \frac{\partial N_2}{\partial y} & \frac{\partial N_2}{\partial x} & \cdots \end{bmatrix} \begin{Bmatrix} u_1 \\ v_1 \\ u_2 \\ v_2 \\ \vdots \end{Bmatrix}$$

$$= [B] \{\delta\}$$

Also for axisymmetric case

$$\begin{Bmatrix} \varepsilon_x \\ \varepsilon_y \\ \varepsilon_{xy} \\ \varepsilon_\theta \end{Bmatrix} = \begin{bmatrix} \frac{\partial N_1}{\partial x} & 0 & \frac{\partial N_2}{\partial x} & 0 & \cdots \\ 0 & \frac{\partial N_1}{y} & 0 & \frac{\partial N_2}{y} & \cdots \\ \frac{\partial N_1}{\partial y} & \frac{\partial N_1}{\partial x} & \frac{\partial N_2}{\partial y} & \frac{\partial N_2}{\partial x} & \cdots \\ \frac{N_1}{r} & 0 & \frac{N_2}{r} & 0 & \cdots \end{bmatrix} \begin{Bmatrix} u_1 \\ v_1 \\ u_2 \\ v_2 \\ \vdots \end{Bmatrix}$$

$$= [B]\{\delta\}$$

Also since

$$\frac{\partial N_i}{\partial \xi} = \frac{\partial N_i}{\partial x}\frac{\partial x}{\partial \xi} + \frac{\partial y}{\partial \xi}\frac{\partial N_i}{\partial y}$$

$$\frac{\partial N_i}{\partial \eta} = \frac{\partial N_i}{\partial x}\frac{\partial x}{\partial \eta} + \frac{\partial y}{\partial \eta}\frac{\partial N_i}{\partial y}$$

where ξ and η are the local coordinates used to define shape functions, we have

$$\begin{Bmatrix} \frac{\partial N_i}{\partial \xi} \\ \frac{\partial N_i}{\partial \eta} \end{Bmatrix} = \begin{bmatrix} \frac{\partial x}{\partial \xi} & \frac{\partial y}{\partial \xi} \\ \frac{\partial x}{\partial \eta} & \frac{\partial y}{\partial \eta} \end{bmatrix} \begin{Bmatrix} \frac{\partial N_i}{\partial x} \\ \frac{\partial N_i}{\partial y} \end{Bmatrix} = [J] \begin{Bmatrix} \frac{\partial N_i}{\partial x} \\ \frac{\partial N_i}{\partial y} \end{Bmatrix}$$

where $[J]$ is called Jacobian matrix. Hence

$$\begin{Bmatrix} \frac{\partial N_i}{\partial x} \\ \frac{\partial N_i}{\partial y} \end{Bmatrix} = [J]^{-1} \begin{Bmatrix} \frac{\partial N_i}{\partial \xi} \\ \frac{\partial N_i}{\partial \eta} \end{Bmatrix}$$

Using interpolation defined earlier for coordinate at a point in terms of nodal coordinates, we have

$$[J] = \begin{bmatrix} \frac{\partial N_1}{\partial \xi} & \frac{\partial N_2}{\partial \xi} & \cdots \\ \frac{\partial N_1}{\partial \eta} & \frac{\partial N_2}{\partial \eta} & \cdots \end{bmatrix} \begin{bmatrix} x_1 & y_1 \\ x_2 & y_2 \\ \vdots & \end{bmatrix}$$

Hence once $\frac{\partial N_i}{\partial x}$ and $\frac{\partial N_i}{\partial y}$ are known, matrix [B] can be calculated by upper expressions shown.

Matrix [D] for different cases are given by for plane stress case:

$$[D] = \frac{E}{1 - \nu^2} \begin{bmatrix} 1 & \nu & 0 \\ \nu & 1 & 0 \\ 0 & 0 & \frac{1-\nu}{2} \end{bmatrix}$$

for plane strain case:

$$[D] = \frac{E}{(1 + \nu)(1 - 2\nu)} \begin{bmatrix} 1-\nu & \nu & 0 \\ \nu & 1-\nu & 0 \\ 0 & 0 & \frac{1-2\nu}{2} \end{bmatrix}$$

for axisymmetric case:

$$[D] = \frac{E(1 - \nu)}{(1 + \nu)(1 - 2\nu)} \begin{bmatrix} 1 & \frac{\nu}{1-\nu} & 0 & \frac{\nu}{1-\nu} \\ \frac{\nu}{1-\nu} & 1 & 0 & \frac{\nu}{1-\nu} \\ 0 & 0 & \frac{1 - 2\nu}{2(1-\nu)} & 0 \\ \frac{\nu}{1-\nu} & \frac{\nu}{1-\nu} & 0 & 1 \end{bmatrix}$$